STUDIES OF THE NONLINEAR SCHRÖDINGER EQUATION AND ITS APPLICATION TO WATER WAVES

THESIS BY

DAVID U. MARTIN

IN PARTIAL FULFILLMENT OF THE REQUIREMENTS
FOR THE DEGREE OF
DOCTOR OF PHILOSOPHY

CALIFORNIA INSTITUTE OF TECHNOLOGY

PASADENA, CALIFORNIA

1981

(SUBMITTED MAY 5, 1981)

ACKNOWLEDGMENTS

I wish to thank Professor Philip G. Saffman for the guidance and counsel he has provided in the course of this work. His breadth of knowledge and eye for detail were invaluable.

A number of friends and colleagues have given support and encouragement, for which I am deeply grateful. My good friend Dr. Henry C. Yuen deserves particular mention.

The skill and high professional standards of Janet Nay were very much appreciated. Her typing of the manuscript was both swift and accurate.

My thanks also to my wife Peg, who was endlessly patient.

ABSTRACT

Various properties of the nonlinear Schrödinger equation and special solutions thereof are investigated, with emphasis on applications to water waves.

The spreading of modal energy for initial conditions corresponding to unstable perturbations of a uniform wave is investigated numerically and analytically. For a one-dimensional surface, the upper limit of the Benjamin-Feir instability interval appears to provide a good estimate of the maximum spread of the modal energy. The analytical estimate of Thyagaraja is shown to be insufficiently sharp to account for this effective maximum. In the case of a two-dimensional surface, the instability region obtained with the nonlinear Schrödinger equation is infinite in extent, and the numerical results suggest that energy may leak to arbitrarily high unstable harmonics in a quasi-recurring fashion.

Stability results for plane-wave envelopes on a two-dimensional surface are calculated and verified numerically with the nonlinear Schrödinger equation. For standing-wave disturbances, instability is found for both odd and even modes; as the period of the unperturbed solution increases, the instability associated with the odd modes remains, but that associated with the even modes disappears. This is consistent with previous results on the stability of solitons. In addition, traveling-wave instabilities are identified for even mode perturbations which are absent in the long-wave limit. Extrapolation to the case of an unperturbed solution with

infinite period suggests that these instabilities may also be present for the envelope solitons. Thus the soliton is unstable to odd, standing-wave perturbations, and very likely also to even, traveling-wave perturbations.

Bifurcation techniques are used to obtain a new class of small-amplitude water waves of permanent form. Stokes waves are used as a starting point, and the critical value of steepness at which bifurcation can occur is computed for various choices of modulation wavelength and angular orientation. It is found that, for a two-dimensional surface, bifurcation can occur at small values of wave steepness. Second order corrections to the wave amplitude, modulation, frequency, and speed, which apply when one moves off the bifurcation point onto a new branch of solutions, are also computed. Two types of new solutions are found, one symmetric with respect to the carrier wave propagation direction, and one asymmetric.

Finally, the nonlinear Schrödinger equation is used to study the interaction of deep-water gravity waves with currents. The case of a uniform wave encountering a steady current is treated numerically and analytically, and the results are shown to correspond to known results in the linear limit. As an example of modulated waves encountering a current, the development of an instability of Benjamin-Feir type is calculated in both the presence and absence of current. Finally, the case of an envelope soliton encountering a current is treated numerically, and the results are compared to those obtained by applying a perturbation scheme.

TABLE OF CONTENTS

CHAPTER PAGE

INTRODUCTION

It is now well established that many weakly-nonlinear dispersive wave systems can be described by the nonlinear Schrödinger equation. One case of interest is that of irrotational, nearly monochromatic gravity waves on water of infinite depth and constant density. In this case, the nonlinear Schrödinger equation governs the development of the "complex envelope" of the free surface displacement, where the complex envelope reflects slow modulations of both amplitude and phase.

The uniform (i.e., space-independent) solution of the nonlinear Schrödinger equation corresponds to the nonlinear water wave of permanent form discovered by Stokes [15] in 1849 (including only the lowest order nonlinear term of the frequency). The Stokes wavetrain is subject to a modulational instability first noted by Lighthill [8] and analyzed in detail by Benjamin and Feir [2]. This instability and its long-term results can be studied via the nonlinear Schrödinger equation. One finds that, in the absence of viscosity, one sees a sequence of modulations and subsequent demodulations corresponding to what is known as Fermi-Pasta-Ulam recurrence [4]. Various explanations of the recurrence phenomenon have been proposed for the case of a one-dimensional surface. In the first chapter, two such explanations, both of which rely on limiting the spreading of energy in the solution spectrum, are compared and tested numerically.

The second chapter deals with the extension of ideas on recurrence developed for the case of a one-dimensional surface to the case of a two-dimensional surface. Yuen and Ferguson [19] identified a relationship between the initial perturbation and the long-time evolution of an unstable, uniform solution of the nonlinear Schrödinger equation in one dimension. In particular, they demonstrated numerically that the long-time evolution of the unstable solution is composed of the growth and decay of all the harmonics of the initial perturbation that lie within the unstable region, each one taking its turn at dominating the solution profile. They reasoned that this relationship, in combination with the fact that the instability region is of finite extent (being confined to low modes), precludes the irreversible spread of energy among all modes often expected of nonlinear systems undergoing instability. In the second chapter, it is demonstrated numerically that the relationship found for the one-dimensional case can be extended to the two-dimensional case. However, the instability region in the two-dimensional case is unbounded, and thus the argument used in the one-dimensional case to predict that energy is confined to low modes no longer applies. In fact, the results suggest that in this situation, the energy may leak to arbitrarily high unstable harmonics in a quasi-recurring fashion.

Another solution of the nonlinear Schrödinger equation of particular interest is the "envelope soliton," which is a wave packet with various special properties. It maintains its form while propagating, and can survive interactions with other wave packets. Zakharov and Shabat [25] showed that an arbitrary initial wave packet on a one-dimensional surface will ultimately evolve into a state dominated by a

number of envelope solitons. For the case of long-wave disturbances on a one-dimensional surface, the envelope soliton is stable (Rowlands [13]). On a two-dimensional surface, however, even the soliton is unstable (Zakharov and Rubenchik [24]; Saffman and Yuen [14]). The third chapter treats the problem of dnoidal (periodic) solutions on a two-dimensional surface. Dnoidal solutions bridge the gap between uniform waves and solitons, and the instabilities to which they are subject suggest the existence of a soliton instability independent of those noted by Zakharov and Rubenchik and Saffman and Yuen.

Three form-preserving solutions of the nonlinear Schrödinger equation have been noted thus far: the uniform solution, dnoidal solution, and soliton. Of these, only the uniform solution represents a wave (as opposed to just an envelope) of permanent form. However, there are a number of results suggesting that other such solutions exist. Longuet-Higgins [9], working with the full water wave equations rather than the nonlinear Schrödinger equation, found that long-wave, one-dimensional perturbations which are unstable for carrier waves of moderate amplitude (in accordance with Benjamin and Feir) are restabilized for wavetrains of large amplitude. For given perturbation wavelength, there exists in the large-amplitude stable regime a wave for which the disturbance is stationary relative to the undisturbed flow. (We call this a point of neutral stability. Note that it is not necessarily a point of exchange of stability). The existence of bifurcation is thereby suggested; that is, at a value of $k_0 a_0$ yielding neutral stability, Stokes-type uniform wavetrain solutions may intersect another branch or branches of solutions corresponding to waves of permanent form. Chen and Saffman [3] have

indeed demonstrated that solutions do bifurcate from the Stokes wave at points which appear to be those of neutral stability. These results are one-dimensional and occur at high values of $k_o a_o$. Thus, they cannot be treated with a simple water wave model like the nonlinear Schrödinger equation. It will be seen in the fourth chapter, in fact, that no bifurcation occurs for one-dimensional solutions of the nonlinear Schrödinger equation.

In a two-dimensional context, however, Peregrine and Thomas [12] have found that, for the limit of infinitely long perturbations, restabilization occurs for smaller and smaller values of $k_o a_o$ as the perturbation becomes more and more oblique. It can be inferred from their calculation that neutral stability also occurs at smaller amplitude as the disturbance becomes more oblique, and that two-dimensional bifurcation may occur at small amplitudes, and hence be describable by the nonlinear Schrödinger equation when the waves are sufficiently oblique. This approach is pursued in the fourth chapter, and bifurcation from the uniform solution of the nonlinear Schrödinger equation at low values of $k_o a_o$ is found. The bifurcated solutions correspond to two-dimensional modulated wavetrains of permanent form. The family of bifurcations is degenerate. There are subfamilies corresponding to modulations symmetric or asymmetric with respect to the direction of propagation of the carrier wave, and for every $|N| = |k_o/k_x| \gg 1$ there is a range of $\theta = \arctan(k_y/k_x)$ yielding bifurcation (where k_o represents carrier wavenumber, k_x represents the longitudinal modulation wavenumber, and k_y represents the transverse modulation wavenumber). The importance of these solutions is subject to analysis of stability and energetics.

Longuet-Higgins and Stewart [10,11] were among the first to study the interaction of water waves with currents. They worked with linear waves, and pointed out that the use of a naive energy transport equation leads one into trouble. In particular, they identified a quantity which they called "radiation stress" which must appear in such an equation.

Whitham [17] demonstrated that the results of Longuet-Higgins and Stewart can be obtained from conservation laws. Subsequently [18], he showed that they can be derived easily via the averaged Lagrangian technique.

In the fifth chapter, a forced version of the nonlinear Schrödinger equation is derived to model the effect of a current on waves. This equation allows for weak nonlinearity, and also includes dispersive terms, thus avoiding singularities which can arise from the intersection of characteristics. Solutions are obtained in various special cases, and compared to the results of other models.

Notational conventions used throughout this work are as follows:

A	complex wave amplitude governed by the nonlinear Schrödinger equation
$\underline{c}_g$	group velocity vector $\left(= \frac{\omega_o}{2k_o^2} \underline{k}_o \right)$
c_g	magnitude of $\underline{c}_g$ $\left(= \frac{\omega_o}{2k_o} \right)$
g	gravitational acceleration
$\underline{k}_o$	carrier wavenumber vector
k_o	magnitude of $\underline{k}_o$
t	time coordinate

$\underline{x}$	horizontal coordinates = (x,y)
x	horizontal coordinate in direction of carrier wave propagation
y	horizontal coordinate normal to x
z	vertical coordinate
n	surface displacement
ϕ	velocity potential
ω_o	linear carrier wave frequency ($= \sqrt{gk_o}$)

CHAPTER 1

SPREADING OF ENERGY IN SOLUTIONS OF THE NONLINEAR SCHRÖDINGER EQUATION ON A ONE-DIMENSIONAL SURFACE

For the case of one space dimension, Yuen and Ferguson [19] noted a relationship between recurrence phenomena associated with, and stability properties of, the nonlinear Schrödinger equation. In particular, they showed, by numerical examples, that for initial conditions corresponding to a perturbed uniform solution, each unstable harmonic of the perturbation takes its turn at dominating the solution profile, and this process continues, cyclically.

Thyagaraja [16] has shown analytically that periodic solutions of the one-space-dimensional nonlinear Schrödinger equation must necessarily confine most of their energy to low wavenumbers. More specifically, he proves that for a solution

$$\psi(x,t) = \sum_{n=-\infty}^{\infty} c_n(t)\exp(2\pi i n x), \tag{1.1}$$

where x is the spatial variable and t represents time, there will be a time-independent bound $\hat{N}$ on the quantity

$$N_{rms} = \left[\left(\sum_{n=-\infty}^{\infty} n^2 |c_n(t)|^2\right)\left(\sum_{n=-\infty}^{\infty} |c_n(t)|^2\right)^{-1}\right]^{1/2} \tag{1.2}$$

which is a measure of the extent of energy spread. In particular, N_{rms} represents the root-mean-square component number with weighting function

$$|c_n|^2 \left(\sum_{n=-\infty}^{\infty} |c_n|^2 \right)^{-1}. \tag{1.3}$$

The bound $\hat{N}$ depends only on the values of constants of motion, as determined by the initial condition. Thyagaraja also shows that if

$$N_0 > \hat{N}K, \tag{1.4}$$

where K is an arbitrary positive number, then for all time

$$\sum_{|n|>N_0} |c_n(t)|^2 < \left(\sum_{n=-\infty}^{\infty} |c_n(t)|^2 \right) K^{-2}. \tag{1.5}$$

Thus, Thyagaraja has provided an *a priori* bound on the spreading of energy for general initial conditions. He argues that this bound is responsible for the recurrence observed by Yuen and Ferguson.

In the following, we shall make several comparisons of Thyagaraja's bound to the upper limit of the instability interval (which was proposed by Yuen and Ferguson as a measure of effective energy spread), and to actual values obtained from numerical solutions of the following version of the one-space-dimensional nonlinear Schrödinger equation:

$$i \frac{\partial \psi}{\partial t} = \frac{\partial^2 \psi}{\partial x^2} + \mu |\psi|^2 \psi \quad (\mu > 0). \tag{1.6}$$

As a first test case we consider the initial condition

$$\psi = \psi_0 (1 - 0.1 \cos 2\pi x) \tag{1.7}$$

on the interval [0,1]. Note that the harmonics of wavenumber N are unstable if, and only if,

$$0 < 4\pi^2 N^2 < 2\mu\psi_o^2, \tag{1.8}$$

as established by Benjamin and Feir [2]. Application of the formulae provided by Thyagaraja yields

$$N_{rms} \leq \hat{N} = M/2\pi, \tag{1.9}$$

where

$$M = \frac{1}{2}\left\{\mu I_o + \left[\mu^2 I_o^2 + 4(J_o/I_o + \mu I_o/2)\right]^{1/2}\right\}, \tag{1.10}$$

$$I_o = 1.005\ \psi_o^2, \tag{1.11}$$

$$J_o = 0.02\pi^2\psi_o^2 - 0.51502\mu\psi_o^4. \tag{1.12}$$

It is easily verified from (1.11) and (1.12) that

$$J_o/I_o + \mu I_o/2 > -0.01\mu\psi_o^2 > -0.01\mu I_o. \tag{1.13}$$

Use of (1.10) gives

$$M > (\mu I_o/2)\left\{1 + \left[1 - 0.04/(\mu I_o)\right]^{1/2}\right\}. \tag{1.14}$$

If we assume that the initial modulation wavenumber lies in the instability interval, i.e., that

$$4\pi^2 < 2\mu\psi_o^2, \tag{1.15}$$

then it follows from (1.11) that

$$\mu I_o \geq 2.01\pi^2, \tag{1.16}$$

and hence, from (1.14), that

$$M > 0.999\mu I_o. \tag{1.17}$$

Let $2\pi N_u$ represent the cutoff wavenumber for instability. Equation (1.8) gives

$$4\pi^2 N_u^2 = 2\mu\psi_o^2, \tag{1.18}$$

and thus

$$\mu I_o = 2.01\pi^2 N_u^2. \tag{1.19}$$

Substitution of (1.9) and (1.19) into (1.17) yields

$$\hat{N} > 3.15 N_u^2. \tag{1.20}$$

The assumption that the initial modulation lies in the unstable region implies that

$$N_u > 1, \tag{1.21}$$

and thus $\hat{N}$ is significantly larger than N_u.

In order to compare Thyagaraja's bounds to numerical results, the five cases considered in Yuen and Ferguson were reexamined, and a sixth case involving a multicomponent unstable initial disturbance was also investigated. In this last case, 14 components lay in the instability interval, and the amplitude of each component was initially one hundredth of the carrier wave amplitude. Choice of phase did not seem to affect the relevant characteristics of the solution. The component amplitudes (including that of the carrier wave) do oscillate, but simple recurrence of the sort observed by Yuen and Ferguson is not apparent.

The values of the bounds $\hat{N}$ and N_u for each of the six cases are presented in Table 1.1. In accordance with the analysis, the relationship

$$\hat{N} \simeq 3.15 N_u^2 \tag{1.22}$$

holds in all cases. (Note, however, that the analysis assumed a single-component initial disturbance).

Figure 1.1 depicts the energy in the N lowest components as a function of N at times of near maximal energy spreading for cases 2, 5, and 6. The bounds $\hat{N}$ and N_u are indicated (although $\hat{N}$ is off scale in cases 5 and 6).

For cases 1, 2, 5, and 6, Table 1.2 compares the maximum over time of N_{rms} and N_{99}, defined as the smallest value of N_o such that

$$\sum_{n=-N_o}^{N_o} |c_n(t)|^2 \simeq 0.99 \sum_{n=-\infty}^{\infty} |c_n(t)|^2 \tag{1.23}$$

for the duration of the run, to the corresponding bounds, $\hat{N}$ and $\hat{N}_{99}$ given by Thyagaraja. Note that max (N_{rms}) is well approximated by the values of N_u also included in Table 1.2. On the other hand, $\hat{N}$ is much larger than max (N_{rms}) and $\hat{N}_{99}$ is much larger than N_{99}.

The accuracy of the code used to solve the one-dimensional nonlinear Schrödinger equation was tested by computing I_o and J_o, which are constants of the motion, at various times during the runs. For cases 1, 2, and 5, they were found to vary by at most one part in a thousand. In case 6, the calculated value of I_o was found to vary by 0.8 parts in a thousand until $t = 940$, at which point a large variation was initiated, culminating in a total shift of 3.2 parts per thousand. The calculated value of J_o was found to vary by 2 parts in a thousand until $t = 940$, at which point a shift of 16 parts per thousand took place. Computation was stopped at that point for lack of numerical accuracy.

In summary, we have found that the results of direct numerical computation support the analytical upper bounds on the spread of modal energy established by Thyagaraja. However, the bounds are not sufficiently sharp to account for the relationship between initial instability and spreading observed by Yuen and Ferguson. In fact, for all the cases examined, the upper limit of the unstable region appears to provide a better estimate of the maximum spread of the modal energy, favoring the empirical relationship proposed by Yuen and Ferguson. [Compare N_u and the computed max (N_{rms}) in Table 1.2.]

CHAPTER 2

THE RELATIONSHIP BETWEEN BENJAMIN-FEIR INSTABILITY AND RECURRENCE FOR THE NONLINEAR SCHRÖDINGER EQUATION IN TWO SPACE DIMENSIONS

To describe weakly-nonlinear, deep-water gravity waves, the following version of the nonlinear Schrödinger equation is appropriate (Zakharov [23]):

$$i\left(\frac{\partial A}{\partial t} + \frac{\omega_o}{2k_o}\frac{\partial A}{\partial x}\right) - \frac{\omega_o}{8k_o^2}\frac{\partial^2 A}{\partial x^2} + \frac{\omega_o}{4k_o^2}\frac{\partial^2 A}{\partial y^2} - \frac{1}{2}\omega_o k_o^2 |A|^2 A = 0, \qquad (2.1)$$

where surface displacement is given by

$$\eta = \mathrm{Re}\left[Ae^{i(k_o x - \omega_o t)} + \frac{1}{2}k_o A^2 e^{i(2k_o x - 2\omega_o t)}\right] + O(A^3). \qquad (2.2)$$

For a one-dimensional surface, equation (2.1) reduces to

$$i\left(\frac{\partial A}{\partial t} + \frac{\omega_o}{2k_o}\frac{\partial A}{\partial x}\right) - \frac{\omega_o}{8k_o^2}\frac{\partial^2 A}{\partial x^2} - \frac{1}{2}\omega_o k_o^2 |A|^2 A = 0. \qquad (2.3)$$

Two properties of particular significance which are associated with equation (2.3) are:

1) Benjamin-Feir Instability - The uniform solution

$$A = a_o e^{-\frac{i}{2}\omega_o k_o^2 a_o^2 t} \qquad (2.4)$$

is unstable under infinitesimal perturbations of the form $b_+ e^{ik\xi} + b_- e^{-ik\xi}$ (where $\xi = x - \frac{\omega_o}{2k_o}t$ is the coordinate moving with the group velocity) provided that k satisfies

$$0 < \left(\frac{k}{2k_o}\right)^2 < 2(k_o a_o)^2. \tag{2.5}$$

Maximum instability occurs when $\frac{k}{2k_o} = k_o a_o$.

2) Fermi-Pasta-Ulam Recurrence - For many solutions of (2.3), the initial condition undergoes strong modulation, but eventually returns to a close approximation of its orginal state. The cycle repeats periodically in time, though the recurrence is not in general perfect. This recurrence phenomenon was first reported by Fermi et al. [4] in a study of nonlinear lattice vibration. Its occurrence in the nonlinear Schrödinger equation in connection with deep-water waves has been reported by Lake et al. [7] and Yuen et al. [22].

Yuen and Ferguson [19] demonstrated that, for solutions of (2.3) corresponding to unstable perturbations of a uniform wavetrain, the complexity of recurrence is related to the number of harmonics of the perturbation which fall within the Benjamin-Feir instability interval. In particular, they show that the evolution of such solutions is a composite of the evolution of all unstable harmonics of a prescribed perturbing mode, with each and every harmonic taking its turn at dominating the solution profile.

Equation (2.1) exhibits the Benjamin-Feir instability for perturbations of the form $b_+ e^{i(k\xi+\kappa y)} + b_- e^{-i(k\xi+\kappa y)}$ where k and κ satisfy

$$0 < \left(\frac{k}{2k_o}\right)^2 - 2\left(\frac{\kappa}{2k_o}\right)^2 < 2(k_o a_o)^2. \tag{2.6}$$

Maximum instability occurs when $\left(\frac{k}{2k_o}\right)^2 - 2\left(\frac{\kappa}{2k_o}\right)^2 = (k_o a_o)^2$. Figure 2.1 represents this instability region in k,κ space. Moreover, some solutions of (2.1) exhibit recurrence (Yuen and Ferguson [20]).

In order to investigate the possibility of generalizing to two space dimensions the relationship between Benjamin-Feir instability and recurrence observed in the case of one space dimension, we have carried out numerical calculations for a carrier wave with

$$\left.\begin{aligned} \omega_o &= 100 \\ k_o a_o &= .1 \end{aligned}\right\} \tag{2.6}$$

modulated initially by the complex amplitude

$$A = a_o + \alpha \cos k\left(x - \frac{\omega_o}{2k_o} t\right) \cos \kappa y \tag{2.7}$$

where

$$|\alpha| = .05\, a_o \tag{2.8}$$

and the phase of α is chosen to give growing solutions. The wavenumbers k and κ were chosen to satisfy

$$\left.\begin{aligned} (k/2k_o)^2 &= 2(k_o a_o)^2 \\ 2(\kappa/2k_o)^2 &= (k_o a_o)^2 \end{aligned}\right\}. \tag{2.9}$$

Thus

$$(k/2k_o)^2 - 2(\kappa/2k_o)^2 = (k_o a_o)^2 \tag{2.10}$$

and therefore the Benjamin-Feir instability is maximized.

Figure 2.2 depicts the amplitude and power spectrum of the solutions arising from the initial condition described above at times representative of the various stages through which the solution progresses. The axis variables are given by

$$X = k_o^2 a_o \left(x - \frac{\omega_o}{2k_o} t \right), \quad Y = k_o^2 a_o y, \quad T = \omega_o k_o^2 a_o^2 t, \tag{2.11}$$

and A is normalized (i.e., A/a_o is plotted).

Figure 2.3 exhibits contour plots of the amplitude functions presented in Figure 2.2.

Two recurrence cycles appear in the sequence depicted — inspection of the power spectra shows that only the (0,0) mode (corresponding to the carrier wave), the (k,κ) mode (corresponding to the initial perturbation), and the $(5k,7\kappa)$ mode participate. Each mode dominates the solution some of the time, and sometimes they participate in combination.

The fact that the $(5k,7\kappa)$ mode was singled out to participate allows us to test the hypothesis that the Benjamin-Feir instability determines significant modes; and indeed, it is easily verified from (7.8) that

$$(5k/2k_o)^2 - 2(7\kappa/2k_o)^2 = (k_o a_o)^2 \tag{2.12}$$

and thus the $(5k,7\kappa)$ mode, like the (k,κ) mode maximizes the Benjamin-Feir instability. There are other unstable harmonics of the prescribed (k,κ) mode, but they are at frequencies beyond the resolution of our computation. Specifically, sixteenth harmonics were the upper limit for the calculation, and the next few unstable harmonics are $(29k,41\kappa)$, $(169k,239\kappa)$, and $(985k,1393\kappa)$.

The $(5k,7\kappa)$ component was initially zero. Thus it appears that energy had to be passed through a chain of stable modes to trigger the $(5k,7\kappa)$ mode, but due to their stability they remained small. Thus, as in the case of one space dimension, the number of modes participating is small, and consequently the recurrence of situations characterized by the dominance of those modes is not surprising. In the case of two space dimensions, however, there is no maximum wavenumber cutoff. Thus, given enough time, a solution could march out to higher wavenumbers, and in so doing depart from the realm of validity of the underlying equation.

CHAPTER 3

STABILITY OF PLANE WAVE SOLUTIONS OF THE NONLINEAR SCHRÖDINGER EQUATION ON A TWO-DIMENSIONAL SURFACE

In the case of one space dimension, it is known that there are stable soliton solutions of the nonlinear Schrödinger equation (Zakharov and Shabat [25], Yuen and Lake [21]) and also that the uniform solution exhibits the Benjamin-Feir instability (Benjamin and Feir [2], Lake et al. [7]). In two space dimensions, even the soliton solutions have been shown to be unstable (Zakharov and Rubenchik [24], Saffman and Yuen [14]). In the following, we will work in two space dimensions and treat dnoidal (periodic) solutions which bridge the gap between solitons and uniform waves.

We proceed by obtaining equations governing the stability of plane periodic solutions, and devising numerical techniques to solve these equations. We apply these techniques to dnoidal waves, and check the results in the uniform wave, soliton, and long-wave perturbation limits. We conclude with a presentation of some numerical solutions of initial value problems which verify our stability curves.

3.1 Steady Solutions on a Two-Dimensional Surface

The appropriate form of the nonlinear Schrödinger equation for deep-water gravity waves on a two-dimensional surface is

$$i\left(\frac{\partial A}{\partial t} + \frac{\omega_o}{2k_o}\frac{\partial A}{\partial x}\right) - \frac{\omega_o}{8k_o^2}\frac{\partial^2 A}{\partial x^2} + \frac{\omega_o}{4k_o^2}\frac{\partial^2 A}{\partial y^2} - \frac{1}{2}\omega_o k_o^2 |A|^2 A = 0. \qquad (3.1)$$

To simplify the subsequent discussion, it is convenient to transform (3.1) into the dimensionless form

$$i\partial B/\partial T + \frac{1}{2}\,\partial^2 B/\partial X^2 + \frac{1}{2}\,\alpha\,\partial^2 B/\partial Y^2 + |B|^2 B = 0, \qquad (3.2)$$

where

$$T = -\omega_0 T, \quad X = 2k_0(x - \omega_0 t/2k_0), \quad Y = 2k_0 y, \quad B = k_0 A/\sqrt{2} \qquad (3.3)$$

For $\alpha = -2$, (3.2) reduces to (3.1).

Let

$$Z = X \cos\delta + Y \sin\delta. \qquad (3.4)$$

Then a solution of (3.2) of the form $B(z)$ must satisfy

$$i\partial B/\partial T + \frac{1}{2}\,(\cos^2\delta + \alpha \sin^2\delta)\partial^2 B/\partial Z^2 + |B|^2 B = 0. \qquad (3.5)$$

Thus this equation describes plane modulations at an angle δ from the direction of propagation of carrier wave energy. The nature of (3.5) varies according to the sign of the coefficient $\partial^2 B/\partial Z^2$. Thus the critical point for the case $\alpha = -2$ is $\sin^2\delta = 1/3$ — i.e., $\delta = 35.26°$. For $\delta < 35.26°$, (3.5) possesses steady localized (soliton) solutions, and a family of periodic (dnoidal) solutions connecting those solitons to the uniform wavetrain. As δ increases past 35.26°, the relative sign between the nonlinear and the dispersive terms changes from positive to negative. The equation now possesses stationary solutions corresponding to depressions in an otherwise uniform wavetrain ("dark pulses"), but no steady localized solutions exist in the form of solitons.

Without loss of generality, attention can be restricted to the case of plane waves propagating in the X direction. The reason for this is that, given a propagation direction corresponding to a coordinate $\hat{X}$, a coordinate $\hat{Y}$ can be found such that the form of (3.2) is

unchanged by a transformation from the coordinates X,Y to the coordinates $\hat{X},\hat{Y}$ with appropriate scaling of $\hat{X}$ and $\hat{Y}$. Thus a plane solution can be assumed to take the form

$$B_0 = \phi_0(X)e^{i\gamma^2 T}, \tag{3.6}$$

where ϕ_0 satisfies the equation

$$-\gamma^2\phi_0 + \frac{1}{2}\,\partial^2\phi_0/\partial X^2 + \phi_0^3 = 0. \tag{3.7}$$

There is a family of periodic solutions of (3.7) of the form

$$\phi_0(X) = \beta\ \mathrm{dn}\left[\beta(X - X_0),m\right], \tag{3.8}$$

where

$$0 \leq m \leq 1 \tag{3.9}$$

and

$$\beta = \gamma[2/(2 - m^2)]^{1/2}. \tag{3.10}$$

The dn function is of period $2F$, where

$$F = F\left(\frac{1}{2}\,\pi,m\right) = \int_0^{\pi/2} (1 - m^2\sin^2\theta)^{-1/2}d\theta. \tag{3.11}$$

Thus ϕ_0 is of period $2F/\beta$. At $m = 0$, ϕ_0 is constant; at $m = 1$, ϕ_0 assumes the infinite wavelength soliton form

$$\phi_0(X) = \sqrt{2}\gamma\ \mathrm{sech}\ (\sqrt{2}\gamma X). \tag{3.12}$$

Note that the dnoidal waves constitute a two-parameter family of solutions, the two parameters being m and γ. For a fixed m, amplitude

increases and period decreases as γ increases. For a fixed γ, the period increases as m increases.

3.2 The Stability of Plane Periodic Envelopes Subjected to Infinitesimal Cross-Wave Perturbations

We now perturb the solutions B_0 described in the preceding section. Consider a disturbance of the form $B_1(X,Y,T)e^{i\gamma^2 T}$, where $|B_1| << |B_0|$ for all X, Y, and T. Substituting $B = B_0 + B_1 e^{i\gamma^2 T}$ into (3.4) and linearizing about B_0 yields.

$$(i\partial/\partial T - \gamma^2)B_1 + \tfrac{1}{2}\,\partial^2 B_1/\partial X^2 + \tfrac{1}{2}\,\alpha\,\partial^2 B_1/\partial Y^2 + 2\phi_0^2 B_1 + \phi_0^2 B_1^* = 0. \quad (3.13)$$

The appearance of B_1^* in this equation implies that no single-mode solutions exist. That is, any mode present must appear in combination with its conjugate mode. Therefore we take

$$B_1 = \phi_1(X)e^{i\kappa Y}e^{(\Omega+i\Lambda)T} + \hat{\phi}_1(X)e^{-i\kappa Y}e^{(\Omega-i\Lambda)T}, \quad (3.14)$$

where κ represents the transverse perturbation wavenumber, ϕ_1 and $\hat{\phi}_1$ are complex, and $|\phi_1|, |\hat{\phi}_1| << \phi_0$.

Substituting (3.14) into (3.13), equating coefficients of $e^{\pm(\kappa Y+\Lambda T)}$, and simplifying, we find that the stability problem is reduced to determining the eigenvalues c^2 of

$$(L_0 + \tfrac{1}{2}\,\alpha\,\kappa^2)(L_1 + \tfrac{1}{2}\,\alpha\,\kappa^2)u = c^2 u \quad (3.15)$$

subject to periodic boundary conditions, for given values of κ, where

$$L_0 = -\tfrac{1}{2}\,d^2/dX^2 + \gamma^2 - \phi_0^2, \quad (3.16)$$

$$L_1 = -\frac{1}{2} d^2/dX^2 + \gamma^2 - 3\phi_0^2, \tag{3.17}$$

$$c = \Lambda \pm i\Omega. \tag{3.18}$$

In the immediately following discussion, we will restrict ourselves to consideration of real c^2. We note, however, that complex values are also relevant to a discussion of stability, and we will consider the complex case in a subsequent section.

Solution of (3.15) is complicated by the fact that, although L_0 and L_1 are self-adjoint, the compound operator $(L_0 + \frac{1}{2}\alpha\kappa^2)(L_1 + \frac{1}{2}\alpha\kappa^2)$ is not. Thus standard theory is not applicable, and unusual solutions can result.

Note that the problem can be simplified by narrowing our focus to search only for even or odd eigenfunctions. If an arbitrary function satisfies (3.15), then both its even and odd components satisfy (3.15) for the same eigenvalue c^2, due to the linearity and even parity of L_0 and L_1. Note also that the even and odd components of a periodic function share its periodicity.

It is easily demonstrated that even eigenfunctions of (3.15) of period $2F/\beta$ (the period of ϕ_0) are equivalent to eigenfunctions u_+ on $[-F/\beta, F/\beta]$ satisfying

$$u_+'(F/\beta) = 0 = u_+'(-F/\beta), \tag{3.19}$$

$$u_+'''(F/\beta) = 0 = u_+'''(-F/\beta), \tag{3.20}$$

Likewise, odd eigenfunctions of (3.15) of period $2F/\beta$ are equivalent to eigenfunctions u_- on $[-F/\beta, F/\beta]$ satisfying

$$u_-(F/\beta) = 0 = u_-(-F/\beta), \tag{3.21}$$

$$u''(F/\beta) = 0 = u''_-(-F/\beta). \tag{3.22}$$

Thus to obtain real eigenvalues, c^2, corresponding to even eigenfunctions, we solve the following boundary value problem on $[0,F/\beta]$ for fixed κ and a range of values of c^2:

$$(L_0 + \tfrac{1}{2}\alpha\kappa^2)(L_1 + \tfrac{1}{2}\alpha\kappa^2)u_+ = c^2 u_+, \quad u_+(0) = 1,$$

$$u'_+(F/\beta) = 0 = u'''_+(F/\beta), \quad u'_+(0) = 0. \tag{3.23}$$

We seek a value of c^2 which causes $u'''_+(0)$ to vanish.

Likewise, for odd eigenfunctions, we require that $u_-(0) = 0$, $u'_-(0) = 1$, $u_-(F/\beta) = 0$, and $u''_-(F/\beta) = 0$. We then fix κ and vary c^2 until $u''_-(0) = 0$.

Alternatively, we can add the equation

$$\partial(c^2)/\partial X = 0 \tag{3.24}$$

and specify the additional boundary condition

$$u'''_+(0) = 0 \tag{3.25}$$

or

$$u''_-(0) = 0. \tag{3.26}$$

We have employed both techniques, using one as a check on the other. The results of these numerical investigations are presented in Figures 3.1 (even modes) and 3.2 (odd modes). The parameter associated with the curves is the modulus m of the dnoidal function associated with ϕ_0. The parameter γ is scaled out – c^2/γ^4 is given as a function of κ/γ.

There are several pertinent observations:

(1) Regions of instability ($c^2 < 0$) exist for both even and odd modes. As m increases, the maximum growth rate $|c|_{max}$ decreases for both even and odd modes (approaching 0 as m approaches 1 in the even case). The wavenumber, κ_{max}, of the most unstable mode increases with m for even modes, and decreases as m increases for odd modes. For both even and odd modes, the cutoff wavenumber, κ_{high}, beyond which there is no instability, decreases as m increases. For even modes, there is a low cutoff, κ_{low}, which increases with m.

(2) Only the lowest few eigenvalues are shown in Figures 3.1 and 3.2. For $0 \leq m < 1$, there are infinitely many larger eigenvalues.

(3) The given curves relate the dimensionless quantities c^2/γ^4 and κ/γ. To convert to the corresponding physical quantities, $\tilde{c}^2$ and $\tilde{\kappa}$, the following formulae are appropriate:

$$\tilde{c}^2 = \omega_0^2 c^2, \quad \tilde{\kappa}/k_0 = 2\kappa, \quad \gamma = \frac{1}{2} k_0 a_0 (2 - m^2)^{1/2}. \tag{3.27}$$

3.3 The Limit m = 0

When $m = 0$, ϕ_0 is a constant. Thus we are looking at the effect of perturbing the uniform wave. This case is less constrained than the case $0 < m < 1$, because the period of ϕ_0 is indefinite. The operators L_0 and L_1 reduce to

$$L_0 = -\frac{1}{2} d^2/dX^2, \quad L_1 = -\frac{1}{2} d^2/dX^2 - 2\gamma^2. \tag{3.28}$$

Thus the eigenvalue problem reduces to the solution of an ODE with constant coefficients. Solving it yields

$$c^2 = r(r - 2\gamma^2), \tag{3.29}$$

where

$$r = \frac{1}{2} K^2 + \frac{1}{2} \alpha \kappa^2 \tag{3.30}$$

and K represents the (dimensionless) component of the perturbation wavenumber in the direction of propagation of the carrier wave. Thus we have instability for

$$0 < r < 2\gamma^2 \tag{3.31}$$

with maximum stability at

$$r = \gamma^2. \tag{3.32}$$

It is easy to verify that this analysis is in agreement with the numerical results of the preceding section. Note that the results are independent of parity when m = 0.

Translating (3.31) and (3.32) into the physical variables $\tilde{K}$ and $\tilde{\kappa}$ via the formulae

$$\tilde{K} = 2k_0 K \tag{3.33}$$

and (3.27), and specializing to water waves by taking $\alpha = -2$, we find that we have instability when

$$0 < (\tilde{K}/2k_0)^2 - 2(\tilde{\kappa}/2k_0)^2 < 2k_0^2 a_0^2 \tag{3.34}$$

with maximum instability at

$$(\tilde{K}/2k_0)^2 - 2(\tilde{\kappa}/2k_0)^2 = k_0^2 a_0^2. \tag{3.35}$$

This is the two-dimensional version of the Benjamin-Feir [2] instability criterion. The form of the one-dimensional Benjamin-Feir criterion is preserved, but the parameter of interest is now

$$(\tilde{K}/2k_o)^2 - 2(\tilde{\kappa}/2k_o)^2$$

rather than

$$(\tilde{K}/2k_o)^2.$$

An obvious corollary of this result is that for any $\tilde{K}$, $\tilde{\kappa}$ can be chosen to achieve instability. Moreover, if $\tilde{K}/2k_o \geq k_o a_o$, then $\tilde{\kappa}$ can be chosen to achieve maximum instability.

3.4 The Limit m = 1

As noted previously, ϕ_o assumes the soliton form given in (3.12) when m = 1. Saffman and Yuen [14] have studied the stability of a plane soliton to infinitesimal two-dimensional perturbations with arbitrary κ. They employed numerical techniques analogous to those described above, but involving decaying rather than periodic boundary conditions.

To summarize their results for the soliton, the value for the maximum growth rate $|c|_{max}$ is found to be

$$|c|_{max} \doteq 0.63\gamma^2 = 0.16k_o^2a_o^2 = |\tilde{c}|_{max}/\omega_o. \tag{3.36}$$

The most unstable mode is achieved at a wavenumber κ_{max} given by

$$\kappa_{max}^2 \doteq 0.65\gamma^2 \tag{3.37}$$

which, when applied to wave waves, becomes

$$\tilde{\kappa}_{max}/k_o = 0.806k_o a_o, \tag{3.38}$$

where $\tilde{\kappa}_{max}$ is the most unstable wavenumber measured in the physical coordinate y. The cutoff wavenumber, beyond which there is no instability, is found to be

$$\kappa^2_{\text{cutoff}} \doteq 1.18\gamma^2 \tag{3.39}$$

corresponding to a cutoff for water waves given by

$$\tilde{\kappa}_{\text{cutoff}}/k_o = 1.09 k_o a_o. \tag{3.40}$$

The traces labelled m = 1 in Figures 3.1 and 3.2 represent the data of Saffman and Yuen [14]. It is clear from these graphs that in the case of odd modes, the periodic results approach the soliton results as m approaches 1. In the case of even modes, the stable portions of the periodic curves passing through the origin approach the soliton curve as m approaches 1. The unstable portions of the periodic curves gradually disappear as m approaches 1, in accordance with the lack of even standing-wave instabilities in the soliton case. (In a subsequent section, we shall see that even traveling-wave instabilities may survive in the soliton case.) The fate as m approaches 1 of the stable portions of the periodic curves containing unstable arcs is uncertain. They appear to lie in the soliton's continuous spectrum region (see Saffman and Yuen [14]), in which no eigenfunctions satisfying decaying boundary conditions can exist. There does not appear to be an analogous region in the periodic case.

3.5 The Limit $\kappa \simeq 0$, $c^2 \simeq 0$

In the soliton case, Zakharov and Rubenchik [24] have obtained results concerning the nature of the spectrum near $c^2 = \kappa^2 = 0$. Ablowitz and Segur [1] extended these results to allow for finite depth and surface tension effects.

The technique devised by Zakharov and Rubenchik can be adapted to the periodic case, but certain formulae must be altered in order to preserve periodicity. In particular, we must find four functions, $\psi^{\pm}$ and $\chi^{\pm}$ (where the superscripts + and - denote even and odd functions, respectively), satisfying

$$L_0 L_1 \psi^{\pm} = 0, \tag{3.41}$$

$$L_1 L_0 \chi^{\pm} = 0. \tag{3.42}$$

We can obtain the solutions ψ^- and χ^+ in the same fashion as Zakharov and Rubenchik:

$$\psi^- = \partial\phi_0/\partial X, \tag{3.43}$$

$$\chi^+ = \phi_0 \tag{3.44}$$

but their solutions for ψ^+ and χ^- must be modified.

In the following, we shall use the notation

$$f' = df/dX$$

for arbitrary f. We must set

$$\psi^+(X) = c_1^+ \psi_1^+(X) + c_2^+ \psi_2^+(X), \tag{3.45}$$

where

$$\psi_1^+(X) = -\partial\phi_0(X)/\partial\gamma^2, \tag{3.46}$$

$$\psi_2^+(X) = \begin{cases} \phi_0'(X) \displaystyle\int_{X_0}^{X} \frac{d\xi}{\phi_0'(\xi)^2} & \text{for } X \in [0, F/\beta], \\ \phi_0'(X) \displaystyle\int_{-X_0}^{X} \frac{d\xi}{\phi_0'(\xi)^2} & \text{for } X \in [-F/\beta, 0], \end{cases} \tag{3.47}$$

$$c_1^+ = \psi_2^{+'}(F/\beta), \qquad c_2^+ = -\psi_1^{+'}(F/\beta) \tag{3.48}$$

and X_0 on $(0,F/\beta)$ must be chosen so that

$$\psi_2^{+'}(0^-) = \psi_2^{+'}(0^+). \tag{3.49}$$

Numerics were employed for the actual computations. The untidy form of ψ_2^+ is due to the fact that ϕ_0' vanishes at 0 and $\pm F/\beta$. It is, however, easily verified that ψ_2^+ is C^∞, provided that X_0 is properly chosen. The choice of c_1^+ and c_2^+ guarantees that

$$\psi^{+'}(\pm F/\beta) = 0 \tag{3.50}$$

and it follows from

$$L_1\psi_1^+ = \phi_0, \quad L_1\psi_2^+ = 0 \tag{3.51}$$

that

$$\psi^{+'''}(\pm F/\beta) = 0. \tag{3.52}$$

Thus ψ^+ is an acceptable even eigenfunction for the eigenvalue $c^2 = 0$ when $\kappa^2 = 0$.

Likewise we must set

$$\chi^-(X) = c_1^-\chi_1^-(X) + c_2^-\chi_2^-(X) \tag{3.53}$$

where

$$\chi_1^-(X) = -X\phi_0(X) \tag{3.54}$$

$$\chi_2^-(X) = \phi_0(X)\int_0^X \frac{d\xi}{\phi_0(\xi)^2} \tag{3.55}$$

$$c_1^- = \chi_2^-(F/\beta), \qquad c_2^- = -\chi_1^-(F/\beta). \tag{3.56}$$

The definition of χ_2^- is simplified by the fact that ϕ_0 never vanishes. The choice of c_1^- and c_2^- guarantees that

$$\chi^-(\pm F/\beta) = 0, \tag{3.57}$$

$$L_0\chi_1^- = \partial\phi_0/\partial X, \qquad L_0\chi_2^- = 0 \tag{3.58}$$

that

$$\chi^{-''}(\pm F/\beta) = 0, \tag{3.59}$$

and that χ^- is periodic as required.

With these definitions of $\psi^\pm$ and $\chi^\pm$, the analysis of Zakharov and Rubenchik [24] goes through, and the form of their result is unchanged:

$$(c^\pm)^2 = \frac{\alpha}{2}\kappa^2 \frac{\langle \chi^\pm, (L_0 + L_1)\psi^\pm \rangle}{\langle \chi^\pm, \psi^\pm \rangle} + O(\kappa^4). \tag{3.60}$$

where the inner product is defined by

$$\langle f, g \rangle = \int_{-F/\beta}^{F/\beta} f^* g \, dx. \tag{3.61}$$

For very small κ^2, this result was found to agree with the numerical results presented earlier.

3.6 Traveling Instabilities

The stability results for even modes, as depicted in Figure 3.1, are rather striking. For $0 < m < 1$, the stability curves consist of two disjoint segments. For each such m, there is an interval of the κ/γ

axis on which no real eigenvalues can be found. These intervals are clearly promising places to look for complex eigenvalues, corresponding to traveling instabilities. The numerical technique involving the additional equation (3.24) and an additional boundary condition, (3.25) or (3.26), was used to search for such eigenvalues, and the results are plotted in Figures 3.3 and 3.4. Figure 3.3 shows Re c/γ^2 vs. κ/γ, and Figure 3.4 shows Im c/γ^2 vs. κ/γ. The correspondence of Figures 3.3 and 3.4 to Figure 3.1 is easily established by inspection, and the gaps in Figure 3.1 are clearly filled by the complex eigenvalues.

Extrapolation from the curves plotted in Figure 3.4 to the case $m = 1$ suggests that traveling instabilities may also exist in the soliton case. This conclusion cannot be reached with certainty on the basis of the data shown, for the maximum instability at $m = 0.98$ is slightly less than the maximum instability at $m = 0.9$. However, the conjecture is not unreasonable. In the case of the soliton, as in the periodic case, a point is reached as κ increases from 0 at which no real solutions exist. Complex solutions spring from this point in the periodic case, and the soliton case is presumably analogous. This raises the interesting question (not yet answered) of how the complex solution plot can merge into the continuous spectrum associated with the soliton case.

Note that the long-wave analysis of Zakharov and Rubenchik [24] and Ablowitz and Segur [1], which would permit traveling instabilities, revealed none because none exist for small κ. On the other hand, the numerical results of Saffman and Yuen [14] are limited to standing-wave instabilities (as the authors themselves point out).

3.7 Numerical Verification

In order to test the predictions of the stability curves of Figures 3.1-3.4, various runs were made with a code which solves the two-space-dimensional nonlinear Schrödinger equation. The results are presented in terms of the original physical variables which are related to our dimensionless variables by (3.5).

It follows from (3.14) that for unstable cases we expect the perturbation

$$B_1 = k_0 A_1/\sqrt{2} \tag{3.62}$$

(where B_1 is dimensionless and A_1 is dimensional) to grow like $e^{|\Omega T|} = e^{|\omega_0 \Omega t|}$. In stable cases ($\Omega = 0$), note that $|B_1|$ depends upon X and $\kappa Y + \Lambda T$, and thus $|A_1|$ depends upon x and $2\kappa k_0 y - \omega_0 \Lambda t$. Thus we expect $|A_1|$ to move parallel to the y-axis with speed

$$v_y = \omega_0 \Lambda/(2\kappa k_0). \tag{3.63}$$

When both Ω and Λ are non-zero, we expect both growth and movement. Some representative cases are described in the following.

Case 1: $\omega_0 = 100$, $k_0 a_0 = 0.1$, $m = 0.9$, $\kappa/\gamma = 0.7$, perturbation initially even in $x_g = x - \omega_0 t/2k_0$, initial amplitude of A_1 is 5% of the initial amplitude of A_0 ($= \sqrt{2} B_0/k_0$). According to Figure 3.1, A_0 should be stable to this perturbation. The eigenvalue is given by

$$\Lambda^2/\gamma^4 \simeq 0.1166, \qquad \gamma = \frac{1}{2} k_0 a_0 \sqrt{2 - m^2} \simeq 5.454 \times 10^{-2}. \tag{3.64}$$

Thus the predicted speed is 0.001304. In Figure 3.5, $|A_1|/a_0$ is plotted in the group velocity frame at t = 0,2,4,$\cdots$,10. It is easily verified

that the profile has moved about five grid divisions in the positive y-direction between t = 0 and t = 10 (the position of the trench between the two humps can be identified with fair precision). There are 32 grid divisions in the y interval [0, 0.07903], and thus the predicted shift is

$$\left(\frac{0.01304}{0.07903}\right) \cdot 32 \doteq 5.3 \text{ grid divisions.} \tag{3.65}$$

Case 2: Same conditions as Case 1, except that the perturbation is initially odd in x_g. According to Figure 3.2, one should see an instability with

$$|\Omega|^2/\gamma^4 = 0.6405 \tag{3.66}$$

and thus

$$|\omega_o \Omega| = 0.2381. \tag{3.67}$$

Observed amplitudes (computed by taking the square root of the mean of the squares of the amplitudes at each point) were plotted on semilog paper, and growth was found to be exponential through t = 9 with the predicted growth rate. By t = 10, the growth rate had decreased slightly (indicating departure from the realm of linear analysis).

Figure 3.6 depicts $|A_1|/a_o$ for this case in the group velocity frame at t = 0,2,4,•••,10.

Case 3:

$$\omega_o = 100, \qquad k_o a_o = 0.1, \qquad m = 0, \qquad \left(\frac{\tilde{K}}{2k_o}\right)^2 = 2(k_o a_o)^2,$$

$$\left(\frac{\tilde{K}}{2k_o}\right)^2 - 2\left(\frac{\tilde{\kappa}}{2k_o}\right)^2 = (k_o a_o)^2, \tag{3.68}$$

initially the amplitude of A_1 is 5% of the amplitude of A_0. It follows from (3.34) and (3.35) that the x-component of the perturbation, taken alone, would yield neutral stability, but the inclusion of the y-component leads to maximum instability. Thus, from our analysis of the case $m = 0$,

$$|\Omega| = \gamma^2 = \frac{1}{2}(k_o a_o)^2 \tag{3.69}$$

and $|A_1|$ should therefore grow initially like $e^{t/2}$. A semilog plot of the root-mean-square amplitude of A_1 for the time interval $t = 0$-10 indicates that growth is exponential at least through $t = 6$ before it begins to level off. (The leveling is due to the fact that the instability has attained a significant magnitude, and thus removed itself from the realm in which our linear analysis is applicable.) Thus at $t = 5$, we expect an increase by a factor of

$$e^{2.5} = 12.18 \tag{3.70}$$

over the value at $t = 0$. This is in agreement with the observed growth factor.

Case 4: $\omega_o = 100$, $k_o a_o = 0.1$, $m = 0.98$, $\kappa/\gamma = 0.5$, perturbation initially even in $x_g = x - \omega_o t/2k_o$, initial amplitude of A_1 is 5% of the initial amplitude of A_0. According to Figures 3.3 and 3.4, we should see a traveling instability with

$$\Omega/\gamma^2 = 0.350, \qquad \Lambda/\gamma^2 = 0.826. \tag{3.71}$$

These values yield a predicted growth rate of $e^{0.09085t}$ and a predicted speed of about 1.1 grid units/time units. Both these predictions are

in agreement with observed values. A semilog plot of the average perturbation amplitude indicates that growth is exponential through t = 20, and Figure 3.7 illustrates the development in time of the perturbation amplitude.

CHAPTER 4

BIFURCATIONS OF STOKES WAVES ON A TWO-DIMENSIONAL SURFACE

Weakly-nonlinear, deep-water gravity waves can be described by the nonlinear Schrödinger equation:

$$i\left\{\frac{\partial A}{\partial t} + \frac{\omega_o}{2k_o}\frac{\partial A}{\partial x}\right\} - \frac{\omega_o}{8k_o^2}\frac{\partial^2 A}{\partial x^2} + \frac{\omega_o}{4k_o^2}\frac{\partial^2 A}{\partial y^2} = \frac{1}{2}\omega_o k_o^2 |A|^2 A, \tag{4.1}$$

where A varies slowly in x, y, and t, and the surface displacement is given by

$$\eta = \mathrm{Re}\left[Ae^{i(k_o x - \omega_o t)} + \frac{1}{2}k_o A^2 e^{i(2k_o x - 2\omega_o t)}\right] + O(A^3). \tag{4.2}$$

Equation (4.1) is known to have solutions of permanent form. One such is the uniform solution

$$\left.\begin{aligned} A &= a_o e^{-iw_o t} \\ a_o &= \text{constant} \\ w_o &= \frac{1}{2}\omega_o k_o^2 |a_o|^2 \end{aligned}\right\} \tag{4.3}$$

which represents a Stokes wave (including only the lowest order nonlinear term of the frequency correction). Another example is the dnoidal solution

$$\left.\begin{aligned} A &= a_o \mathrm{dn}\left[\sqrt{2}\, k_o^2 a_o\left(x - \frac{\omega_o}{2k_o}t\right), m\right] e^{-iw_o t} \\ 0 &< m < 1 \\ a_o &= \text{constant} \\ w_o &= \left(\frac{2 - m^2}{4}\right)\omega_o k_o^2 |a_o|^2 \end{aligned}\right\} \tag{4.4}$$

As $m \to 0$, solution (4.4) approaches solution (4.3). As $m \to 1$, solution (4.4) approaches the soliton solution

$$\left.\begin{aligned} A &= a_o \operatorname{sech}\left[\sqrt{2}\, k_o^2 a_o\left(x - \frac{\omega_o}{2k_o}\, t\right)\right] e^{-iw_o t} \\ a_o &= \text{constant} \\ w_o &= \frac{1}{4}\, \omega_o k_o^2 |a_o|^2 \end{aligned}\right\} \tag{4.5}$$

The solutions (4.3, (4.4), and (4.5) all represent envelopes of permanent form, but only (4.3) yields an η of permanent form [where η is given by (4.2)]. For (4.4) and (4.5), the wave envelope travels at the group speed $\omega_o/2k_o$ while the individual waves travel at the phase speed $(\omega_o + w_o)/k_o$. It is easily verified that these two speeds cannot be equal, and hence the waves of (4.4) and (4.5) modulate rather than maintain their form.

A generalization of the uniform solution of the form

$$\left.\begin{aligned} A &= a\, e^{-iwt} \\ a &= a(x - ct, y) \end{aligned}\right\} \tag{4.6}$$

and be sought, where a is complex, and

$$c = \frac{\omega_o + w}{k_o}\,. \tag{4.7}$$

The form of η will be preserved under these assumptions — to arbitrary order, for the $O(A^n)$ term of η is proportional to

$$\operatorname{Re}\left[a_n e^{ink_o(x-ct)}\right] \tag{4.8}$$

where a_n is a polynomial in a and a*. Hence the $O(A^n)$ term depends on time only through x - ct, and will be steady in a frame of reference moving with velocity (c,0).

One may expand a about the uniform solution as follows:

$$a = \sum_{m,n=-\infty}^{\infty} a_{mn} E_+^m E_-^n \tag{4.9}$$

where

$$E_\pm = e^{ik_x(x-ct)} e^{\pm ik_y y} \tag{4.10}$$

and k_x, k_y, and the a_{mn} are independent of space and time. In order to ensure that A varies slowly with x and y, it is required that

$$|k_x|, |k_y| \ll k_o. \tag{4.11}$$

This expansion allows one to consider a general perturbation involving waves of a given wavelength at a given angle to the carrier wave vector. Next, the a_{mn}, w, and c are expanded in powers of $\varepsilon \ll 1$:

$$\left.\begin{aligned} a_{mn} &= \sum_{j=0}^{\infty} a_{mn}^{(j)} \varepsilon^j \\ w &= \sum_{j=0}^{\infty} w_j \varepsilon^j \\ c &= \sum_{j=0}^{\infty} c_j \varepsilon^j \end{aligned}\right\} \tag{4.12}$$

To ensure that the solution at order 0 corresponds to the uniform solution, the following values are prescribed:

$$\left.\begin{aligned} a_{00}^{(0)} &= \text{real constant} \\ w_o &= \tfrac{1}{2}\,\omega_o k_o^2 |a_{00}^{(0)}|^2 \\ a_{mn}^{(0)} &= 0 \text{ for } |m| + |n| > 0 \end{aligned}\right\} \tag{4.13}$$

Note that $a_{00}^{(0)}$ can be assumed to be real without loss of generality due to the form of (4.1).

The uniform solution is perturbed with the E_+, E_+^{-1}, E_-, and E_-^{-1} terms at $O(\varepsilon)$. That is,

$$a_{mn}^{(1)} = 0 \text{ for } |m| + |n| > 1. \tag{4.14}$$

Substituting into (4.1) and retaining terms of order ε yields

$$w_1 a_{00}^{(0)} = w_o \cdot \left[a_{00}^{(1)} + a_{00}^{(1)*}\right] \tag{4.15}$$

for the constant terms, and

$$M_1 \begin{pmatrix} a_{10}^{(1)} \\ a_{-10}^{(1)*} \end{pmatrix} = 0 \tag{4.16}$$

$$M_1 \begin{pmatrix} a_{01}^{(1)} \\ a_{0,-1}^{(1)*} \end{pmatrix} = 0 \tag{4.17}$$

for the E_+, E_+^{-1}, E_-, and E_-^{-1} terms, where

$$M_1 = \begin{pmatrix} \frac{k_x c_o}{\omega_o} - \frac{k_x}{2k_o} + u - \frac{1}{2} k_o^2 a_{00}(0)^2 & -\frac{1}{2} k_o^2 a_{00}(0)^2 \\ -\frac{1}{2} k_o^2 a_{00}(0)^2 & -\frac{k_x c_o}{\omega_o} + \frac{k_x}{2k_o} + u - \frac{1}{2} k_o^2 a_{00}(0)^2 \end{pmatrix} \tag{4.18}$$

and

$$u = \frac{1}{2}\left(\frac{k_x}{2k_o}\right)^2 - \left(\frac{k_y}{2k_o}\right)^2 . \tag{4.19}$$

Thus it is required that det $M_1 = 0$, where

$$\det M_1 = \left(u - \frac{1}{2} k_o^2 a_{00}(0)^2\right)^2 - \left(\frac{k_x c_o}{\omega_o} - \frac{k_x}{2k_o}\right)^2 - \frac{1}{4} k_o^4 a_{00}(0)^4 . \tag{4.20}$$

Therefore,

$$\left(\frac{k_x c_o}{\omega_o} - \frac{k_x}{2k_o}\right)^2 = u^2 - k_o^2 a_{00}(0)^2 u. \tag{4.21}$$

If (4.21) is satisfied and $k_o a_{00}^{(0)} \neq 0$, then (4.16) and (4.17) can be satisfied by setting

$$\frac{a_{-10}^{(1)*}}{a_{10}^{(1)}} = \frac{a_{0,-1}^{(1)*}}{a_{01}^{(1)}} = r = \left(\frac{k_x c_o}{\omega_o} - \frac{k_x}{2k_o} + u - \frac{1}{2} k_o^2 a_{00}(0)^2\right) \Big/ \left(\frac{1}{2} k_o^2 a_{00}(0)^2\right) \tag{4.22}$$

where $a_{10}^{(1)}$ and $a_{01}^{(1)}$ are free parameters (at this order — at higher order it will be found that they must have the same magnitude). It was assumed that $k_o a_{00}^{(0)} \neq 0$, for the expansion employed is not really appropriate when $k_o a_{00}^{(0)} = 0$. Bifurcations from Stokes waves are sought, not bifurcations from a surface at rest.

Equation (4.16) is clearly satisfied if

$$a_{10}^{(1)} = 0 = a_{-10}^{(1)} \tag{4.23}$$

and likewise, equation (4.17) is satisfied if

$$a_{01}^{(1)} = 0 = a_{0,-1}^{(1)}. \tag{4.24}$$

Equations (4.9) and (4.10), which specify the form of the solution being sought, show that if the first of these conditions holds, then the wave will appear to propagate in the $(k_x,-k_y)$ direction. Likewise, if the second condition holds, the wave will appear to propagate in the (k_x,k_y) direction.

On the other hand, the condition

$$a_{10}^{(1)} = a_{01}^{(1)},\ a_{-10}^{(1)} = a_{0,-1}^{(1)} \tag{4.25}$$

yields a symmetric, "standing wave" pattern — the eye would perceive motion in the $(k_x,0)$ direction.

It follows from the steady surface condition (4.7) that

$$c_o = \frac{\omega_o + w_o}{k_o}. \tag{4.26}$$

Equations (4.13), (4.21), and (4.26) can be combined to eliminate w_o and c_o, yielding

$$\left(\frac{k_x}{2k_o}\right)^2 \left(k_o a_{00}^{(0)}\right)^4 + \left[\frac{5}{2}\left(\frac{k_x}{2k_o}\right)^2 - \left(\frac{k_y}{2k_o}\right)^2\right]\left(k_o a_{00}^{(0)}\right)^2 + \left[\left(\frac{k_x}{2k_o}\right)^2 - \left[\frac{1}{2}\left(\frac{k_x}{2k_o}\right)^2 - \left(\frac{k_y}{2k_o}\right)^2\right]^2\right] = 0. \tag{4.27}$$

For given k_o, k_x/k_o, and k_y/k_o, this condition gives us the values of $a_{00}^{(0)}$ at which bifurcation may occur — i.e., the amplitude at which Stokes-type solutions may intersect another branch of solutions corresponding to waves of permanent form, with modulations characterized by k_x and k_y. A solution of (4.27) will be denoted by a_c.

It is easily demonstrated that (4.27) admits no positive solutions for $(k_o a_c)^2$ unless $k_x \neq 0 \neq k_y$ (or $k_x = 0 = k_y$, which is clearly a degenerate case). Thus bifurcations from the uniform solution of the nonlinear Schrödinger equation must be two-dimensional and oblique. Specifically, one can show that there are no positive roots of (4.27) unless

$$\tan^2 \theta \geq \frac{1}{2} + \frac{4N^2}{N^2 + 1} \tag{4.28}$$

where

$$\tan \theta = k_y/k_x, \quad N = k_o/k_x. \tag{4.29}$$

When

$$\frac{1}{2} + 2\,|N| > \tan^2 \theta \geq \frac{1}{2} + \frac{4N^2}{N^2 + 1}, \tag{4.30}$$

there are two positive roots of (4.27), while for

$$\tan^2 \theta \geq \frac{1}{2} + 2\,|N| \tag{4.31}$$

there is only one positive root. It is easy to show that the root found when (4.31) holds will satisfy

$$\left[k_o a_{00}^{(0)}\right]^2 \geq 2(|N| - 1). \tag{4.32}$$

Physical consistency requires $|N| \gg 1$ [see (4.11)], and (4.32) will therefore violate the requirement of weak nonlinearity imposed by our use of the nonlinear Schrödinger equation. Thus (4.30) describes the real region of interest.

Figure 4.1 depicts $k_o a_c$ vs. θ for various values of $|N|$. Having obtained a value of $k_o a_c$, one can substitute directly into (4.13) and (4.26) to obtain w_c and c_c.

To verify a candidate bifurcation point (and to move off it), the perturbation solution of (4.1) must be continued. At order ε^2 one needs to allow for non-zero $a_{mn}^{(2)}$ only for $|m| + |n| \leq 2$ in order to balance the forcing terms generated by the $a_{mn}^{(0)}$ and $a_{mn}^{(1)}$. Thus,

$$a_{mn}^{(2)} = 0 \text{ for } |m| + |n| > 2. \tag{4.33}$$

Collecting the constant terms [and exercising (4.15)] then yields

$$w_2 = \omega_o k_o^2 \left[a_c \mathrm{Re}\left[a_{00}^{(2)}\right] + (1 + r + r^2)\left[\left|a_{10}^{(1)}\right|^2 + \left|a_{01}^{(1)}\right|^2\right] + \frac{1}{2}\left|a_{00}^{(1)}\right|^2 \right] \tag{4.34}$$

where

$$r = r(N,\theta) = \left[N + (N - N^2)k_o^2 a_c^2 + \frac{1}{2}\left(\frac{1}{2} - \tan^2\theta\right)\right] \Big/ (N^2 k_o^2 a_c^2) \tag{4.35}$$

[see equation (4.22) for the original definition of r]. The quantity $k_o^2 a_c^2$ is, of course, a function of N and θ due to (4.27) — the variables N and θ are clearly interchangeable with k_x/k_o and k_y/k_o. Collecting the coefficients of the E_+, E_+^{-1}, E_-, and E_-^{-1} terms yields

$$\left.\begin{aligned} M_1 \begin{pmatrix} a_{10}^{(2)} \\ a_{-10}^{(2)*} \end{pmatrix} &= \begin{pmatrix} -5a_{10}^{(1)} - 2a_{-10}^{(1)*} & -a_{10}^{(1)} \\ -5a_{-10}^{(1)*} - 2a_{10}^{(1)} & a_{-10}^{(1)*} \end{pmatrix} \begin{pmatrix} w_1/\omega_o \\ k_x c_1/\omega_o \end{pmatrix} \\ M_1 \begin{pmatrix} a_{01}^{(2)} \\ a_{0,-1}^{(2)*} \end{pmatrix} &= \begin{pmatrix} -5a_{01}^{(1)} - 2a_{0,-1}^{(1)*} & -a_{01}^{(1)} \\ -5a_{0,-1}^{(1)*} - 2a_{01}^{(1)} & a_{0,-1}^{(1)*} \end{pmatrix} \begin{pmatrix} w_1/\omega_o \\ k_x c_1/\omega_o \end{pmatrix} \end{aligned}\right\} . \tag{4.36}$$

It follows from the steady surface condition (4.7) that

$$c_1 = \frac{w_1}{k_o} . \tag{4.37}$$

Equation (4.37), the fact that det M_1 vanishes, and application of the Fredholm alternative to equation (4.36) imply that

$$c_1 = w_1 = 0. \tag{4.38}$$

It follows from (4.15) that

$$\mathrm{Re}\left[a_{00}^{(1)}\right] = 0 \tag{4.39}$$

and one can assume that the imaginary part of $a_{00}^{(1)}$ also vanishes — it is not specified by the equations, and hence can be absorbed without loss of generality by $a_{00}^{(0)}$. Returning to (4.36), which is now known to be homogeneous, note that we can take

$$a_{\pm 1,0}^{(2)} = 0 = a_{0,\pm 1}^{(2)}, \tag{4.40}$$

for any non-zero solutions could be absorbed into the solutions of (4.16) and (4.17), the equations for $a_{\pm 1,0}^{(1)}$ and $a_{0,\pm 1}^{(1)}$.

Collecting the coefficients of the $E_+^m E_-^n$ terms for $|m| + |n| = 2$ yields

$$M_{20}\begin{pmatrix} a_{20}^{(2)} \\ a_{-20}^{(2)*} \end{pmatrix} = k_o^2 a_c \begin{pmatrix} a_{10}^{(1)} a_{-10}^{(1)*} + \frac{1}{2} a_{-10}^{(1)2} \\ a_{10}^{(1)} a_{-10}^{(1)*} + \frac{1}{2} a_{-10}^{(1)*2} \end{pmatrix} \tag{4.41}$$

$$M_{02}\begin{pmatrix} a_{02}^{(2)} \\ a_{0,-2}^{(2)*} \end{pmatrix} = k_o^2 a_c \begin{pmatrix} a_{01}^{(1)} a_{0,-1}^{(1)*} + \frac{1}{2} a_{01}^{(1)2} \\ a_{01}^{(1)} a_{0,-1}^{(1)*} + \frac{1}{2} a_{0,-1}^{(1)*2} \end{pmatrix} \tag{4.42}$$

$$M_{11}\begin{pmatrix} a_{11}^{(2)} \\ a_{-1,-1}^{(2)*} \end{pmatrix} = k_o^2 a_c \begin{pmatrix} a_{10}^{(1)} a_{0,-1}^{(1)*} + a_{-1,0}^{(1)*} a_{01}^{(1)} + a_{10}^{(1)} a_{01}^{(1)} \\ a_{10}^{(1)} a_{0,-1}^{(1)*} + a_{-10}^{(1)*} a_{01}^{(1)} + a_{-10}^{(1)*} a_{0,-1}^{(1)*} \end{pmatrix} \tag{4.43}$$

$$M_{1,-1}\begin{pmatrix} a_{1,-1}^{(2)} \\ a_{-1,1}^{(2)*} \end{pmatrix} = k_o^2 a_c \begin{pmatrix} a_{10}^{(1)} a_{01}^{(1)*} + a_{-10}^{(1)*} a_{0,-1}^{(1)} + a_{10}^{(1)} a_{0,-1}^{(1)} \\ a_{10}^{(1)} a_{01}^{(1)*} + a_{-10}^{(1)*} a_{0,-1}^{(1)} + a_{-10}^{(1)*} a_{01}^{(1)*} \end{pmatrix} \tag{4.44}$$

where

$$M_{20} = M_{02} = \begin{pmatrix} \frac{2k_x c_o}{\omega_o} - \frac{k_x}{k_o} + 4u - \frac{1}{2} k_o^2 a_c^2 & -\frac{1}{2} k_o^2 a_c^2 \\ -\frac{1}{2} k_o^2 a_c^2 & -\frac{2k_x c_o}{\omega_o} + \frac{k_x}{k_o} + 4u - \frac{1}{2} k_o^2 a_c^2 \end{pmatrix} \tag{4.45}$$

$$M_{11} = \begin{pmatrix} \frac{2k_x c_o}{\omega_o} - \frac{k_x}{k_o} + 2\left(\frac{k_x}{2k_o}\right)^2 - \frac{1}{2} k_o^2 a_c^2 & -\frac{1}{2} k_o^2 a_c^2 \\ -\frac{1}{2} k_o^2 a_c^2 & -\frac{2k_x c_o}{\omega_o} + \frac{k_x}{k_o} + 2\left(\frac{k_x}{2k_o}\right)^2 - \frac{1}{2} k_o^2 a_{00}^{(0)2} \end{pmatrix} \tag{4.46}$$

$$M_{1,-1} = \begin{pmatrix} -\frac{k_y^2}{k_o^2} - \frac{1}{2}k_o^2a_c^2 & -\frac{1}{2}k_o^2a_c^2 \\ -\frac{1}{2}k_o^2a_c^2 & -\frac{k_y^2}{k_o^2} - \frac{1}{2}k_o^2a_c^2 \end{pmatrix} \tag{4.47}$$

It follows from (4.45) and (4.21) (the requirement that det M_1 vanish) that

$$\det M_{20} = \det M_{02} = 12u^2. \tag{4.48}$$

Equation (4.27) has no positive solutions when $u = 0$ (except in the degenerate case $k_x = 0 = k_y$). Thus $u \neq 0$, M_{20} and M_{02} are nonsingular, and the equations (4.41) and (4.42) can be solved.

Inspection of (4.43) reveals that it is satisfied by

$$a_{11}^{(2)} = 0 = a_{-1,-1}^{(2)} \tag{4.49}$$

if

$$a_{10}^{(1)} = 0 = a_{-10}^{(1)} \tag{4.50}$$

or

$$a_{01}^{(1)} = 0 = a_{0,-1}^{(1)}. \tag{4.51}$$

If neither of these conditions is satisfied, a solution still exists, for it follows from (4.21) (the vanishing of det M_1) and (4.28) (the condition ensuring that the bifurcation equation has positive roots) that det M_{11} does not vanish.

Inspection of (4.44) reveals that it is satisfied by

$$a_{1,-1}^{(2)} = 0 = a_{-1,1}^{(2)} \tag{4.52}$$

if

$$a_{10}^{(1)} = 0 = a_{0,-1}^{(1)} \tag{4.53}$$

or

$$a_{01}^{(1)} = 0 = a_{0,-1}^{(1)}. \tag{4.54}$$

If neither of these conditions is satisfied, there is still solution, for $\det M_{1,-1}$ vanishes if and only if $k_y/k_o = 0$. However, equation (4.27) has no positive solutions when $k_y/k_o = 0$ (except in the degenerate case $k_x = 0 = k_y$). Thus $M_{1,-1}$ is nonsingular.

At order ε^2, the steady surface condition (4.7) yields

$$c_2 = \frac{w_2}{k_o}. \tag{4.55}$$

Equations (4.34) and (4.55) will yield values for w_2 and c_2 given a value for $a_{00}^{(2)}$. In order to determine $a_{00}^{(2)}$ in terms of the parameters $a_{10}^{(1)}$ and $a_{01}^{(1)}$, one must consider (4.1) at third order in the E_+, E_+^{-1}, E_-, and E_-^{-1} terms. This yields

$$\left.\begin{aligned} M_2 \begin{pmatrix} a_{10}^{(1)} \\ a_{-10}^{(1)*} \end{pmatrix} + M_1 \begin{pmatrix} a_{10}^{(3)} \\ a_{-10}^{(3)*} \end{pmatrix} &= \begin{pmatrix} f_{10}^{(3)} \\ g_{10}^{(3)} \end{pmatrix} \\ M_2 \begin{pmatrix} a_{01}^{(1)} \\ a_{0,-1}^{(1)*} \end{pmatrix} + M_1 \begin{pmatrix} a_{01}^{(3)} \\ a_{0,-1}^{(3)*} \end{pmatrix} &= \begin{pmatrix} f_{01}^{(3)} \\ g_{01}^{(3)} \end{pmatrix} \end{aligned}\right\} \tag{4.56}$$

where

$$M_2 = \begin{pmatrix} \frac{k_x c_2}{\omega_o} - k_o^2 a_c a_{00}^{(2)} & - k_o^2 a_c a_{00}^{(2)} \\ - k_o^2 a_c a_{00}^{(2)} & - \frac{k_x c_2}{\omega_o} - k_o^2 a_c a_{00}^{(2)} \end{pmatrix} \tag{4.57a}$$

$$f_{10}^{(3)}/a_{10}^{(1)} = \left[- \frac{k_o^2}{2} (1 + 2r) + k_o^2 a_c (r\hat{a}_{20}^{(2)} + \hat{a}_{20}^{(2)} + r^3 \hat{a}_{-20}^{(2)*}) \right] \left| a_{10}^{(1)} \right|^2$$
$$+ \left[k_o^2 (r^2 - r) + k_o^2 a_c \left((r^2 + r)\hat{a}_{1,-1}^{(2)} + (r + 1)\hat{a}_{11}^{(2)} \right.\right.$$
$$\left.\left. + r\hat{a}_{-1,1}^{(2)} + r^3 \hat{a}_{-1,-1}^{(2)*} \right) \right] \left| a_{01}^{(1)} \right|^2 \tag{4.57b}$$

$$g_{10}^{(3)*}/a_{10}^{(1)*} = \left[k_o^2 \left(- \frac{1}{2} r^3 - r^2 \right) + k_o^2 a_c \left(r^2 \hat{a}_{-20}^{(2)} + r^3 \hat{a}_{-20}^{(2)} + \hat{a}_{20}^{(2)*} \right) \right] \left| a_{10}^{(1)} \right|^2$$
$$+ \left[k_o^2 (- r^2 + r) + k_o^2 a_c \left((r^3 + r^2)\hat{a}_{-1,-1}^{(2)} + (r^2 + r)\hat{a}_{-1,1}^{(2)} \right.\right.$$
$$\left.\left. + \hat{a}_{11}^{(2)*} + r^2 \hat{a}_{1,-1}^{(2)*} \right) \right] \left| a_{01}^{(1)} \right|^2 \tag{4.57c}$$

and $f_{01}^{(3)}$ and $g_{01}^{(3)}$ are given by analogous expressions with the subscripts transposed. The notation $\hat{a}_{mn}$ is defined by

$$a_{mn}^{(2)} = \hat{a}_{mn}^{(2)} a_{\text{sgn } m,o}^{(1)|m|} a_{o,\text{sign } n}^{(1)|n|} \tag{4.58}$$

the legitimacy of which follows from (4.41)-(4.47), which determine the $a_{mn}^{(2)}$, and (4.22), which relates $a_{-10}^{(1)}$ to $a_{10}^{(1)}$ and $a_{0,-1}^{(1)}$ to $a_{01}^{(1)}$. It also follows from (4.41)-(4.47) that

$$\hat{a}_{mn}^{(2)} = \hat{a}_{nm}^{(2)}. \tag{4.59}$$

The matrix M_1 is singular, and application of the Fredholm alternative yields

$$\left.\begin{aligned} a_{10}^{(1)} \cdot \left[(1 - r^2)\,\frac{k_x c_2}{\omega_o} - (1 + r)^2 k_o^2 a_c a_{00}^{(2)}\right] &= f_{10}^{(3)} + r g_{10}^{(3)} \\ a_{01}^{(1)} \cdot \left[(1 - r^2)\,\frac{k_x c_2}{\omega_o} - (1 + r)^2 k_o^2 a_c a_{00}^{(2)}\right] &= f_{01}^{(3)} + r g_{01}^{(3)} \end{aligned}\right\} \tag{4.60}$$

If

$$a_{10}^{(1)} = 0 \text{ or } a_{01}^{(1)} = 0 \tag{4.61}$$

then the corresponding equation in (4.60) is automatically satisfied. However, if

$$a_{10}^{(1)} \neq 0 \neq a_{01}^{(1)}, \tag{4.62}$$

then in order to make the two equations in (4.60) consistent, it will in general be necessary to take

$$|a_{10}^{(1)}| = |a_{01}^{(1)}|. \tag{4.63}$$

Any phase difference can be absorbed by shifting the origin along the y-axis. Thus one can say

$$\frac{a_{01}^{(1)}}{a_{10}^{(1)}} = 0, \infty, \text{ or } 1 \tag{4.64}$$

and when (4.60) is satisfied, (4.56) can be solved for

$$\begin{pmatrix} a_{10}^{(3)} \\ a_{-10}^{(3)*} \end{pmatrix} \quad \text{and} \quad \begin{pmatrix} a_{01}^{(3)} \\ a_{0,-1}^{(3)*} \end{pmatrix} . \tag{4.65}$$

There is a one-parameter family of solutions for each of these vectors, but the additional conditions

$$\left.\begin{aligned} \begin{pmatrix} a_{10}^{(3)} \\ a_{-10}^{(3)*} \end{pmatrix} \quad &\text{orthogonal to} \quad \begin{pmatrix} a_{10}^{(1)} \\ a_{-10}^{(1)*} \end{pmatrix} \\ \begin{pmatrix} a_{01}^{(3)} \\ a_{0,-1}^{(3)*} \end{pmatrix} \quad &\text{orthogonal to} \quad \begin{pmatrix} a_{01}^{(1)} \\ a_{0,-1}^{(1)*} \end{pmatrix} \end{aligned}\right\} \tag{4.66}$$

give uniqueness. This is legitimate, for any components proportional to the order ε vectors should be absorbed into the solutions of (4.16) and (4.17), the equations determining those vectors.

Equations (4.60), (4.55), (4.39), (4.34), and (4.22) can be combined to eliminate w_2 and c_2, yielding

$$\begin{aligned} \mathrm{Re}\left[a_{00}^{(2)}\right] &= \frac{\mathrm{Re}\left[\left(f_{10}^{(3)} + r g_{10}^{(3)}\right)/a_{10}^{(1)}\right] - (1-r^2)k_x k_o (1+r+r^2)\left(|a_{10}^{(1)}|^2 + |a_{01}^{(1)}|^2\right)}{(1-r^2)k_x k_o a_c - (1+r)^2 k_o^2 a_c} \\ \mathrm{Im}\left[a_{00}^{(2)}\right] &= -\frac{\mathrm{Im}\left[\left(f_{10}^{(3)} + r g_{10}^{(3)}\right)/a_{10}^{(1)}\right]}{(1+r)^2 k_o^2 a_c} \end{aligned} \tag{4.67}$$

where it was assumed that

$$a_{10}^{(1)} \neq 0. \tag{4.68}$$

In the computations we have performed, $a_{00}^{(2)}$ has been found to be real. There is clearly some danger that the denominator of the expression for $\mathrm{Re}\left[a_{00}^{(2)}\right]$ will vanish. Employing (4.27) (the bifurcation equation), it is found that this will occur when

$$\tan^2 \theta = \frac{1}{2} + \frac{4N^2}{N^2 + 1} \tag{4.69}$$

— that is, when a_c^2 is a double root of (4.27). Thus, unless the numerator also vanishes at this point, there are solutions only for

$$\tan^2 \theta > \frac{1}{2} + \frac{4N^2}{N^2 + 1} \tag{4.70}$$

[by virtue of (4.28)].

Having obtained a value for $a_{00}^{(2)}$, one can substitute into (4.34) and (4.55) to obtain w_2 and c_2. Figures 4.2, 4.3, and 4.4 depict $c/c_{lin} = (c_o + c_2)/(\omega_o/k_o)$ vs. $k_o a_{00}$ for Stokes wave solutions, and bifurcations therefrom corresponding to various values of $|N| = |k_o/k_x|$ and $\theta = \arctan(k_y/k_x)$. In these figures, the minimum and maximum values represented on an axis are indicated near the corresponding axis label. Figure 4.5 depicts the surface displacement for a Stokes wave with $k_o a_{00}^{(0)} = .319$ and a wavelength of 10 m; the surface for a bifurcation from this wave with $N = 5$, $\theta = 70°$, and $a_{10}^{(1)} = .25 = a_{01}^{(1)}$; and a similar bifurcation with $a_{10}^{(1)} = .5$, $a_{01}^{(1)} = 0$.

In summary, a new class of fully two-dimensional, steady solutions for waves on deep water has been found; the free surface is of permanent form with a constant propagation speed. These solutions are found as bifurcations from the uniform Stokes wave train.

Unlike the bifurcation found by Chen and Saffman [3] for one-dimensional waves, these two-dimensional bifurcations occur at small values of wave steepness $k_o a_o$. This permits the use of the two-dimensional nonlinear Schrödinger equation, instead of the exact Euler equations, which greatly simplifies our calculations. The critical value of $k_o a_o$ at which bifurcation can occur, $k_o a_c$, has been computed for various choices of modulation wavelength and angular orientation. Also, second-order corrections to the wave amplitude, modulation, frequency, and speed have been computed, which apply when one moves off the bifurcation point onto the new branch of solutions. The significance of these new-found steady solutions is yet to be determined by analyses of stability and energetics.

CHAPTER 5

THE NONLINEAR SCHRÖDINGER EQUATION AND WAVE/CURRENT INTERACTIONS

In order to account for the effect of a non-uniform current on a wave train, one must obtain correction terms for the nonlinear Schrödinger equation. One approach is to employ the theory of Whitham [17] for the time development of the wavenumber vector $\underline{k}$ and amplitude a in the presence of a surface current $\underline{U}(\underline{x},t)$:

$$\frac{\partial \underline{k}}{\partial t} + \frac{\partial}{\partial \underline{x}} (\omega + \underline{U}\cdot\underline{k}) = 0 \tag{5.1}$$

$$\frac{\partial a^2}{\partial t} + \frac{\partial}{\partial \underline{x}} \cdot \left[\left(\frac{\partial \omega}{\partial \underline{k}} + \underline{U} \right) a^2 \right] + \frac{a^2}{2} \frac{\partial U_1}{\partial x} = 0 \tag{5.2}$$

where ω is the frequency, ω, $\underline{k}$, and a all being slowly-varying functions of the horizontal spatial vector $\underline{x}$ and of the time t. The first equation conserves the wavenumber and the second conserves the wave action to the order considered. These equations must be complemented by the dispersion relation relating ω to $\underline{k}$ and a:

$$\omega(\underline{k},a) = \sqrt{gk} \left(1 + \frac{1}{2} k^2 a^2 \right) \tag{5.3}$$

for weak nonlinearity.

We now consider a wave train with a dominant wave which has carrier wave vector $\underline{k}_0 = (k_0,0)$ and write

$$\underline{k} = \underline{k}_0 + \delta\underline{k} = (k_0,0) + (\delta k_x, \delta k_y) \tag{5.4}$$

$$\omega = \omega_0 + \delta\omega \tag{5.5}$$

where $\omega_o = \omega(\underline{k}_o, 0)$. The functions $\delta\underline{k}$ and $\delta\omega$ vary slowly with $\underline{x}$ and t, and are small compared to $\underline{k}_o$ and ω_o, respectively. Substituting (5.4) and (5.5) into (5.3) and performing a Taylor series expansion about $\underline{k}_o$ yields

$$\omega = \omega_o + \frac{\omega_o}{2k_o}(\delta k_x) - \frac{\omega_o}{8k_o^2}(\delta k_x)^2 + \frac{\omega_o}{4k_o^2}(\delta k_y)^2 + \frac{1}{2}\omega_o k_o^2 a^2 + o(|\delta\underline{k}|^2, a^2) \tag{5.6}$$

The system of equations (5.1), (5.2) and (5.6) governs the time evolution of the wave train.

In order to obtain the nonlinear Schrödinger equation from this formulation, one must add the dispersive terms $\frac{\omega_o}{8k_o^2 a}\frac{\partial^2 a}{\partial x^2}$ and $-\frac{\omega_o}{4k_o^2 a}\frac{\partial^2 a}{\partial y^2}$ to the right-hand side of equation (5.6) (see Yuen and Lake [21]). One then defines the complex wave envelope

$$A = ae^{i\theta} \tag{5.7}$$

where the perturbed phase function θ is defined by

$$\frac{\partial\theta}{\partial\underline{x}} = \delta\underline{k}, \quad \frac{\partial\theta}{\partial t} = -\delta\omega \tag{5.8}$$

and the system reduces to a single equation for A:

$$i\left(\frac{\partial A}{\partial t} + \frac{\omega_o}{2k_o}\frac{\partial A}{\partial x}\right) - \frac{\omega_o}{8k_o^2}\frac{\partial^2 A}{\partial x^2} + \frac{\omega_o}{4k_o^2}\frac{\partial^2 A}{\partial y^2} - \frac{1}{2}\omega_o k_o^2 |A|^2 A +$$

$$+ i\underline{U}\cdot\frac{\partial A}{\partial\underline{x}} + i\left[(i\underline{k}_o\cdot\underline{U}) + \left(\frac{3}{4}\frac{\partial}{\partial x}, \frac{1}{2}\frac{\partial}{\partial y}\right)\cdot\underline{U}\right]A = 0. \tag{5.9}$$

In Appendix A, equation (5.9) is derived using a perturbation technique. The perturbation approach is considerably more tedious, but does yield some additional information. In particular, it is found that

the surface displacement and velocity potential are given by

$$\eta(x,y,t) = \eta_0 + \mathrm{Re}\left[A e^{i(\underline{k}_0 \cdot \underline{x} - \omega_0 t)} + \frac{1}{2} k_0 A^2 e^{i(2\underline{k}_0 \cdot \underline{x} - 2\omega_0 t)}\right] + O(A^3) \quad (5.10)$$

$$\phi(x,y,z,t) = \phi_0 + \mathrm{Re}\left[B e^{i(\underline{k}_0 \cdot \underline{x} - \omega_0 t)} \; e^{k_0 z}\right] + O(A^3) \quad (5.11)$$

where η_0 represents mean displacement, ϕ_0 represents mean flow, and the following relations hold:

$$\underline{U} = \left.\frac{\partial \phi_0}{\partial \underline{x}}\right|_{z=0} \quad (5.12)$$

$$\eta_0 = -\frac{1}{g}\left[\frac{\partial \phi_0}{\partial t} + \frac{1}{2}\,\underline{U}\cdot\underline{U}\right] \quad (5.13)$$

$$\left.\frac{\partial \phi_0}{\partial z}\right|_{z=0} = \frac{\partial \eta_0}{\partial t} + \underline{U}\cdot\frac{\partial \eta_0}{\partial \underline{x}} + \left(\frac{\partial}{\partial \underline{x}}\cdot\underline{U}\right)\eta_0 + \frac{\omega_0}{2k_0}\,\underline{k}_0 \cdot \frac{\partial |A|^2}{\partial \underline{x}} + \begin{matrix}\text{higher}\\ \text{order}\\ \text{terms}\end{matrix} \quad (5.14)$$

$$B\big|_{z=0} = -\frac{i\omega_0}{k_0} A + \frac{\omega_0}{2k_0^3}\,\underline{k}_0 \cdot \frac{\partial A}{\partial \underline{x}} + i\omega_0 \eta_0 A + O(A^3) \quad (5.15)$$

$$\frac{\partial B}{\partial z} = -\frac{i}{k_0}\,\underline{k}_0 \cdot \frac{\partial B}{\partial \underline{x}} - \frac{1}{2k_0}\left[\left(\frac{\partial}{\partial \underline{x}} \cdot \frac{\partial}{\partial \underline{x}} B\right) - \left(\frac{1}{k_0}\,\underline{k}_0 \cdot \frac{\partial}{\partial \underline{x}}\right)^2 B\right] + O(A^3). \quad (5.16)$$

Equations (5.12)-(5.14) can be solved with perturbation techniques. One might suspect that the term in equation (5.14) involving $\frac{\partial |A|^2}{\partial \underline{x}}$ would affect ϕ_0, and therefore $\underline{U}$ via equation (5.12), and hence equation (5.9). However, as indicated in Appendix A, equation (5.9) is accurate only to $O(A^4)$, and the effect of the $\frac{\partial |A|^2}{\partial \underline{x}}$ term is negligible at this order.

5.1 Effect of Current on Uniform and Nearly-Uniform Waves

In this subsection, equation (5.9) will be used to study the effect of prescribed currents on waves on a one-dimensional surface. For this case, equation (5.9) reduces to

$$i\left\{\frac{\partial A}{\partial t} + \left(\frac{\omega_o}{2k_o} + U\right)\frac{\partial A}{\partial x} + \left(ik_oU + \frac{3}{4}\frac{\partial U}{\partial x}\right)A\right\} - \frac{\omega_o}{8k_o^2}\frac{\partial^2 A}{\partial x^2} - \frac{1}{2}\omega_o k_o^2|A|^2A = 0. \quad (5.17)$$

A pseudo-spectral method (see Fornberg and Whitham [5]) is used to solve equation (5.17). All figures are scaled against a carrier wavelength of 10 m.

The time development (in the group velocity frame, $\xi = x - c_g t$) of the envelope of an initially uniform wave subjected to a sinusoidal current pattern is depicted in Figure 5.1. Figure 5.2 depicts the time development (in the group velocity frame) of the associated wavenumber shift profile (i.e., the spatial derivative of the phase of A). The slope of the carrier is $k_o a_o = 0.1$, and the group velocity is $c_g = 1.975$ m/sec. The current is given by

$$U = 0.025\, c_g \sin(k_o x/200). \quad (5.18)$$

That is, the current pattern is steady in the bottom-fixed frame.

Clearly, both the amplitude and wavenumber shift profiles assume the sinusoidal form of the current pattern. However, they do not remain stationary with respect to the current pattern. Moreover, their magnitudes grow throughout the time interval of the solution.

The fact that they are not stationary with respect to the current is not really a surprise. For a sufficiently small disturbance, one can

think of the solution as a perturbation of the uniform wave consisting of two components — a forced term at rest with respect to the current pattern, and a homogeneous term traveling at the group velocity. Thus it should be possible to simplify the picture by specifying an initial condition corresponding to the sum of the uniform solution and the forced portion of the perturbation, thereby eliminating the need for a homogeneous term. The following analysis provides the necessary formulae for the forced solution.

Assume that

$$U = \varepsilon u(\varepsilon x) \tag{5.19}$$

where $\varepsilon << 1$. Set

$$A = ae^{i\theta} \tag{5.20}$$

where a and θ are real. Substituting (5.20) into (5.17) yields

$$-\theta_t a - (c_g + U)\theta_x a - k_o U a - \frac{\omega_o}{8k_o^2}(a_{xx} - \theta_x^2 a) - \frac{1}{2}\omega_o k_o^2 a^3 = 0. \tag{5.21}$$

and

$$a_t + (c_g + U)a_x + \frac{3}{4}U_x a - \frac{\omega_o}{8k_o^2}(2\theta_x a_x + \theta_{xx} a) = 0. \tag{5.22}$$

Let

$$\left.\begin{aligned} a &= a_o + a_1 + \cdots \\ \theta &= \theta_o + \theta_1 + \cdots \end{aligned}\right\} \tag{5.23}$$

where

$$\left.\begin{aligned} &a_o \sim O(1),\ \theta_o \sim O(1) \\ &a_n = \varepsilon^n \hat{a}_n(\varepsilon_x) \sim O(\varepsilon^n) \qquad \text{for } n > 0 \\ &\theta_n = \varepsilon^{n-1} \hat{\theta}_n(\varepsilon_x) \sim O(\varepsilon^{n-1}) \qquad \text{for } n > 0 \end{aligned}\right\}. \tag{5.24}$$

Substituting (5.23) into (5.21) and (5.22) and retaining terms of $O(1)$ yields

$$-\theta_{o_t} a_o - c_g \theta_{o_x} a_o - \frac{\omega_o}{8k_o^2}(a_{o_{xx}} - \theta_{o_x}^2 a_o) - \frac{1}{2}\omega_o k_o^2 a_o^3 = 0 \tag{5.25}$$

and

$$a_{o_t} + c_g a_{o_x} - \frac{\omega_o}{8k_o^2}(2\theta_{o_x} a_{o_x} + \theta_{o_{xx}} a_o) = 0. \tag{5.26}$$

The uniform wave

$$a_o = \text{constant} \tag{5.27}$$

$$\theta_o = -\frac{1}{2}\omega_o k_o^2 a_o^2 t \tag{5.28}$$

satisfies these equations as, of course, it must.

With this choice for a_o and θ_o, equation (5.21) at $O(\varepsilon)$ yields

$$-\theta_{o_t} a_1 - \theta_{1_t} a_o - c_g \theta_{1_x} a_o - k_o a_o U - \frac{3}{2}\omega_o k_o^2 a_o^2 a_1 = 0. \tag{5.29}$$

Equation (5.22) has no $O(\varepsilon)$ terms, but at $O(\varepsilon^2)$ yields

$$a_{1_t} + c_g a_{1_x} + \frac{3}{4} a_o U_x - \frac{\omega_o}{8k_o^2} a_o \theta_{1_{xx}} = 0. \tag{5.30}$$

Equations (5.29) and (5.30) can be solved using the fact that, by assumption, a_1 and θ_1 depend only on x [see equation (5.24)]. One finds that

$$a_1 = - a_o \frac{U}{c_g} \cdot \frac{1}{1 + k_o^2 a_o^2/2} \tag{5.31}$$

$$\theta_1' = -(k_o U + \omega_o k_o^2 a_o a_1)/c_g \tag{5.32}$$

assuming $a_o \neq 0$.

Clearly the ratio U/c_g must satisfy

$$U/c_g << 1 \tag{5.33}$$

in order for the perturbation scheme to be consistent. It follows from equation (5.18) that this condition is satisfied for the calculation represented by Figures 5.1 and 5.2.

In Appendix B, it is demonstrated that an analogous perturbation solution for the case $a_o = 0$ is consistent with the results of Longuet-Higgins and Stewart [10, 11] to $O[(U/c_g)^3]$. It is also demonstrated that the perturbation results for $a_o = 0$ correspond to the results of equations (5.31) and (5.32) in the limit $a_o \to 0$. Thus equations (5.31) and (5.32) correspond to known results in the proper limit.

A final analytical exercise of some interest is to relax the assumptions of (5.24) and (5.19) which require slow variation of U, a and θ. One can assume instead that

$$\left.\begin{aligned} U &= \varepsilon u(x) \\ a_o &\sim O(1) \sim \theta_o \\ a_n &= \varepsilon^n \hat{a}_n(x) \sim O(\varepsilon^n) \qquad \text{for } n > 0 \\ \theta_n &= \varepsilon^n \hat{\theta}_n(x) \sim O(\varepsilon^n) \qquad \text{for } n > 0 \end{aligned}\right\}. \tag{5.34}$$

The somewhat surprising result is that (5.29) and (5.30), and hence (5.31) and (5.32) are once again obtained.

Figure 5.3 depicts the result of a computation identical to that of Figure 5.1 except that the initial condition consists of the uniform wave with the forced perturbation specified by (5.31) and (5.32). Figure 5.4 is the analog of Figure 5.2 for this initial condition. As expected, the forced solution remains stationary with respect to the current pattern. Moreover, the forced amplitude and wavenumber shift profiles maintain essentially constant magnitudes. Thus the homogeneous term is responsible for the growth observed in Figures 5.1 and 5.2.

The solutions presented thus far involve the modulation of a uniform wave due to interaction with a current. Consider now the case of an already modulated wave interacting with a current. Figure 5.5 represents the time development, in the absence of current, of the envelope of a wave which consists initially of a uniform component and a (much smaller) sinusoidal component with wavenumber $k_p = k_o/10$. Figure 5.6 represents the time development of the associated wavenumber shift profile. The slope of the carrier wave is $k_o a_o = 0.1$. It is easily verified that the modulation wavenumber lies in the Benjamin-Feir instability interval:

$$0 < (k_p/2k_o) < \sqrt{2}\, k_o a_o \qquad (5.35)$$

and the growth of the modulation is clearly discernible in Figure 5.5.

Figure 5.7 represents the time development of the envelope of a wave initially the same as that of Figure 5.5, but interacting with the current pattern specified by equation (5.18). Figure 5.8 represents the time development of the associated wavenumber shift profile. The effect of the disturbance is quite evident, and jibes with the effect seen in Figures 5.1 and 5.2 (the time steps are different due to the fact that resolution problems arise sooner in the computation associated with

Figures 5.7 and 5.8). That is, the development of Figures 5.7 and 5.8 appears to be a linear combination of the development of the uniform component due to the current interaction and the development of the modulation due to the Benjamin-Feir instability. One could, presumably, simplify the picture by including in the initial condition yet another modulation corresponding to the perturbation forced on the uniform component by the current.

The preceding remarks apply to a case in which the envelope is close to uniform. When initial modulations are not small, a generalization of the uniform wave analysis cannot be expected to apply. However, it is possible to proceed in another direction.

5.2 A Perturbation Scheme for Families of Non-Uniform Solutions

Given a parameterized family of solutions of an unforced nonlinear equation [e.g., (5.17) without terms involving the current], one is inclined to feel that when small forcing terms are added, there should be solutions approximated by unforced solutions with slowly-varying parameters. This notion is formalized in the following. The resulting formulae are then applied to the case of soliton solutions of the nonlinear Schrödinger equation interacting with currents.

Suppose the family of functions $A_0(\underline{x},t,\underline{p})$ satisfies

$$\frac{\partial A_0}{\partial t} + O(A_0) = 0 \tag{5.35}$$

for every set of parameters $\underline{p}$ within some range, where O is an operator which does not involve $\frac{\partial}{\partial t}$. Now consider the problem

$$\frac{\partial A}{\partial t} + O(A) = \mathcal{F}(A,\underline{x},t) \tag{5.36}$$

where $\mathcal{F}$ is an operator which does not involve $\frac{\partial}{\partial t}$, and

$$|\mathcal{F}| = O(\varepsilon), \quad \varepsilon << 1 \tag{5.37}$$

It seems natural to assume that there will be a solution of (5.36) approximated by

$$A = A_0\left(\underline{x},t,\underline{p}(t)\right) + A_1 \tag{5.38}$$

where

$$|A_1| = O(\varepsilon) = |\dot{\underline{p}}|. \tag{5.39}$$

That is, the forcing term will cause changes in the parameters, and an additional term, A_1, will be needed to allow for changes unrelated to the parameters.

Substituting (5.38) into (5.36) yields (5.35) at O(1), as intended. At $O(\varepsilon)$, one obtains

$$\frac{\partial A_1}{\partial t} + \mathcal{D}O(A_0)A_1 + \nabla_{\underline{p}}A_0 \cdot \dot{\underline{p}} = \mathcal{F}(A_0,\underline{x},t). \tag{5.40}$$

Define

$$B_j = \frac{\partial A_0}{\partial p_j} \tag{5.41}$$

and it follows from (5.35) that

$$\frac{\partial B_j}{\partial t} + \mathcal{D}O(A_0)B_j = 0. \tag{5.42}$$

Thus if $\hat{A}_1$ is a solution of (5.40), then so is $\hat{A}_1 + \sum_j c_j B_j$ for any choice of the constants c_j.

Let

$$\left.\begin{aligned} A_1 &= \sum_j h_j(t)B_j + \hat{A}_1 \\ \mathcal{F}(A_0,\underline{x},t) &= \sum_j f_j(t)B_j + \hat{f} \end{aligned}\right\} \tag{5.43}$$

where

$$\left.\begin{aligned}(B_j,\hat{A}_1) &= 0\\ (B_j,\hat{f}) &= 0\end{aligned}\right\} \quad \text{for all } j \text{ and } t \tag{5.44}$$

where the notation (f,g) represents the inner product of f and g. Then (5.40) reduces to

$$\left.\begin{aligned}&\dot{h}_j + \dot{p}_j = f_j\\ &\frac{\partial \hat{A}_1}{\partial t} + \mathcal{DO}(A_0)\hat{A}_1 = \hat{f}\end{aligned}\right\}. \tag{5.45}$$

Using $\dot{h}_j$ to balance accounts could clearly lead to substantial increases in $|A_1|$ - secular growth. Thus it is best to take

$$\dot{p}_j = f_j,\ \dot{h}_j = 0. \tag{5.46}$$

In fact, one can take

$$h_j = 0,\ A_1 = \hat{A}_1 \tag{5.47}$$

all of which sustains the notion that A_1 should represent change unrelated to parameter changes.

To compute the f_j, one has the formula

$$\left(B_\ell \mathcal{F}(A_0,\underline{x},t)\right) = \sum_j (B_\ell,B_j) f_j \tag{5.48}$$

which follows from (5.43) and (5.44). This is identical to the result obtained by Keener and McLaughlin [6] with a Green's function approach.

Keener and McLaughlin apply this formula to the case of soliton solutions of the nonlinear Schrödinger equation. In the case of a single soliton, in particular, they show that the solution

$$r(x,t) = -2i\eta \operatorname{sech}\left\{2\eta[(x - x_o) + 4\xi t]\right\} \exp\left\{i[2\xi x + 4(\xi^2 - \eta^2)t + \phi]\right\} \tag{5.49}$$

of

$$-i\frac{\partial r}{\partial t} + \frac{\partial^2 r}{\partial x^2} + 2|r|^2 r = 0 \tag{5.50}$$

where η, ξ, x_o and ϕ are constants, can be generalized to provide an approximate solution of

$$-i\frac{\partial r}{\partial t} + \frac{\partial^2 r}{\partial x^2} + 2|r|^2 r = f \tag{5.51}$$

where the perturbation f satisifies

$$|f| \ll 1. \tag{5.52}$$

The generalized result is

$$r(x,t) = -2i\eta(t) \operatorname{sech}\left(2\eta(t)\left[x - x_o(t) + 4\int_o^t \xi(t')dt'\right]\right) \times$$
$$\times \exp\left\{i\left[2\xi(t)x + 4\int_o^t [\xi^2(t') - \eta^2(t')]dt' + \phi(t)\right]\right\} \tag{5.53}$$

where η, ξ, x_o and ϕ now vary slowly in time.

The time variation of these quantities is governed by

$$\frac{d\zeta}{dt} = -\frac{1}{2}\Gamma^- e^{-i\theta}[\underline{f}(.,t),\underline{r}_1(t)] \tag{5.54}$$

$$\frac{d}{dt}\ell n\Gamma = -\frac{1}{2}[\underline{f}(.,t),\underline{r}_2(t)] + \frac{1}{2}(\zeta - \zeta^*)\frac{d\zeta}{dt} \tag{5.55}$$

where

$$\left.\begin{aligned} \zeta &= \xi + i\eta \\ \Gamma &= |\Gamma|e^{i\phi} \\ |\Gamma| &= 2\eta e^{2\eta x_o} \end{aligned}\right\} \tag{5.56}$$

$$\Gamma^- = (\zeta - \zeta^*)^2/\Gamma \tag{5.57}$$

$$\theta = \int_0^t 4\zeta^2 dt' = \int_0^t 4(\xi^2 - \eta^2)dt' + i\int_0^t 8\xi\eta dt' \tag{5.58}$$

$$(\underline{u},\underline{v}) = \int_{-\infty}^{\infty} \underline{u}^{\dagger}(x)\cdot\underline{v}(x)dz \tag{5.59}$$

$$\underline{f} = \begin{pmatrix} f \\ f^* \end{pmatrix} \tag{5.60}$$

$$\underline{r}_1 = -\frac{1}{\gamma^-}\left[1 - \frac{(\zeta - \zeta^*)^2}{\gamma^-\gamma^{-*}} e^{2i(\zeta-\zeta^*)x}\right]^{-1} \times \begin{pmatrix} r \\ \dfrac{(\zeta - \zeta^*)^2}{\gamma^-\gamma^{-*}} e^{2i(\zeta-\zeta^*)x} r^* \end{pmatrix} \tag{5.61}$$

$$\underline{r}_2 = 2\left[1 - \frac{(\zeta - \zeta^*)^2}{\gamma^-\gamma^{-*}} e^{2i(\zeta-\zeta^*)x}\right]^{-1} \times$$

$$\times \begin{pmatrix} \left(\dfrac{1}{(\zeta - \zeta^*)} + ix\right) r \\ \left(\dfrac{1}{(\zeta - \zeta^*)} + ix\,\dfrac{(\zeta - \zeta^*)^2}{\gamma^-\gamma^{-*}} e^{2i(\zeta-\zeta^*)x}\right) r^* \end{pmatrix} \tag{5.62}$$

$$\gamma^- = \Gamma^- e^{-i\theta} \tag{5.63}$$

To convert solutions of (5.17) to solutions of (5.51) or vice versa, one must use the transformation

$$\left.\begin{aligned} A &\leftrightarrow \alpha r \\ \beta\left(x - \frac{\omega_o}{2k_o} t\right) &\leftrightarrow x \end{aligned}\right\} \tag{5.64}$$

where

$$\left.\begin{aligned} \alpha &= \left(\frac{4}{\omega_o k_o^2}\right)^{1/2} \\ \beta &= \left(\frac{\omega_o}{8k_o^2}\right)^{-1/2} \end{aligned}\right\} . \tag{5.65}$$

It follows that

$$f = i\beta U \frac{\partial r}{\partial x} + \frac{3}{4} i\beta \frac{\partial U}{\partial x} r - k_o U r. \tag{5.66}$$

5.3 Soliton/Current Interaction

We now compare numerical computation with the results of the perturbation analysis of the preceding section. All figures are scaled against a carrier wavelength of 10 m.

Figure 5.9 represents the time development, computed via the nonlinear Schrödinger equation, of the amplitude profile of an envelope soliton interacting with the current pattern specified by equation (5.18). Figure 5.10 represents the time development of the associated wavenumber shift profile. The envelope clearly holds its shape very well, with only slight magnitude variations. The development of the wavenumber shift profile, on the other hand, is virtually identical to that of Figure 5.2, save for the introduction of Gibbs phenomenon.

Figure 5.11 is a plot of the soliton maximum versus time for the solution depicted in Figure 5.9. The curve appears to correspond closely to the curve that would be obtained by plotting the amplitude of the center point versus time in Figure 5.1.

Figure 5.12 depicts the time development of the soliton maximum and its location, and the wavenumber shift according to the perturbation approach. The plots of the soliton maximum versus time in Figures 5.11 and 5.12 are similar, but there are clearly significant differences. The first local maximum encountered in Figure 5.11 is larger than that of Figure 5.12. This maximum also appears to occur sooner in Figure 5.11, and the function of Figure 5.11 decreases faster thereafter. These discrepancies may be due to the fact that the perturbation approach has been pursued only far enough to determine the soliton parameters as a function of time. The term A_1 in equation (5.38) has not been computed.

The time development of the location of the soliton maximum presented in Figure 5.12 is in good agreement with the results of Figure 5.9. The spatial resolution of Figure 5.9 is 7.8125 m. At 0 sec and 101 sec, the maximum occurs at 1000 m in Figure 5.9. At 202 sec, it occurs at 992.1875 m. At 303 sec, it occurs at 984.375 m. At 404 sec and 505 sec, it occurs at 976.5625 m.

The time development of the soliton wavenumber shift presented in Figure 5.12 appears to correspond closely to the curve that would be obtained by plotting the wavenumber shift at the location of the soliton maximum, as given by Figure 5.10, versus time.

APPENDIX A

A DERIVATION OF THE FORCED NONLINEAR SCHRÖDINGER EQUATION FOR THE CASE OF WAVE/CURRENT INTERACTIONS ON A TWO-DIMENSIONAL SURFACE

For the case of irrotational gravity waves on water of infinite depth and constant density, the governing equations are

$$(\partial^2_{x_1} + \partial^2_{x_2} + \partial^2_z) = S(\underline{x},z,t) \qquad \text{on } z \leq \eta(\underline{x},t) \tag{A.1}$$

$$\eta_t + \phi_{x_1}\eta_{x_1} + \phi_{x_2}\eta_{x_2} = \phi_z \qquad \text{on } z = \eta(\underline{x},t) \tag{A.2}$$

$$\phi_t + \frac{1}{2}(\phi^2_{x_1} + \phi^2_{x_2} + \phi^2_z) + g\eta = 0 \qquad \text{on } z = \eta(\underline{x},t) \tag{A.3}$$

$$\phi_z\Big|_{z=-\infty} = 0 \tag{A.4}$$

where

$$\left.\begin{aligned} x_1, x_2 &= \text{horizontal coordinates} \\ \underline{x} &= (x_1, x_2) \\ z &= \text{vertical coordinate} \\ t &= \text{time coordinate} \\ \eta(\underline{x},t) &= \text{surface displacement} \\ \phi(\underline{x},z,t) &= \text{velocity potential} \\ g &= \text{acceleration of gravity} \end{aligned}\right\} \tag{A.5}$$

and S is a function representing underwater disturbances.

We now consider the case of a weakly nonlinear slowly modulating, nearly monochromatic wave. Harmonics higher than the second are assumed to be of negligible magnitude, but modulations are taken into account (which is important due to the modulational instability of Stokes waves).

To quantify these notions, we assume that

$$\eta = \sum_{n=-2}^{2} \eta_n + O(\varepsilon^3), \quad \phi = \sum_{n=-2}^{2} \phi_n + O(\varepsilon^3) \tag{A.6}$$

where

$$\varepsilon << 1; \ \eta_0, \eta_1 \sim O(\varepsilon); \ \eta_2 \sim O(\varepsilon^2); \ \phi_n \sim O(\varepsilon^n) \tag{A.7}$$

and

$$\eta_{-n} = \eta_n^*, \ \phi_{-n} = \phi_n^*. \tag{A.8}$$

The terms η_0 and ϕ_0 are intended to represent long waves (mean level and mean flow fluctuations), while $\eta_1 + \eta_1^*$ and $\phi_1 + \phi_1^*$ represent short waves and $\eta_2 + \eta_2^*$ and $\phi_2 + \phi_2^*$ represent second harmonics.

We restrict ourselves to consideration of a low-frequency S so that

$$\nabla^2\phi_0 = S, \ \nabla^2\phi_1 = 0, \ \nabla^2\phi_2 = 0. \tag{A.9}$$

It is therefore reasonable to separate the η_n and ϕ_n into carrier wave and modulation factors as follows:

$$\eta_n = a_n(\underline{x},t)e^{in(\underline{k}_o \cdot \underline{x} - \omega_o t)} \tag{A.10}$$

$$\phi_n = b_n(\underline{x},z,t)e^{in(\underline{k}_o \cdot \underline{x} - \omega_o t)} e^{|n|k_o z}, \tag{A.11}$$

where the a_n and b_n are slowly varying functions of their arguments,

$$k_o = |\underline{k}_o|, \tag{A.12}$$

and it follows from (A.8) that

$$a_{-n} = a_n^*, \ b_{-n} = b_n^*. \tag{A.13}$$

The use of $|n|$ in the factor $e^{|n|k_o z}$ is necessary for the satisfaction of (A.4).

We quantify our scaling as follows:

$$a_n = a_n^{(1)} + a_n^{(2)} + a_n^{(3)} + O(\varepsilon^4) \text{ for } n = 0, \pm 1; \; a_{\pm 2} = a_{\pm 2}^{(2)} + a_{\pm 2}^{(3)} + O(\varepsilon^4) \tag{A.14}$$

$$b_o = b_o^{(0)} + b_o^{(1)} + b_o^{(2)} + b_o^{(3)} + O(\varepsilon^4), \; b_{\pm 1} = b_{\pm 1}^{(1)} + b_{\pm 1}^{(2)} + b_{\pm 1}^{(3)} + O(\varepsilon^4),$$

$$b_{\pm 2} = b_{\pm 2}^{(2)} + b_{\pm 2}^{(3)} + O(\varepsilon^4) \tag{A.15}$$

where

$$a_n^{(j)}, \; b_n^{(j)} \sim O(\varepsilon^j) \tag{A.16}$$

$$a_n^{(j)} = a_n^{(j)}(\hat{\underline{x}}, \hat{t}), \; b_n^{(j)} = b_n^{(j)}(\hat{\underline{x}}, \hat{z}, \hat{t}) \text{ for } n \neq \pm 1 \text{ or } j \neq 1 \tag{A.17}$$

$$a_{\pm 1}^{(1)} = a_{\pm 1}^{(1)}(\hat{\underline{x}}, \hat{t}, \hat{\hat{t}}), \; b_{\pm 1}^{(1)} = b_{\pm 1}^{(1)}(\hat{\underline{x}}, \hat{z}, \hat{t}, \hat{\hat{t}}) \tag{A.18}$$

$$\hat{\underline{x}} = \varepsilon \underline{x}, \; \hat{z} = \varepsilon z, \; \hat{t} = \varepsilon t, \; \hat{\hat{t}} = \varepsilon^2 t. \tag{A.19}$$

The extra argument for $a_{\pm 1}^{(1)}$ and $b_{\pm 1}^{(1)}$ is needed to suppress secularity; this will become clear in subsequent calculations.

Expanding ϕ and derivatives of ϕ evaluated at $z = \eta$ into expressions involving ϕ and derivatives of ϕ evaluated at $z = 0$ allows us to write the governing equations (A.2) and (A.3) as follows:

$$\eta_t + \sum_{j=1}^{2} \left[\eta_{x_j} \cdot \phi_{x_j} + \eta \phi_{x_j z} \right] = \phi_z + \eta \phi_{zz} + \frac{1}{2} \eta^2 \phi_{zzz} + O(\varepsilon^4) \text{ on } z = 0 \tag{A.20}$$

$$\phi_t + \eta \phi_{tz} + \frac{1}{2} \eta^2 \phi_{tzz} + \frac{1}{2} \sum_{j=1}^{2} \left(\phi_{x_j}^2 + 2\eta \phi_{x_j} \phi_{x_j z} \right) + \frac{1}{2} \left(\phi_z^2 + 2\eta \phi_z \phi_{zz} \right) +$$

$$+ g\eta = O(\varepsilon^4) \text{ on } z = 0. \tag{A.21}$$

Substituting η and ϕ, as given by (A.6), into equations (A.20) and (A.21), and equating coefficients of the $e^{in(k_o \cdot x - \omega_o t)}$ [see (A.10) and (A.11)] to 0 yields

$$(\partial_t \eta_o) + \sum_{j=1}^{2} \Big[(\partial_{x_j} \phi_{-1})(\partial_{x_j} \eta_1) + (\partial_{x_j} \phi_o)(\partial_{x_j} \eta_o) + (\partial_{x_j} \phi_1)(\partial_{x_j} \eta_{-1}) +$$

$$+ \eta_o \cdot \Big[(\partial_z \partial_{x_j} \phi_{-1})(\partial_{x_j} \eta_1) + (\partial_z \partial_{x_j} \phi_1)(\partial_{x_j} \eta_{-1}) \Big] \Big] =$$

$$= (\partial_z \phi_o) + \eta_1 \cdot (\partial_z^2 \phi_{-1}) + \eta_o \cdot (\partial_z^2 \phi_o) + \eta_{-1} \cdot (\partial_z^2 \phi_1) +$$

$$+ \eta_o \eta_1 \cdot (\partial_z^3 \phi_{-1}) + \eta_o \eta_{-1} \cdot (\partial_z^3 \phi_1) + O(\varepsilon^4) \text{ on } z = 0 \qquad \text{(A.22)}$$

$$(\partial_t \phi_o) + \eta_1 \cdot (\partial_z \phi_t \phi_{-1}) + \eta_o \cdot (\partial_z \partial_t \phi_o) + \eta_{-1} \cdot (\partial_z \partial_t \phi_1) + \eta_o \eta_1 \cdot (\partial_z^2 \partial_t \phi_{-1}) +$$

$$+ \eta_o \eta_{-1} \cdot (\partial_z^2 \partial_t \phi_1) + \frac{1}{2} \sum_{j=1}^{2} \Big[2(\partial_{x_j} \phi_{-1})(\partial_{x_j} \phi_1) + (\partial_{x_j} \phi_o)^2 +$$

$$+ 2\eta_{-1} (\partial_{x_j} \phi_o)(\partial_z \partial_{x_j} \phi_1) + 2\eta_o \cdot (\partial_{x_j} \phi_{-1})(\partial_z \partial_{x_j} \phi_1) + 2\eta_1 \cdot (\partial_{x_j} \phi_o)(\partial_z \partial_{x_j} \phi_{-1}) +$$

$$+ 2\eta_o \cdot (\partial_{x_j} \phi_1)(\partial_z \partial_{x_j} \phi_{-1}) \Big] + \frac{1}{2} \Big[2(\partial_z \phi_{-1})(\partial_z \phi_1) + (\partial_z \phi_o)^2 +$$

$$+ 2\eta_{-1} \cdot (\partial_z \phi_o)(\partial_z^2 \phi_1) + 2\eta_o \cdot (\partial_z \phi_{-1})(\partial_z^2 \phi_1) + 2\eta_1 \cdot (\partial_z \phi_o)(\partial_z^2 \phi_{-1}) +$$

$$+ 2\eta_o \cdot (\partial_z \phi_1)(\partial_z^2 \phi_{-1}) \Big] + g\eta_o = O(\varepsilon^4) \text{ on } z = 0 \qquad \text{(A.23)}$$

$$(\partial_t \eta_1) = (\partial_z \phi_1) + \sum_{j=1}^{2} \sum_{n=-1}^{2} (\partial_{x_j} \eta_n)(\partial_{x_j} \phi_{1-n}) - \sum_{n=-1}^{2} \eta_n \cdot (\partial_z^2 \phi_{1-n}) +$$

$$+ \sum_{\underline{n} \in S(-1,1,1)}^{2} \left[\sum_{j=1}^{2} (\partial_{x_j} \eta_{n_1}) \eta_{n_2} (\partial_z \partial_{x_j} \phi_{n_3}) - \frac{1}{2} \eta_{n_1} \eta_{n_2} (\partial_z^3 \phi_{n_3}) \right] +$$

$$- \frac{1}{2} \eta_o^2 \cdot (\partial_z^3 \phi_1) = O(\varepsilon^4) \text{ on } z = 0 \qquad \text{(A.24)}$$

$$(\partial_t \phi_1) + g\eta_1 + \sum_{n=-1}^{2} \left[\eta_n \cdot (\partial_z \partial_t \phi_{1-n}) + \frac{1}{2} \sum_{j=1}^{2} (\partial_{x_j} \phi_n)(\partial_{x_j} \phi_{1-n}) \right.$$

$$\left. + \frac{1}{2} (\partial_z \phi_n)(\partial_z \phi_{1-n}) \right] + \sum_{\underline{n} \in S(-1,1,1)}^{2} \times$$

$$\times \left[\frac{1}{2} \eta_{n_1} \eta_{n_2} \cdot (\partial_z^2 \partial_t \phi_{n_3}) + \sum_{j=1}^{2} \eta_{n_1} \cdot (\partial_{x_j} \phi_{n_2})(\partial_z \partial_{x_j} \phi_{n_3}) + \right.$$

$$\left. + \eta_{n_1} \cdot (\partial_z \phi_{n_2})(\partial_z^2 \phi_{n_3}) \right] + \frac{1}{2} \eta_o^2 \cdot (\partial_z^2 \partial_t \phi_1) + \sum_{j=1}^{2} \eta_o \cdot (\partial_{x_j} \phi_o)(\partial_z \partial_{x_j} \phi_1) +$$

$$+ \eta_o \cdot (\partial_z \phi_o)(\partial_z^2 \phi_1) = O(\varepsilon^4) \text{ on } z = 0 \qquad \text{(A.25)}$$

$$(\partial_t \eta_2) - (\partial_z \phi_2) + \sum_{j=1}^{2} (\partial_{x_j} \eta_1)(\partial_{x_j} \phi_1) - \eta_1 \cdot (\partial_z^2 \phi_1) + \sum_{j=1}^{2} (\partial_{x_j} \eta_2)(\partial_{x_j} \phi_0) +$$

$$- \eta_0 (\partial_z^2 \phi_2) - \eta_2 \cdot (\partial_z^2 \phi_0) + \sum_{j=1}^{2} \Big[(\partial_{x_j} \eta_1) \eta_0 (\partial_z \partial_{x_j} \phi_1) +$$

$$+ (\partial_{x_j} \eta_1) \eta_1 (\partial_z \partial_{x_j} \phi_0) \Big] +$$

$$- \eta_0 \eta_1 (\partial_z^3 \phi_1) = 0(\varepsilon^4) \text{ on } z = 0 \qquad \text{(A.26)}$$

$$(\partial_t \phi_2) + g\eta_2 + \eta_1 \cdot (\partial_z \partial_t \phi_1) + \frac{1}{2} \sum_{j=1}^{2} (\partial_{x_j} \phi_1)^2 + \frac{1}{2} (\partial_z \phi_1)^2 + \eta_0 \cdot (\partial_z \partial_t \phi_2) +$$

$$+ \eta_2 \cdot (\partial_z \partial_t \phi_0) + \sum_{j=1}^{2} (\partial_{x_j} \phi_0)(\partial_{x_j} \phi_2) + (\partial_z \phi_0)(\partial_z \phi_2) + \eta_0 \eta_1 \cdot (\partial_z^2 \partial_t \phi_1) +$$

$$+ \sum_{j=1}^{2} \Big[\eta_0 \cdot (\partial_{x_j} \phi_1)(\partial_z \partial_{x_j} \phi_1) + \eta_1 \cdot (\partial_{x_j} \phi_0)(\partial_z \partial_{x_j} \phi_1) \Big] + \eta_0 \cdot (\partial_z \phi_1)(\partial_z^2 \phi_1) +$$

$$+ \eta_1 \cdot (\partial_z \phi_0)(\partial_z^2 \phi_1) = 0(\varepsilon^4) \text{ on } z = 0 \qquad \text{(A.27)}$$

where the notation $\sum_{\underline{n} \varepsilon S(-1,1,1)}^{2}$ indicates summation over all distinct permutations of the triplet (-1,1,1). That is,

$$\sum_{\underline{n} \varepsilon S(-1,1,1)}^{2} f(n_1, n_2, n_3) = f(-1,1,1) + f(1,-1,1) + f(1,1,-1). \qquad \text{(A.28)}$$

At $O(\varepsilon)$, equation (A.24) reduces to

$$-i\omega_o a_1^{(1)} - k_o b_1^{(1)} = 0 \quad \text{on } z = 0 \tag{A.29}$$

while equation (A.25) reduces to

$$-i\omega_o b_1^{(1)} + g a_1^{(1)} = 0 \quad \text{on } z = 0. \tag{A.30}$$

If (A.29) and (A.30) are to have a nontrivial solution, it must be the case that

$$\omega_o^2 = g k_o \tag{A.31}$$

and it will then follow that

$$b_1^{(1)} = -\frac{i\omega_o}{k_o} a_1^{(1)} \quad \text{on } z = 0. \tag{A.32}$$

At $O(\varepsilon)$, equation (A.22) reduces to

$$(\partial_{\hat{z}} b_o^{(0)}) = 0 \quad \text{on } z = 0 \tag{A.33}$$

while (A.23) reduces to

$$a_o^{(1)} = -(\varepsilon \partial_{\hat{t}} b_o^{(0)})/g \quad \text{on } z = 0. \tag{A.34}$$

It follows from (A.4), (A.9), and (A.33) that

$$\left.\begin{aligned} \nabla^2 b_o^{(0)} &= S \text{ on } z < 0 \\ \partial_z b_o^{(0)} &= 0 \text{ on } z = 0 \\ \partial_z b_o^{(0)} &= 0 \text{ on } z = -\infty \end{aligned}\right\}. \tag{A.35}$$

This determines $b_o^{(0)}$ which then determines $a_o^{(1)}$ via (A.34).

Equations (A.26) and (A.27) vanish at $O(\varepsilon)$. At $O(\varepsilon^2)$, equation (A.24) reduces to

$$- i\omega_o a_1^{(2)} - k_o b_1^{(2)} + (\varepsilon\partial_{\hat{t}} a_1^{(1)}) - (\varepsilon\partial_{\hat{z}} b_1^{(1)}) + i\underline{k}_o a_1^{(1)}\cdot(\varepsilon\partial_{\hat{\underline{x}}} b_o^{(0)}) + - k_o^2 a_o^{(1)} b_1^{(1)} = 0 \qquad \text{on } z = 0 \tag{A.36}$$

while (A.25) reduces to

$$- i\omega_o b_1^{(2)} + g a_1^{(2)} + (\varepsilon\partial_{\hat{t}} b_1^{(1)}) - i\omega_o k_o a_o^{(1)} b_1^{(1)} + i\underline{k}_o b_1^{(1)}\cdot(\varepsilon\partial_{\hat{\underline{x}}} b_o^{(0)}) + + k_o b_1^{(1)}\cdot(\varepsilon\partial_{\hat{z}} b_o^{(0)}) = 0 \qquad \text{on } z = 0. \tag{A.37}$$

The last term of (A.37) will vanish due to (A.33). Multiplying (A.36) by $i\omega_o$ and (A.37) by k_o, and subtracting the latter result from the former, yields

$$i\omega_o(\partial_{\hat{t}} a_1^{(1)}) - k_o(\partial_{\hat{t}} b_1^{(1)}) - i\omega_o(\partial_{\hat{z}} b_1^{(1)}) + - (\omega_o a_1^{(1)} + ik_o b_1^{(1)})\underline{k}_o\cdot(\partial_{\hat{\underline{x}}} b_o^{(0)}) = 0 \qquad \text{on } z = 0. \tag{A.38}$$

Substituting ϕ_1 as given by (A.11) into (A.9) yields

$$(\partial_{\hat{z}} b_1^{(1)}) = - \frac{i\underline{k}_o}{k_o}\cdot(\partial_{\hat{\underline{x}}} b_1^{(1)}) \tag{A.39}$$

at $O(\varepsilon^2)$. With this and (A.32), we can substitute for $b_1^{(1)}$ in (A.38). The result is

$$(\partial_{\hat{t}} a_1^{(1)}) + \frac{\omega_o}{2k_o^2}\underline{k}_o\cdot(\partial_{\hat{\underline{x}}} a_1^{(1)}) + i\underline{k}_o\cdot(\partial_{\hat{\underline{x}}} b_o^{(0)}) a_1^{(1)} = 0 \qquad \text{on } z = 0 \tag{A.40}$$

which is an intuitively sound equation governing the time development of $a_1^{(1)}$, for the group velocity is given by

$$\underline{c}_g = \frac{\omega_o}{2k_o^2}\,\underline{k}_o \tag{A.41}$$

and the $O(\varepsilon)$ component of the current is given by,

$$\underline{U}^{(1)} = (\partial_{\underline{x}} b_o^{(0)})\Big|_{z=0.} \tag{A.42}$$

Equations (A.32) and (A.39) can also be used to simplify the relationship between $b_1^{(2)}$ and $a_1^{(2)}$ implicit in equations (A.36) and (A.37). The result is:

$$b_1^{(2)} = -\frac{i\omega_o}{k_o}\,a_1^{(2)} + (\varepsilon\partial_{\hat{t}} a_1^{(1)})/k_o + \frac{\omega_o}{k_o^3}\,\underline{k}_o\cdot(\varepsilon\partial_{\underline{x}} a_1^{(1)}) +$$

$$+ \frac{i}{k_o}\,\underline{k}_o\cdot(\varepsilon\partial_{\hat{\underline{x}}} b_o^{(0)})a_1^{(1)} + i\omega_o a_o^{(1)} a_1^{(1)}$$

$$= -\frac{i\omega_o}{k_o}\,a_1^{(2)} + \frac{\omega_o}{2k_o^3}\,\underline{k}_o\cdot(\varepsilon\partial_{\hat{\underline{x}}} a_1^{(1)}) + i\omega_o a_o^{(1)} a_1^{(1)} \text{ on } z = 0. \tag{A.43}$$

At $O(\varepsilon^2)$, equation (A.22) reduces to

$$(\partial_{\hat{z}} b_o^{(1)}) = (\partial_{\hat{t}} a_o^{(1)}) \quad \text{on } z = 0 \tag{A.44}$$

while (A.23) reduces to

$$a_o^{(2)} = -\left[(\varepsilon\partial_{\hat{t}} b_o^{(1)}) + \frac{1}{2}\,(\varepsilon\partial_{\hat{\underline{x}}} b_o^{(0)})\cdot(\varepsilon\partial_{\underline{x}} b_0^{(0)})\right]\Big/ g \quad \text{on } z = 0 \tag{A.45}$$

Equations (A.4), (A.9), (A.35), and (A.44) yield

$$\left.\begin{aligned} \nabla^2 b_o^{(1)} &= 0 \text{ on } z < 0 \\ (\partial_z b_o^{(1)}) &= (\partial_t a_o^{(1)}) \text{ on } z = 0 \\ (\partial_z b_o^{(1)}) &= 0 \text{ on } z = -\infty \end{aligned}\right\} \tag{A.46}$$

which determines $b_o^{(1)}$. Equation (A.45) then determines $a_o^{(2)}$.

At $O(\varepsilon^2)$, equation (A.26) reduces to

$$-2i\omega_o a_2^{(2)} - 2k_o b_2^{(2)} - 2k_o^2 a_1^{(1)} b_1^{(1)} = 0 \qquad \text{on } z = 0 \tag{A.47}$$

while (A.27) reduces to

$$-2i\omega_o b_2^{(2)} + g a_2^{(2)} - i\omega_o k_o a_1^{(1)} b_1^{(1)} = 0 \qquad \text{on } z = 0. \tag{A.48}$$

These equations can be solved for $a_2^{(2)}$ and $b_2^{(2)}$, yielding

$$a_2^{(2)} = k_o a_1^{(1)2} \tag{A.49}$$

$$b_2^{(2)} = 0 \quad \text{on } z = 0. \tag{A.50}$$

It follows from (A.9) that $b_2^{(2)}$ will in fact vanish everywhere.

At $O(\varepsilon^3)$, equation (A.24) yields,

$$\begin{aligned}
&- i\omega_o a_1^{(3)} + (\varepsilon\partial_{\hat{t}} a_1^{(2)}) + (\varepsilon^2\partial_{\hat{t}\hat{t}} a_1^{(1)}) = k_o b_1^{(3)} - (\varepsilon\partial_{\hat{z}} b_1^{(2)}) + \\
&\quad + (-i\underline{k}_o a_{-1}^{(1)})\cdot(2i\underline{k}_o b_2^{(2)}) + (\varepsilon\partial_{\hat{\underline{x}}} a_o^{(1)})\cdot(i\underline{k}_o b_1^{(1)}) + \\
&\quad + (i\underline{k}_o a_1^{(1)})\cdot(\varepsilon\partial_{\hat{\underline{x}}} b_o^{(1)}) + \left[(i\underline{k}_o a_1^{(2)}) + (\varepsilon\partial_{\hat{\underline{x}}} a_1^{(1)})\right]\cdot(\varepsilon\partial_{\hat{\underline{x}}} b_o^{(0)}) + \\
&\quad + (2i\underline{k}_o a_2^{(2)})\cdot(-i\underline{k}_o b_{-1}^{(1)}) - a_{-1}^{(1)}\cdot(4k_o^2 b_2^{(2)}) + \\
&\quad - a_o^{(1)}\cdot\left[k_o^2 b_1^{(2)} + 2k_o(\varepsilon\partial_{\hat{z}} b_1^{(1)})\right] - a_o^{(2)}\cdot(k_o^2 b_1^{(1)}) + \\
&\quad - a_1^{(1)}\cdot(\varepsilon^2\partial_{\hat{z}}^2 b_o^{(0)}) - a_2^{(2)}\cdot(k_o^2 b_{-1}^{(1)}) + (-i\underline{k}_o a_{-1}^{(1)})a_1^{(1)}\cdot(ik_o\underline{k}_o b_1^{(1)}) + \\
&\quad + (i\underline{k}_o a_1^{(1)})a_{-1}^{(1)}\cdot(ik_o\underline{k}_o b_1^{(1)}) + (i\underline{k}_o a_1^{(1)})a_1^{(1)}\cdot(-ik_o\underline{k}_o b_{-1}^{(1)}) + \\
&\quad - a_1^{(1)}a_{-1}^{(1)}\cdot(k_o^3 b_1^{(1)}) - \tfrac{1}{2} a_1^{(1)2}\cdot(k_o^3 b_{-1}^{(1)}) - \tfrac{1}{2} a_o^{(1)2}\cdot(k_o^3 b_1^{(1)}) = 0 \\
&\quad \text{on } z = 0
\end{aligned} \tag{A.51}$$

while (A.25) yields

$$-i\omega_o b_1^{(3)} + (\varepsilon\partial_{\hat{t}} b_1^{(2)}) + (\varepsilon^2\partial_{\hat{t}\hat{t}} b_1^{(1)}) + g a_1^{(3)} + a_{-1}^{(1)}\cdot(-4i\omega_o k_o b_2^{(2)}) +$$

$$+ a_o^{(2)}\cdot(-i\omega_o k_o b_1^{(1)}) + a_o^{(1)}\cdot\left[(-i\omega_o k_o b_1^{(2)}) + (-i\omega_o \varepsilon\partial_{\hat{z}} b_1^{(1)}) + (k_o \varepsilon\partial_{\hat{t}} b_1^{(1)})\right] +$$

$$+ a_1^{(1)}\cdot(\varepsilon^2\partial_{\hat{z}}\partial_{\hat{t}} b_o^{(0)}) + a_2^{(2)}\cdot(i\omega_o k_o b_{-1}^{(1)}) + (-i\underline{k}_o b_{-1}^{(1)})\cdot(2i\underline{k}_o b_2^{(2)}) +$$

$$+ (\varepsilon\partial_{\underline{\hat{x}}} b_o^{(0)})\cdot\left[(i\underline{k}_o b_1^{(2)}) + (\varepsilon\partial_{\underline{\hat{x}}} b_1^{(1)})\right] + (\varepsilon\partial_{\underline{\hat{x}}} b_o^{(1)})\cdot(i\underline{k}_o b_1^{(1)}) +$$

$$+ (k_o b_{-1}^{(1)})\cdot(2k_o b_2^{(2)}) + (\varepsilon\partial_{\hat{z}} b_o^{(0)})\cdot\left[(k_o b_1^{(2)}) + (\varepsilon\partial_{\hat{z}} b_1^{(1)})\right] +$$

$$+ (\varepsilon\partial_{\hat{z}} b_o^{(1)})\cdot(k_o b_1^{(1)}) + a_{-1}^{(1)} a_1^{(1)}(-i\omega_o k_o^2 b_1^{(1)}) + \tfrac{1}{2} a_1^{(1)2}\cdot(i\omega_o k_o^2 b_{-1}^{(1)}) +$$

$$+ a_{-1}^{(1)}\cdot(i\underline{k}_o b_1^{(1)})\cdot(ik_o\underline{k}_o b_1^{(1)}) + a_1^{(1)}\cdot(-i\underline{k}_o b_{-1}^{(1)})\cdot(ik_o\underline{k}_o b_1^{(1)}) +$$

$$+ a_1^{(1)}\cdot(i\underline{k}_o b_1^{(1)})\cdot(-ik_o\underline{k}_o b_{-1}^{(1)}) + k_o^3 a_{-1}^{(1)} b_1^{(1)2} + 2k_o^3 a_1^{(1)} b_{-1}^{(1)} b_1^{(1)} +$$

$$+ \tfrac{1}{2} a_o^{(1)2}\cdot(-i\omega_o k_o^2 b_1^{(1)}) + a_o^{(1)}\cdot(\varepsilon\partial_{\underline{\hat{x}}} b_o^{(0)})\cdot(ik_o\underline{k}_o b_1^{(1)}) +$$

$$+ a_o^{(1)}\cdot(\varepsilon\partial_{\hat{z}} b_o^{(0)})\cdot(k_o^2 b_1^{(1)}) = 0 \qquad \text{on } z = 0 \tag{A.52}$$

Substituting for $b_{\pm 1}^{(1)}$, $b_2^{(2)}$, and $a_2^{(2)}$ simplifies (A.51) to

$$-i\omega_o a_1^{(3)} = k_o b_1^{(3)} + (\varepsilon\partial_{\hat{t}} a_1^{(2)}) + (\varepsilon^2\partial_{\hat{t}\hat{t}} a_1^{(1)}) - (\varepsilon\partial_{\hat{z}} b_1^{(2)}) +$$

$$+ (\varepsilon\partial_{\underline{\hat{x}}} a_o^{(1)})\cdot\left(\frac{\omega_o}{k_o}\underline{k}_o a_1^{(1)}\right) + (i\underline{k}_o a_1^{(1)})\cdot(\varepsilon\partial_{\underline{\hat{x}}} b_o^{(1)}) +$$

$$+ \left[(i\underline{k}_o a_1^{(2)}) + (\varepsilon\partial_{\underline{\hat{x}}} a_1^{(1)})\right]\cdot(\varepsilon\partial_{\underline{\hat{x}}} b_o^{(0)}) + \tfrac{5}{2} i\omega_o k_o^2 \left|a_1^{(1)}\right|^2 a_1^{(1)} +$$

$$- a_o^{(1)}\cdot\left[k_o^2 b_1^{(2)} + 2k_o(\varepsilon\partial_{\hat{z}} b_1^{(1)})\right] + i\omega_o k_o a_o^{(2)} a_1^{(1)} - a_1^{(1)}\cdot(\varepsilon^2\partial_{\hat{z}}^2 b_o^{(0)}) +$$

$$+ \tfrac{1}{2} i\omega_o k_o^2 a_o^{(1)2} a_1^{(1)} = 0 \quad \text{on } z = 0 \tag{A.53}$$

and simplifies (A.52) to

$$-i\omega_o b_1^{(3)} + g a_1^{(3)} + (\varepsilon \partial_{\hat{t}} b_1^{(2)}) + (\varepsilon^2 \partial_{\hat{\hat{t}}} b_1^{(1)}) - \omega_o^2 a_o^{(2)} a_1^{(1)} +$$

$$+ a_o^{(1)} \cdot \left[(-i\omega_o k_o b_1^{(2)}) + (-i\omega_o \varepsilon \partial_{\hat{z}} b_1^{(1)}) + (-i\omega_o \varepsilon \partial_{\hat{t}} a_1^{(1)}) \right] +$$

$$+ \frac{3}{2} \omega_o^2 k_o \left| a_1^{(1)} \right|^2 a_1^{(1)} + (\varepsilon \partial_{\hat{\underline{x}}} b_o^{(0)}) \left[(i \underline{k}_o b_1^{(2)}) - \frac{i\omega_o}{k_o} (\varepsilon \partial_{\hat{\underline{x}}} a_1^{(1)}) \right] +$$

$$+ (\varepsilon \partial_{\hat{\underline{x}}} b_o^{(1)}) \cdot \left(\frac{\omega_o}{k_o} \underline{k}_o a_1^{(1)} \right) - i\omega_o (\varepsilon \partial_{\hat{z}} b_o^{(1)}) a_1^{(1)} - \frac{1}{2} \omega_o^2 k_o a_o^{(1)2} a_1^{(1)} +$$

$$+ \omega_o a_o^{(1)} \underline{k}_o \cdot (\varepsilon \partial_{\hat{\underline{x}}} b_o^{(0)}) a_1^{(1)} = 0 \qquad \text{on } z = 0 \tag{A.54}$$

Multiplying (A.53) by $i\omega_o$ and (A.54) by k_o, and subtracting the latter result from the former yields

$$\left[i\omega_o (\varepsilon \partial_{\hat{t}} a_1^{(2)}) - k_o (\varepsilon \partial_{\hat{t}} b_1^{(2)}) \right] + \left[i\omega_o (\varepsilon^2 \partial_{\hat{\hat{t}}} a_1^{(1)}) - k_o (\varepsilon^2 \partial_{\hat{\hat{t}}} b_1^{(1)}) \right] +$$

$$- i\omega_o (\varepsilon \partial_{\hat{z}} b_1^{(2)}) + \frac{i\omega_o^2}{k_o} \underline{k}_o \cdot (\varepsilon \partial_{\hat{\underline{x}}} a_o^{(1)}) a_1^{(1)} - 2\omega_o \underline{k}_o \cdot (\varepsilon \partial_{\hat{\underline{x}}} b_o^{(1)}) a_1^{(1)} +$$

$$+ (\varepsilon \partial_{\hat{\underline{x}}} b_o^{(0)}) \cdot \left[(-\omega_o \underline{k}_o a_1^{(2)} - i k_o \underline{k}_o b_1^{(2)}) + (2i\omega_o \varepsilon \partial_{\hat{\underline{x}}} a_1^{(1)}) \right] - 4\omega_o^2 k_o^2 \left| a_1^{(1)} \right|^2 a_1^{(1)} +$$

$$+ a_o^{(1)} \cdot \left[-i\omega_o k_o (\varepsilon \partial_{\hat{z}} b_1^{(1)}) + i\omega_o k_o (\varepsilon \partial_{\hat{t}} a_1^{(1)}) \right] - i\omega_o (\varepsilon^2 \partial_{\hat{z}}^2 b_o^{(0)}) a_1^{(1)} +$$

$$+ i\omega_o k_o (\varepsilon \partial_{\hat{z}} b_o^{(1)}) a_1^{(1)} - \omega_o k_o a_o^{(1)} \underline{k}_o \cdot (\varepsilon \partial_{\hat{\underline{x}}} b_o^{(0)}) a_1^{(1)} = 0 \quad \text{on } z = 0. \tag{A.55}$$

We must now whittle away at (A.55), eliminating references to the $b_i^{(j)}$. To begin, we apply (A.43) to deduce that

$$k_o (\varepsilon \partial_{\hat{t}} b_1^{(2)}) = -i\omega_o (\varepsilon \partial_{\hat{t}} a_1^{(2)}) + \frac{\omega_o}{2k_o^2} \underline{k}_o \cdot (\varepsilon^2 \partial_{\hat{t}} \partial_{\hat{\underline{x}}} a_1^{(1)}) + i\omega_o k_o (\varepsilon \partial_{\hat{t}} a_o^{(1)}) a_1^{(1)}$$

$$+ i\omega_o k_o a_o^{(1)} \cdot (\varepsilon \partial_{\hat{t}} a_1^{(1)}) \qquad \text{on } z = 0. \tag{A.56}$$

It follows from (A.40) that

$$(\varepsilon^2 \partial_{\hat{t}} \partial_{\hat{\underline{x}}} \underline{a}_1^{(1)}) + \frac{\omega_o}{2k_o^2} \left(\varepsilon \partial_{\hat{\underline{x}}} (\underline{k}_o \cdot \varepsilon \partial_{\hat{\underline{x}}} a_1^{(1)})\right) + i(\varepsilon \partial_{\hat{\underline{x}}} \underline{k}_o \cdot \underline{U}^{(1)}) a_1^{(1)} +$$

$$+ i(\underline{k}_o \cdot \underline{U}^{(1)})(\varepsilon \partial_{\hat{\underline{x}}} a_1^{(1)}) = 0. \qquad \text{(A.57)}$$

Substituting (A.40) and (A.57) into (A.56) yields

$$k_o(\varepsilon \partial_{\hat{t}} b_1^{(2)}) = -i\omega_o(\varepsilon \partial_{\hat{t}} a_1^{(2)}) - \frac{\omega_o^2}{4k_o^4} \underline{k}_o \cdot \left(\varepsilon \partial_{\hat{\underline{x}}} (\underline{k}_o \cdot \varepsilon \partial_{\hat{\underline{x}}} a_1^{(1)})\right) +$$

$$- \frac{\omega_o}{2k_o^2} i\underline{k}_o \cdot (\varepsilon \partial_{\hat{\underline{x}}} \underline{k}_o \cdot \underline{U}^{(1)}) a_1^{(1)} - \frac{\omega_o}{2k_o^2} \cdot i(\underline{k}_o \cdot \underline{U}^{(1)})(\underline{k}_o \cdot \varepsilon \partial_{\hat{\underline{x}}} a_1^{(1)}) +$$

$$+ i\omega_o k_o (\varepsilon \partial_{\hat{t}} a_o^{(1)}) a_1^{(1)} - i a_o^{(1)} \cdot \frac{\omega_o^2}{2k_o} \cdot \underline{k}_o \cdot (\varepsilon \partial_{\hat{\underline{x}}} a_1^{(1)}) +$$

$$+ \omega_o k_o a_o^{(1)} (\underline{k}_o \cdot \underline{U}^{(1)}) a_1^{(1)} \qquad \text{on } z = 0. \qquad \text{(A.58)}$$

It follows from (A.32) that

$$k_o(\varepsilon^2 \partial_{\hat{\hat{t}}} b_1^{(1)}) = -i\omega_o(\varepsilon^2 \partial_{\hat{\hat{t}}} a_1^{(1)}) \quad \text{on } z = 0. \qquad \text{(A.59)}$$

Substituting ϕ_1 as given by (A.11) into (A.9) yields

$$(2\varepsilon \partial_{\hat{\underline{x}}} b_1^{(2)}) \cdot (i\underline{k}_o) + (2\varepsilon \partial_{\hat{z}} b_1^{(2)}) \cdot k_o + (\varepsilon^2 \partial_{\hat{\underline{x}}} \cdot \partial_{\hat{\underline{x}}} b_1^{(1)}) + (\varepsilon^2 \partial_{\hat{z}}^2 b_1^{(1)}) = 0 \qquad \text{(A.60)}$$

at $O(\varepsilon^3)$. From (A.39) (the $O(\varepsilon^2)$ version of the same equation) we can infer that

$$(\varepsilon^2 \partial_{\hat{z}}^2 b_1^{(1)}) = - \left(\frac{\varepsilon}{k_o} \underline{k}_o \cdot \partial_{\hat{\underline{x}}}\right)^2 b_1^{(1)}. \qquad \text{(A.61)}$$

Thus,

$$\varepsilon\partial_{\hat{z}}b_1^{(2)} = (-i\underline{k}_o/k_o)\cdot(\varepsilon\partial_{\underline{\hat{x}}}b_1^{(2)}) - \frac{1}{2k_o}\left[(\varepsilon^2\partial_{\underline{\hat{x}}}\cdot\partial_{\underline{\hat{x}}}b_1^{(1)}) - \left(\frac{\varepsilon}{k_o}\,\underline{k}_o\cdot\partial_{\underline{\hat{x}}}\right)^2 b_1^{(1)}\right]. \tag{A.62}$$

Substituting for $b_1^{(2)}$ and $b_1^{(1)}$ in (A.62) yields

$$\varepsilon\partial_{\hat{z}}b_1^{(2)} = (-i\underline{k}_o/k_o)\cdot\left[-\frac{i\omega_o}{k_o}(\varepsilon\partial_{\underline{\hat{x}}}a_1^{(2)}) + \frac{\omega_o}{2k_o^3}\cdot(\varepsilon\partial_{\underline{\hat{x}}}\underline{k}_o\cdot\varepsilon\partial_{\underline{\hat{x}}}a_1^{(1)}) + \right.$$

$$\left. + i\omega_o(\varepsilon\partial_{\underline{\hat{x}}}a_o^{(1)})a_1^{(1)} + i\omega_o a_o^{(1)}(\varepsilon\partial_{\underline{\hat{x}}}a_1^{(1)})\right] +$$

$$+ \frac{i\omega_o}{2k_o^2}\left[(\varepsilon^2\partial_{\underline{x}}\cdot\partial_{\underline{x}}a_1^{(1)}) - \left(\frac{\varepsilon}{k_o}\,\underline{k}_o\cdot\partial_{\underline{\hat{x}}}\right)^2 a_1^{(1)}\right] =$$

$$= -\frac{\omega_o}{k_o^2}\,\underline{k}_o\cdot(\varepsilon\partial_{\underline{\hat{x}}}a_1^{(2)}) - \frac{i\omega_o}{2k_o^2}\left(\frac{\varepsilon}{k_o}\,\underline{k}_o\cdot\partial_{\underline{\hat{x}}}\right)^2 a_1^{(1)} + \frac{\omega_o}{k_o}\,\underline{k}_o\cdot(\varepsilon\partial_{\underline{\hat{x}}}a_o^{(1)})a_1^{(1)} +$$

$$+ \frac{\omega_o}{k_o}\,a_o^{(1)}\cdot\underline{k}_o\cdot(\varepsilon\partial_{\underline{\hat{x}}}a_1^{(1)}) + \frac{i\omega_o}{2k_o^2}\left[(\varepsilon^2\partial_{\underline{\hat{x}}}\cdot\partial_{\underline{\hat{x}}}a_1^{(1)}) - \left(\frac{\varepsilon}{k_o}\,\underline{k}_o\cdot\partial_{\underline{\hat{x}}}\right)^2 a_1^{(1)}\right] =$$

$$= -\frac{\omega_o}{k_o^2}\,\underline{k}_o\cdot(\varepsilon\partial_{\underline{\hat{x}}}a_1^{(2)}) + \frac{\omega_o}{k_o}\,\underline{k}_o\cdot(\varepsilon\partial_{\underline{\hat{x}}}a_o^{(1)})a_1^{(1)} + \frac{\omega_o}{k_o}\,a_o^{(1)}\cdot\underline{k}_o\cdot(\varepsilon\partial_{\underline{\hat{x}}}a_1^{(1)}) +$$

$$+ \frac{i\omega_o}{2k_o^2}\left[(\varepsilon^2\partial_{\underline{\hat{x}}}\cdot\partial_{\underline{\hat{x}}}a_1^{(1)}) - 2\left(\frac{\varepsilon}{k_o}\,\underline{k}_o\cdot\partial_{\underline{\hat{x}}}\right)^2 a_1^{(1)}\right] \quad \text{on } z = 0. \tag{A.63}$$

Substituting in (A.55) for $(\varepsilon\partial_{\hat{t}}b_1^{(2)})$ as given by (A.58), $(\varepsilon^2\partial_{\hat{t}}\partial_{\hat{t}}b_1^{(1)})$ as given by (A.59), $(\varepsilon\partial_{\hat{z}}b_1^{(2)})$ as given by (A.63), $(\varepsilon\partial_{\underline{\hat{x}}}b_o^{(n)})|_{z=0}$ by $\underline{U}^{(n+1)}$, $b_1^{(2)}$ as given by (A.43), $(\varepsilon\partial_{\hat{z}}b_1^{(1)})$ as given by (A.39), $(\varepsilon\partial_{\hat{t}}a_1^{(1)})$ as given by (A.40), $(\varepsilon^2\partial_{\hat{z}}^2b_o^{(0)})$ according to (A.9) and (A.11), and $(\varepsilon\partial_{\hat{z}}b_o^{(1)})$ according to (A.46) yields

$$2i\omega_o(\varepsilon\partial_{\hat{t}}a_1^{(2)}) + \frac{\omega_o^2}{4k_o^2}\left(\frac{\varepsilon}{k_o}\cdot\underline{k}_o\cdot\partial_{\hat{\underline{x}}}\right)^2 a_1^{(1)} + \frac{i\omega_o}{2k_o^2}\,\underline{k}_o\cdot(\varepsilon\partial_{\hat{\underline{x}}}\underline{k}_o\cdot\underline{U}^{(1)})a_1^{(1)} +$$

$$+ \frac{i\omega_o}{2k_o^2}(\underline{k}_o\cdot\underline{U}^{(1)})(\underline{k}_o\cdot\varepsilon\partial_{\hat{\underline{x}}}a_1^{(1)}) - i\omega_o k_o(\varepsilon\partial_{\hat{t}}a_o^{(1)})a_1^{(1)} +$$

$$+ \frac{i\omega_o^2}{2k_o}a_o^{(1)}\underline{k}_o\cdot(\varepsilon\partial_{\hat{\underline{x}}}a_1^{(1)}) - \omega_o k_o a_o^{(1)}(\underline{k}_o\cdot\underline{U}^{(1)})a_1^{(1)} + 2i\omega_o(\varepsilon^2\partial_{\hat{t}}a_1^{(1)}) +$$

$$+ \frac{i\omega_o^2}{k_o^2}\,\underline{k}_o\cdot(\varepsilon\partial_{\hat{\underline{x}}}a_1^{(2)}) - \frac{i\omega_o^2}{k_o}\,\underline{k}_o\cdot(\varepsilon\partial_{\hat{\underline{x}}}a_o^{(1)})a_1^{(1)} - \frac{i\omega_o^2}{k_o}\,a_o^{(1)}\underline{k}_o\cdot(\varepsilon\partial_{\hat{\underline{x}}}a_1^{(1)}) +$$

$$+ \frac{\omega_o^2}{2k_o^2}\left[(\varepsilon^2\partial_{\hat{\underline{x}}}\cdot\partial_{\hat{\underline{x}}}a_1^{(1)}) - 2\left(\frac{\varepsilon}{k_o}\,\underline{k}_o\cdot\partial_{\hat{\underline{x}}}\right)^2 a_1^{(1)}\right] + \frac{i\omega_o^2}{k_o}\,\underline{k}_o\cdot(\varepsilon\partial_{\hat{\underline{x}}}a_o^{(1)})a_1^{(1)} +$$

$$- 2\omega_o\underline{k}_o\cdot\underline{U}^{(2)}a_1^{(1)} - 2\omega_o(\underline{k}_o\cdot\underline{U}^{(1)})a_1^{(2)} - \frac{i\omega_o}{2k_o^2}(\underline{k}_o\cdot\underline{U}^{(1)})(\underline{k}_o\cdot\varepsilon\partial_{\hat{\underline{x}}}a_1^{(1)}) +$$

$$+ \omega_o k_o(\underline{k}_o\cdot\underline{U}^{(1)})a_o^{(1)}a_1^{(1)} + \underline{U}^{(1)}\cdot(2i\omega_o\varepsilon\partial_{\hat{\underline{x}}}a_1^{(1)}) - 4\omega_o^2k_o^2\left|a_1^{(1)}\right|^2 a_1^{(1)} +$$

$$+ a_o^{(1)}\cdot\left[\frac{i\omega_o^2}{k_o}\,\underline{k}_o\cdot(\varepsilon\partial_{\hat{\underline{x}}}a_1^{(1)}) - \frac{i\omega_o^2}{2k_o}\,\underline{k}_o\cdot(\varepsilon\partial_{\hat{\underline{x}}}a_1^{(1)}) + \omega_o k_o(\underline{k}_o\cdot\underline{U}^{(1)})a_1^{(1)}\right] +$$

$$- i\omega_o Sa_1^{(1)} + i\omega_o(\varepsilon\partial_{\hat{\underline{x}}}\cdot\underline{U}^{(1)})a_1^{(1)} + i\omega_o k_o(\varepsilon\partial_{\hat{t}}a_o^{(1)})a_1^{(1)} +$$

$$- \omega_o k_o a_o^{(1)}\cdot(\underline{k}_o\cdot\underline{U}^{(1)})a_1^{(1)} = 0 \qquad \text{on } z = 0 \tag{A.64}$$

Dividing through by $2i\omega_o$ and collecting terms yields

$$(\varepsilon\partial_{\hat{t}}a_1^{(2)}) + (\varepsilon^2\partial_{\hat{\hat{t}}}a_1^{(1)}) + \frac{\omega_o}{2k_o^2}\,\underline{k}_o\cdot(\varepsilon\partial_{\underline{\hat{x}}}a_1^{(2)}) +$$

$$- \frac{i\omega_o}{k_o^2}\left[\frac{1}{4}\,(\varepsilon^2\partial_{\underline{\hat{x}}}\cdot\partial_{\underline{\hat{x}}}a_1^{(1)}) - \frac{3}{8}\left(\frac{\varepsilon}{k_o}\,\underline{k}_o\cdot\partial_{\underline{\hat{x}}}\right)^2 a_1^{(1)}\right] + 2i\omega_o k_o^2\left|a_1^{(1)}\right|^2 a_1^{(1)} +$$

$$+ (i\underline{k}_o\cdot\underline{U}^{(2)})a_1^{(1)} + (i\underline{k}_o\cdot\underline{U}^{(1)})a_1^{(2)} + \underline{U}^{(1)}\cdot(\varepsilon\partial_{\underline{\hat{x}}}a_1^{(1)}) + \frac{1}{2}\,(\varepsilon\partial_{\underline{\hat{x}}}\cdot U^{(1)})a_1^{(1)} +$$

$$- \frac{1}{2}\,Sa_1^{(1)} + \frac{1}{4k_o^2}\,\underline{k}_o\cdot(\varepsilon\partial_{\underline{\hat{x}}}\underline{k}_o\cdot\underline{U}^{(1)})a_1^{(1)} = 0 \qquad \text{on } z = 0. \tag{A.65}$$

At this stage, the need for the second slow-time variable $\hat{\hat{t}}$ becomes clear. In the case $\underline{U}^{(1)} = 0$, dropping $(\varepsilon^2\partial_{\hat{\hat{t}}}a_1^{(1)})$ from (A.65) would lead to secular terms in the solution for $a_1^{(2)}$.

Combining equations (A.40) and (A.65), setting

$$A = 2a_1, \quad \underline{U} = \left.\frac{\partial b_o}{\partial \underline{x}}\right|_{z=0}, \tag{A.66}$$

ignoring terms of order $O(\varepsilon^4)$ and higher, and locating the x_1-axis along $\underline{k}_o$ and the x_2-axis perpendicular to it yields

$$i\left(\frac{\partial A}{\partial t} + \frac{\omega_o}{2k_o}\,\frac{\partial A}{\partial x_1}\right) - \frac{\omega_o}{8k_o^2}\,\frac{\partial^2 A}{\partial x_1^2} + \frac{\omega_o}{4k_o^2}\,\frac{\partial^2 A}{\partial x_2^2} - \frac{\omega_o k_o^2}{2}\,|A|^2 A + i\underline{U}\cdot\frac{\partial A}{\partial \underline{x}} +$$

$$+ i\left[(i\underline{k}_o\cdot\underline{U}) + \left(\frac{3\partial}{4\partial x_1}\,,\ \frac{1}{2}\,\frac{\partial}{\partial x_2}\right)\cdot\underline{U}\right]A = 0 \tag{A.67}$$

assuming that

$$S\Big|_{z=0} = 0. \tag{A.68}$$

Equation (A.67) is the two-space-dimensional nonlinear Schrödinger equation with current terms.

Given the form of the disturbance term S, one can compute $b_o^{(0)}$ from (A.35). The quantity $a_o^{(1)}$ then follows from (A.34). With $a_o^{(1)}$ in hand, one can compute $b_o^{(1)}$ via (A.46). Substituting $b_o = b_o^{(0)} + b_o^{(1)} + O(\varepsilon^2)$ into (A.66) yields $\underline{U}$ to $O(\varepsilon^3)$. This value of $\underline{U}$ can then be used to compute A to $O(\varepsilon^3)$ via (A.67). Now A is the complex amplitude of the fundamental component of the carrier wave. To compute the actual surface displacement, η, one uses the definition of A, (A.66), the original decomposition of η, (A.6), and (A.10) to write

$$\eta = a_o^{(1)} + a_o^{(2)} + \mathrm{Re}\left[Ae^{i(\underline{k}_o\cdot\underline{x}-\omega_o t)} + \frac{1}{2}k_o A^2 e^{i(2\underline{k}_o\cdot\underline{x}-2\omega_o t)}\right] + O(\varepsilon^3) \quad \text{(A.69)}$$

where $a_o^{(1)}$ is given by (A.34), $a_o^{(2)}$ is given by (A.45), and the term in A^2 follows from (A.49). The frequency ω_o is specified in terms of k_o by (A.31).

In order to obtain a similar expression for the velocity potential ϕ, a bit more work must be done. It follows from (A.32) and (A.43) that

$$\begin{aligned} b_1 &= -\frac{i\omega_o}{k_o}a_1 + \frac{\omega_o}{2k_o^3}\underline{k}_o\cdot\frac{\partial a_1}{\partial\underline{x}} + i\omega_o a_o^{(1)}a_1 + O(\varepsilon^3) \\ &= -\frac{i\omega_o}{k_o}a_1 + \frac{\omega_o}{2k_o^2}\frac{\partial a_1}{\partial x_1} + i\omega_o a_o^{(1)}a_1 + O(\varepsilon^3) \qquad \text{on } z = 0. \end{aligned} \quad \text{(A.70)}$$

From (A.39) and (A.62) it follows that

$$\frac{\partial b_1}{\partial y} = -\frac{i}{k_o}\cdot\underline{k}_o\cdot\frac{\partial b_1}{\partial\underline{x}} - \frac{1}{2k_o}\left[\left(\frac{\partial}{\partial\underline{x}}\cdot\frac{\partial}{\partial\underline{x}}b_1\right) - \left(\frac{1}{k_o}\underline{k}_o\cdot\frac{\partial}{\partial\underline{x}}\right)^2 b_1\right] + O(\varepsilon^3). \quad \text{(A.71)}$$

Equations (A.70) and (A.71) are in principle sufficient to determine b_1 for all $\underline{x}$ and t and $z \leq 0$.

In order to obtain b_0 to $O(\varepsilon^3)$ all that remains to be done is to determine $b_0^{(2)}$. As noted earlier, $b_0^{(0)}$ and $b_0^{(1)}$ follow from (A.34), (A.35), and (A.46). The value of $b_0^{(2)}$ follows from equation (A.22), which reduces at $O(\varepsilon^3)$ to

$$
\begin{aligned}
&(\varepsilon\partial_{\hat{t}} a_0^{(2)}) + (-i\underline{k}_0 b_{-1}^{(1)})\cdot(\varepsilon\partial_{\hat{\underline{x}}} a_1^{(1)}) + (\varepsilon\partial_{\hat{\underline{x}}} b_{-1}^{(1)})(i\underline{k}_0 a_1^{(1)}) + \\
&\quad + (i\underline{k}_0 b_1^{(1)})\cdot(\varepsilon\partial_{\hat{\underline{x}}} a_{-1}^{(1)}) + (\varepsilon\partial_{\hat{\underline{x}}} b_1^{(1)})(-i\underline{k}_0 a_{-1}^{(1)}) + (-i\underline{k}_0 b_{-1}^{(2)})\cdot(i\underline{k}_0 a_1^{(1)}) + \\
&\quad + (-i\underline{k}_0 b_{-1}^{(1)})\cdot(i\underline{k}_0 a_1^{(2)}) + (i\underline{k}_0 b_1^{(2)})\cdot(i\underline{k}_0 a_{-1}^{(1)}) + (i\underline{k}_0 b_1^{(1)})\cdot(-i\underline{k}_0 a_{-1}^{(2)}) + \\
&\quad + (\varepsilon\partial_{\hat{\underline{x}}} b_0^{(0)})\cdot(\varepsilon\partial_{\hat{\underline{x}}} a_0^{(1)}) + a_0^{(1)}\cdot\Big[(-ik_0\underline{k}_0 b_{-1}^{(1)})\cdot(i\underline{k}_0 a_1^{(1)}) + \\
&\qquad\qquad + ik_0\underline{k}_0 b_1^{(1)})\cdot(-i\underline{k}_0 a_{-1}^{(1)})\Big] = \\
&= (\varepsilon\partial_{\hat{z}} b_0^{(2)}) + a_0^{(1)}\cdot(\varepsilon^2\partial_{\hat{z}}^2 b_0^{(0)}) + a_1^{(1)}\cdot(2k_0\varepsilon\partial_{\hat{z}} b_{-1}^{(1)}) + a_{-1}^{(1)}\cdot(2k_0\varepsilon\partial_{\hat{z}} b_1^{(1)}) + \\
&\quad + a_1^{(2)}\cdot(k_0^2 b_{-1}^{(1)}) + a_{-1}^{(2)}\cdot(k_0^2 b_1^{(1)}) + a_1^{(1)}\cdot(k_0^2 b_{-1}^{(2)}) + a_{-1}^{(1)}\cdot(k_0^2 b_1^{(2)}) + \\
&\quad + a_0^{(1)}a_1^{(1)}\cdot(k_0^3 b_{-1}^{(1)}) + a_0^{(1)}a_{-1}^{(1)}\cdot(k_0^3 b_1^{(1)}) \quad \text{on } z = 0. \qquad \text{(A.72)}
\end{aligned}
$$

Applying (A.18), substituting for $b_1^{(1)}$ from (A.32), and simplifying yields

$$
\begin{aligned}
(\varepsilon\partial_{\hat{t}} a_0^{(2)}) + (\varepsilon\partial_{\hat{\underline{x}}} b_0^{(0)})\cdot(\varepsilon\partial_{\hat{\underline{x}}} a_0^{(1)}) &= (\varepsilon\partial_{\hat{z}} b_0^{(2)}) + a_0^{(1)}\cdot(\varepsilon^2\partial_{\hat{z}}^2 b_0^{(0)}) + \\
&\quad + a_1^{(1)}\cdot(2k_0\varepsilon\partial_{\hat{z}} b_{-1}^{(1)}) + a_{-1}^{(1)}\cdot(2k_0\varepsilon\partial_{\hat{z}} b_1^{(1)}) \\
&\quad \text{on } z = 0. \qquad \text{(A.73)}
\end{aligned}
$$

Substituting for $(\varepsilon^2 \partial_{\hat{z}}^2 b_o^{(0)})$ according to (A.35) and (A.68), and substituting for $(\varepsilon \partial_{\hat{z}} b_{\pm 1}^{(1)})$ according to (A.39), (A.8), and (A.11) reduces (A.73) to

$$\frac{\partial b_o^{(2)}}{\partial z} = \frac{\partial a_o^{(2)}}{\partial t} + \underline{U}^{(1)} \cdot \frac{\partial a_o^{(1)}}{\partial \underline{x}} + \left(\frac{\partial}{\partial \underline{x}} \cdot \underline{U}^{(1)} \right) a_o^{(1)} + \frac{\omega_o}{2k_o} \underline{k}_o \cdot \frac{\partial |A|^2}{\partial \underline{x}} + O(\varepsilon^4)$$

$$\text{on } z = 0. \tag{A.74}$$

It follows from (A.9) and (A.11) that

$$\nabla^2 b_o^{(2)} = 0 \qquad \text{on } z \leq 0 \tag{A.75}$$

and from (A.4) and (A.11) that,

$$\frac{\partial b_o^{(2)}}{\partial z} = 0 \qquad \text{on } z = -\infty. \tag{A.76}$$

Equations (A.74), (A.75), and (A.76) are in principle sufficient to determine $b_o^{(2)}$.

As noted earlier, $b_2^{(2)}$ vanishes. Thus, we have

$$\phi = b_o^{(0)} + b_o^{(1)} + b_o^{(2)} + 2\,\mathrm{Re}\left[b_1 e^{i(\underline{k}_o \cdot \underline{x} - \omega_o t)} e^{k_o z} \right] + O(\varepsilon^3) \tag{A.77}$$

where $\phi\big|_{z=0}$ can be evaluated explicitly from the preceding formulae, and ϕ is implicitly determined on the domain $z \leq 0$.

It would be possible to deduce further information from equations (A.24)-(A.27) at $O(\varepsilon^3)$. In particular, (A.24) and (A.25) allow one to write $b_1^{(3)}$ in terms of $a_1^{(3)}$, while (A.26) and (A.27) reduce to formulae for $a_2^{(3)}$ and $b_2^{(3)}$. However, no further detail will be given here, as this additional information would not make it possible to improve the expressions for η and ϕ to $O(\varepsilon^4)$.

APPENDIX B

COMPARISON OF PERTURBED NONLINEAR SCHRÖDINGER RESULTS FOR UNIFORM WAVES ON A CURRENT WITH THE RESULTS OF LONGUET-HIGGINS AND STEWART

In Chapter 5, the formulae (5.31) and (5.32) were shown to give the perturbation of a uniform wave generated by a current of small magnitude relative to the group velocity. In order to compare this result with those obtained by Longuet-Higgins and Stewart [10,11] for linear waves, one must consider the limiting case in which the amplitude of the unperturbed wave approaches zero.

In the terminology of Chapter 5, one must consider the case $a_o = 0$. When this holds, equation (5.21) yields nothing at $O(\varepsilon)$. At $O(\varepsilon^2)$, it gives

$$-\theta_{1t}a_1 - c_g\theta_{1x}a_1 - k_o a_1 U = 0 \tag{B.1}$$

which reduces to

$$\theta_1' = -k_o \frac{U}{c_g} . \tag{B.2}$$

At $O(\varepsilon^2)$, (5.22) yields

$$c_g a_1' = 0. \tag{B.3}$$

At $O(\varepsilon^3)$, (5.21) yields

$$-\theta_{2t}a_1 - \theta_{1t}a_2 - c_g(\theta_{1x}a_2 + \theta_{2x}a_1) - U\theta_{1x}a_1 - k_o a_2 U$$

$$+ \frac{\omega_o}{8k_o^2}\theta_{1x}^2 a_1 - \frac{1}{2}\omega_o k_o^2 a_1^3 = 0. \tag{B.4}$$

which reduces to

$$\theta_2' = \frac{5}{4} k_o \left(\frac{U}{c_g}\right)^2 - \frac{1}{2} \omega_o k_o^2 a_1^2 / c_g. \tag{B.5}$$

Equation (5.22) at $O(\varepsilon^3)$ yields

$$a_{2t} + c_g a_{2x} + \frac{3}{4} U_x a_1 - \frac{\omega_o}{8k_o^2} \theta_{1xx} a_1 = 0 \tag{B.6}$$

which reduces to

$$a_2 = - a_1 \frac{U}{c_g} . \tag{B.7}$$

Note that $\lim_{a_o \to 0} a_1/a_o$ as given by (5.31) is equal to a_2/a_1 as given by (B.7). Similarly, $\lim_{a_o \to 0} \theta_1'$ as given by (5.32) is equal to θ_1' as given by (B.2). Note also that, whether or not a_o vanishes, one must have

$$U/c_g << 1 \tag{B.8}$$

in order for the perturbation scheme to be valid.

The results of Longuet-Higgins and Stewart reduce to

$$(gk)^{1/2} + kU = (gk_o)^{1/2} \tag{B.9}$$

and

$$Ec\left(U + \frac{1}{2} c\right) = E_o c_o \cdot \frac{1}{2} c_o \tag{B.10}$$

where k represents a slowly-varying wavenumber with value k_o where $U = 0$; E represents wave energy (proportional to amplitude squared) with value E_o where $U = 0$; $c = (g/k)^{1/2}$ and $c_o = (g/k_o)^{1/2}$.

In the Schrödinger model, the k of equation (B.9) is approximated by

$$k = k_o + \theta_{1x} + \theta_{2x} + \cdots . \tag{B.11}$$

Thus

$$\begin{aligned}(gk)^{1/2} &\simeq (gk_o)^{1/2} \cdot \left(1 + \frac{\theta_1'}{k_o} + \frac{\theta_2'}{k_o}\right)^{1/2} \\ &\simeq (gk_o)^{1/2} \cdot \left[1 + \frac{1}{2}\left(\frac{\theta_1'}{k_o} + \frac{\theta_2'}{k_o}\right) - \frac{1}{8}\left(\frac{\theta_1'}{k_o}\right)^2\right]\end{aligned} \tag{B.12}$$

and substituting in (B.9) the values of θ_1' and θ_2' given by (B.2) and (B.5) yields

$$(gk)^{1/2} + kU = (gk_o)^{1/2} - \frac{1}{2}\omega_o k_o^2 a_1^2. \tag{B.13}$$

The only difference between (B.9) and (B.13) is the nonlinear term $-\frac{1}{2}\omega_o k_o a_1^2$ which is, of course, invisible in the linear model used by Longuet-Higgins and Stewart.

Replacing E by a^2 and E_o by a_1^2 in (B.10) and solving for a yields

$$a = a_1 \left(\frac{k}{k_o}\right)^{1/4} \left(\frac{U}{c_g} + \frac{c}{2c_g}\right)^{-1/2}. \tag{B.14}$$

It follows from (B.11) and the definition of c that

$$\frac{c}{2c_g} = 1 - \frac{1}{2}\frac{\theta_1'}{k_o} + O(\varepsilon^2). \tag{B.15}$$

Substituting (B.11), (B.15), and (B.2) in (B.14) yields

$$a = a_1\left[1 + \frac{\theta_1'}{k_o} + O(\varepsilon^2)\right]^{1/4}\left[1 - \frac{1}{2}\frac{\theta_1'}{k_o} + \frac{U}{c_g} + O(\varepsilon^2)\right]^{-1/2}$$

$$= a_1\left(1 - \frac{U}{c_g}\right) + O(\varepsilon^3). \qquad \text{(B.16)}$$

Comparison of (B.16) with (B.3) and (B.7) demonstrates consistency to $O(\varepsilon^3)$.

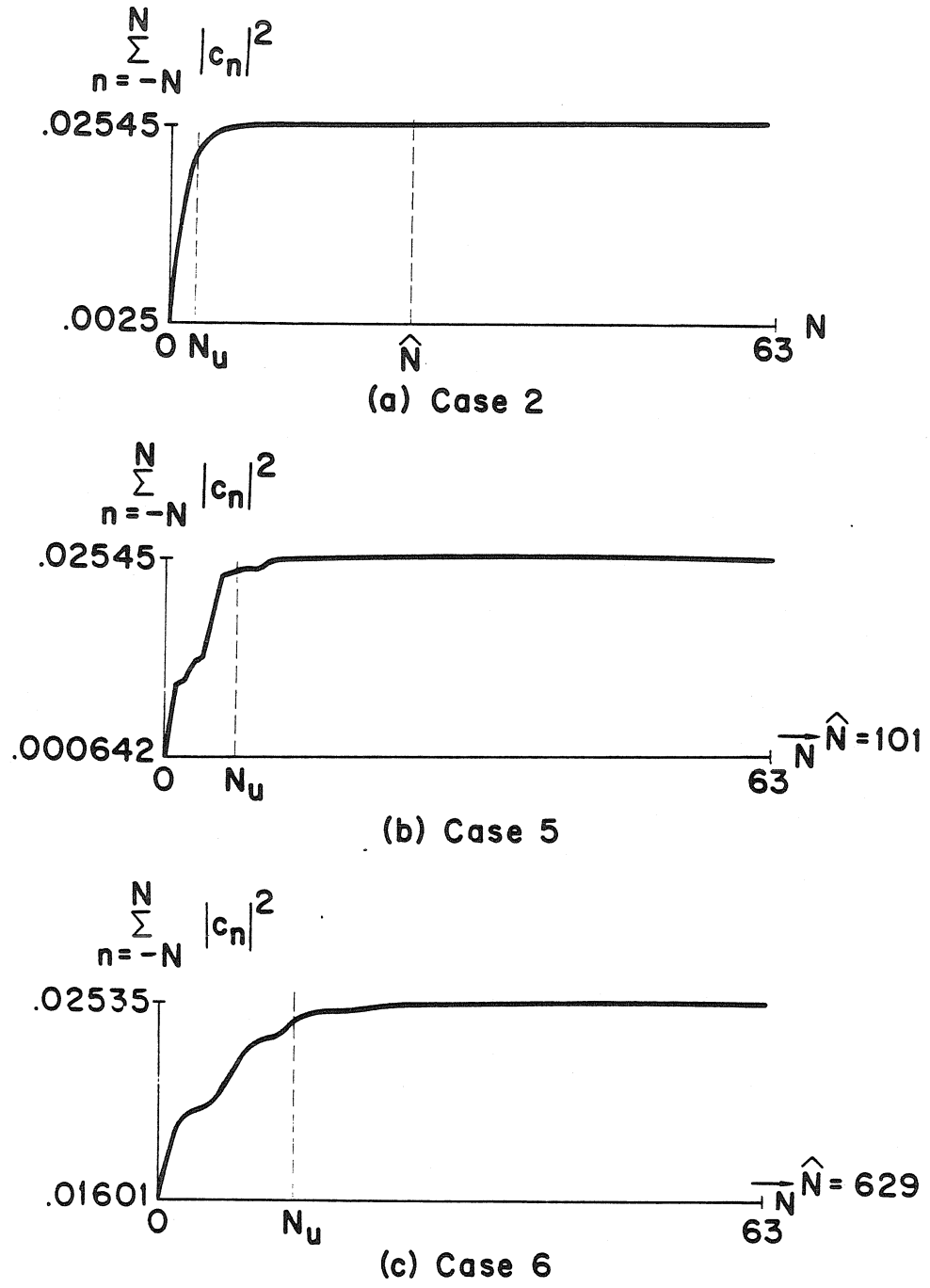

Figure 1.1. Energy in components -N,•••,N as a function of N at times of near-maximal energy spreading. (a) Case 2 at t = 1000; components ±1 and ±2 are unstable. (b) Case 5 at t = 750; components ±1,•••,±5 are unstable. (c) Case 6 at t = 350; components ±1,•••,±14 are unstable.

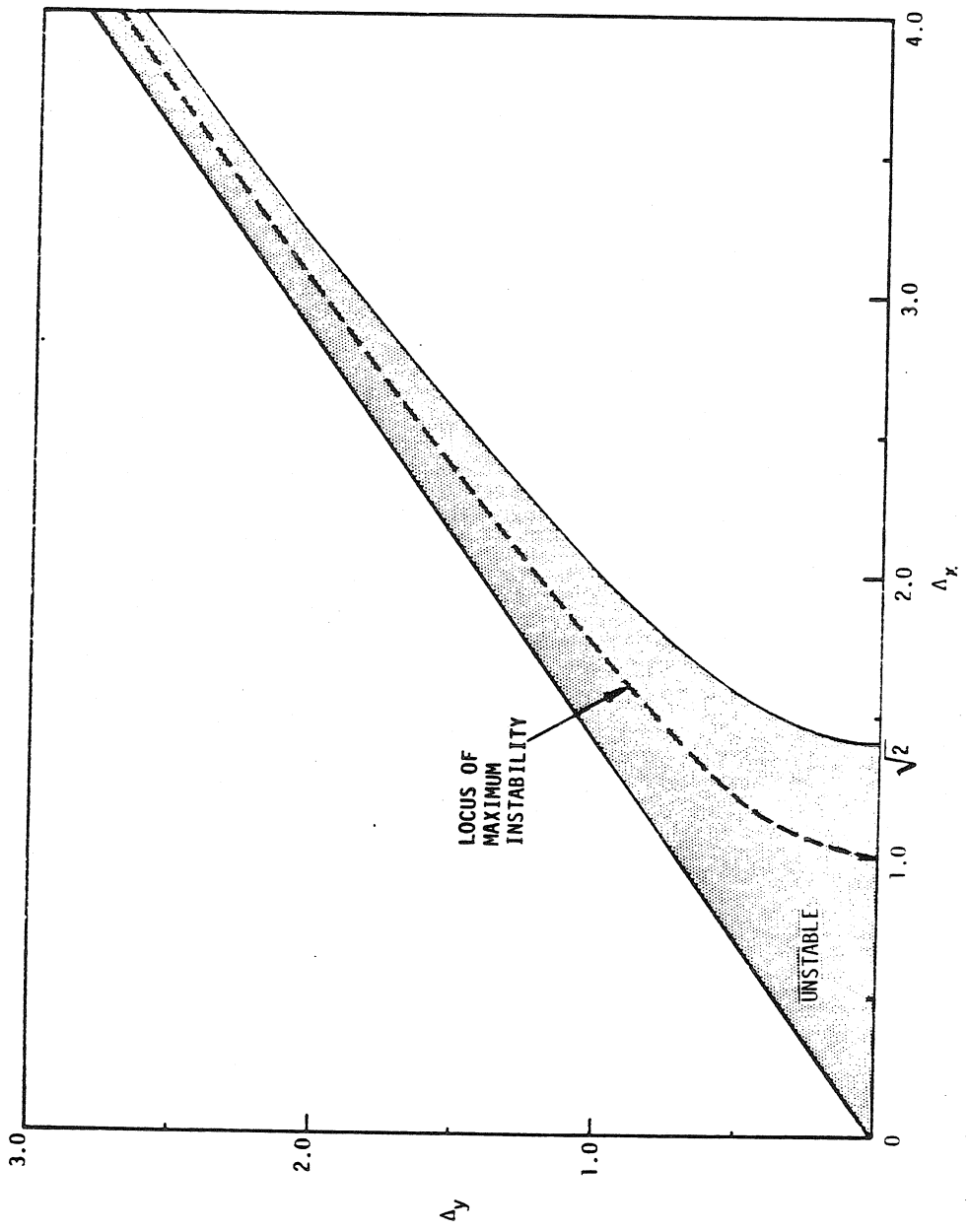

Figure 2.1. Benjamin-Feir instability diagram in two space dimensions. $\Delta_x = (k/2k_o)/(k_o a_o)$, $\Delta_y = (\kappa/2k_o)/(k_o a_o)$

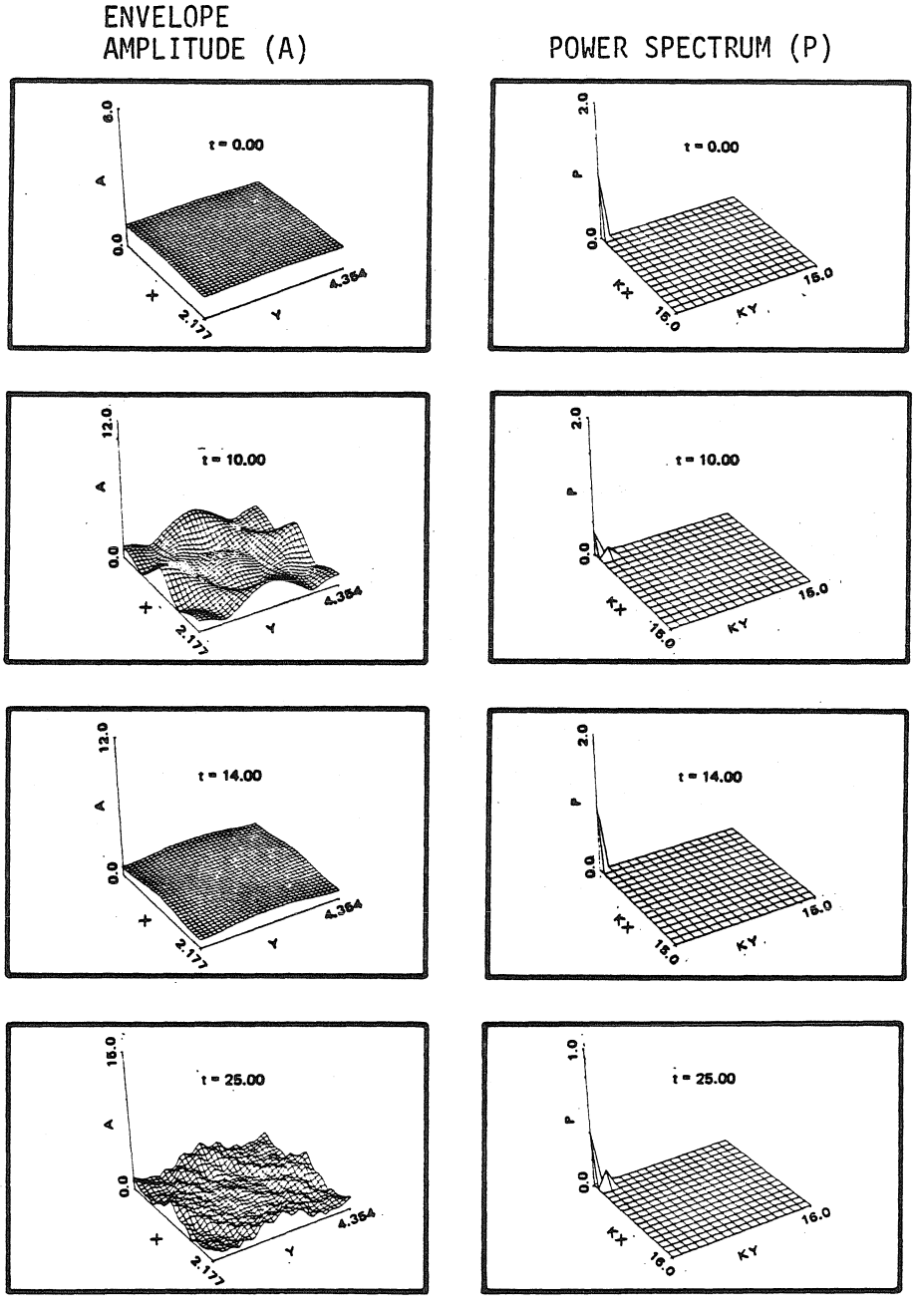

Figure 2.2. Evolution of an unstable perturbation of a uniform wavetrain on a two-dimensional surface.

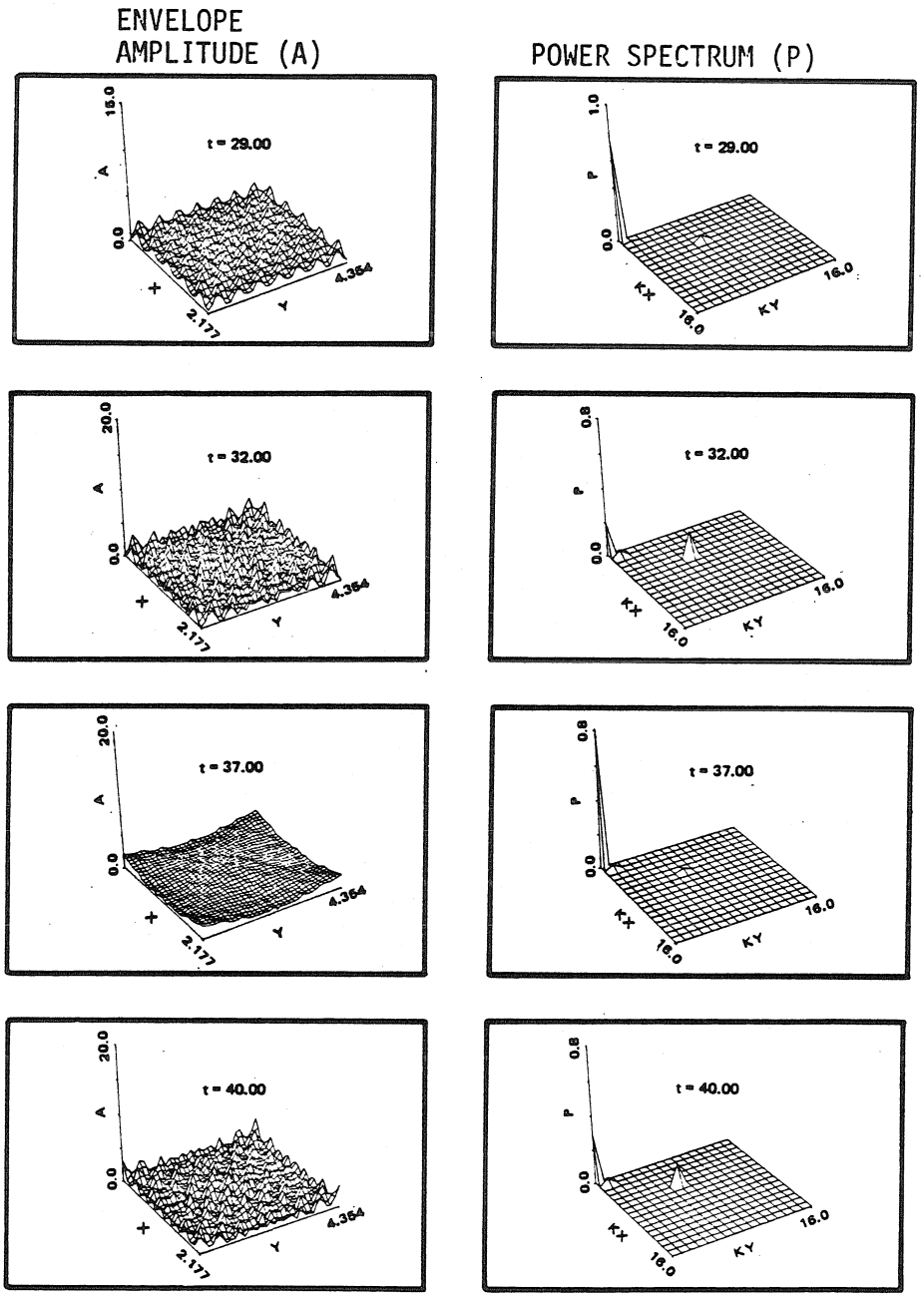

Figure 2.2. (Cont.)

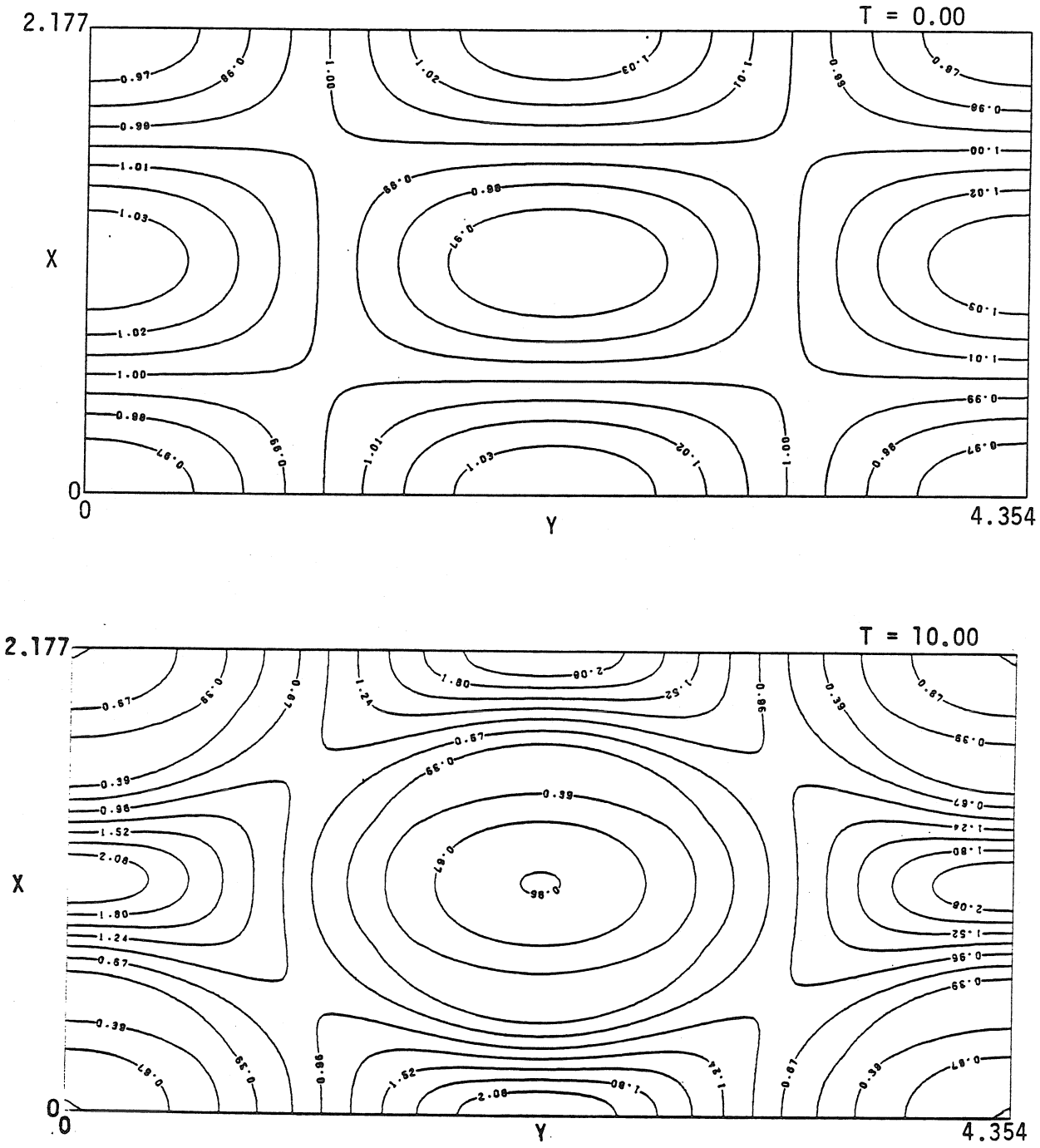

Figure 2.3. Contour plots of the envelope amplitude of Figure 2.2.

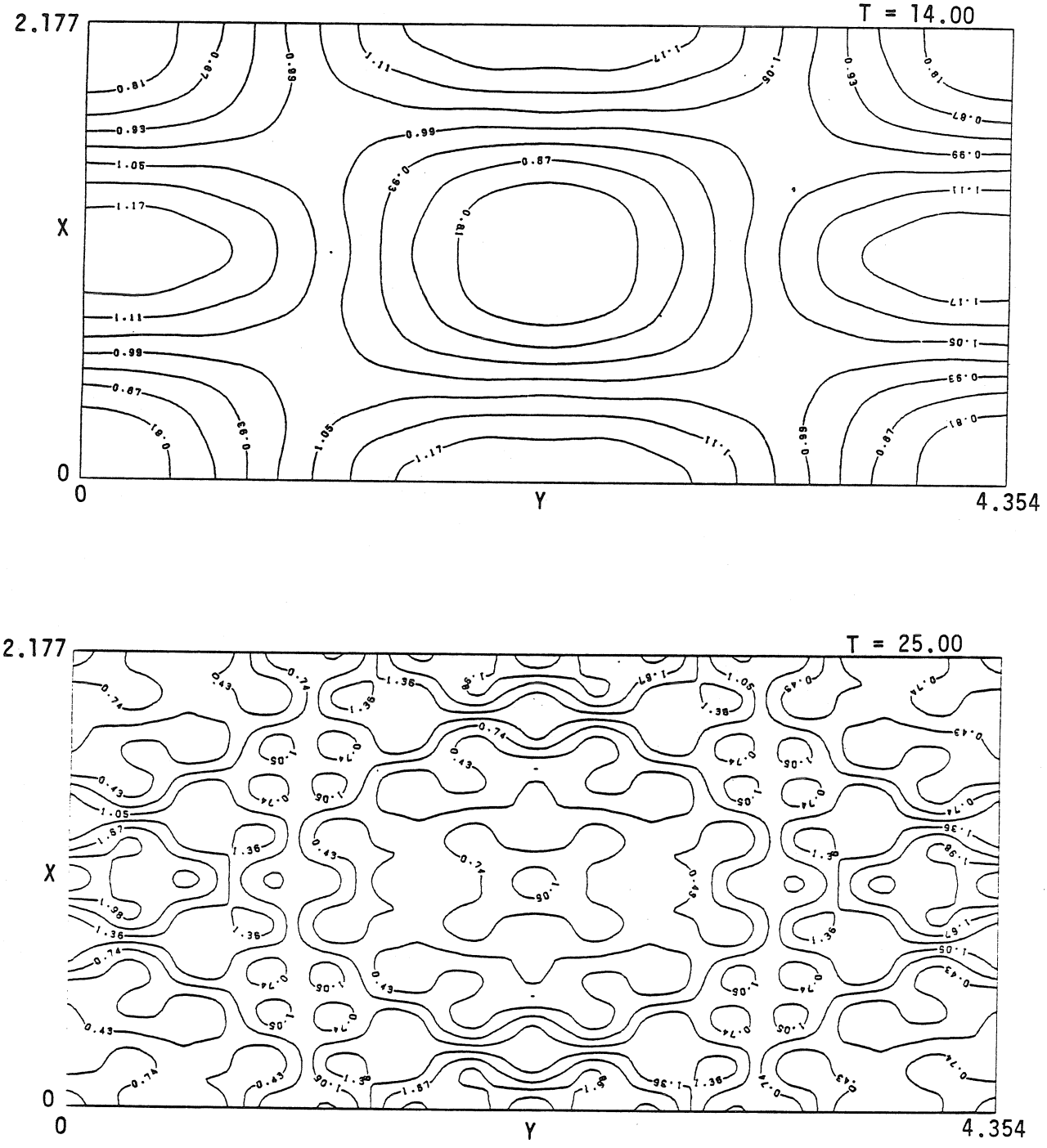

Figure 2.3. (Cont.).

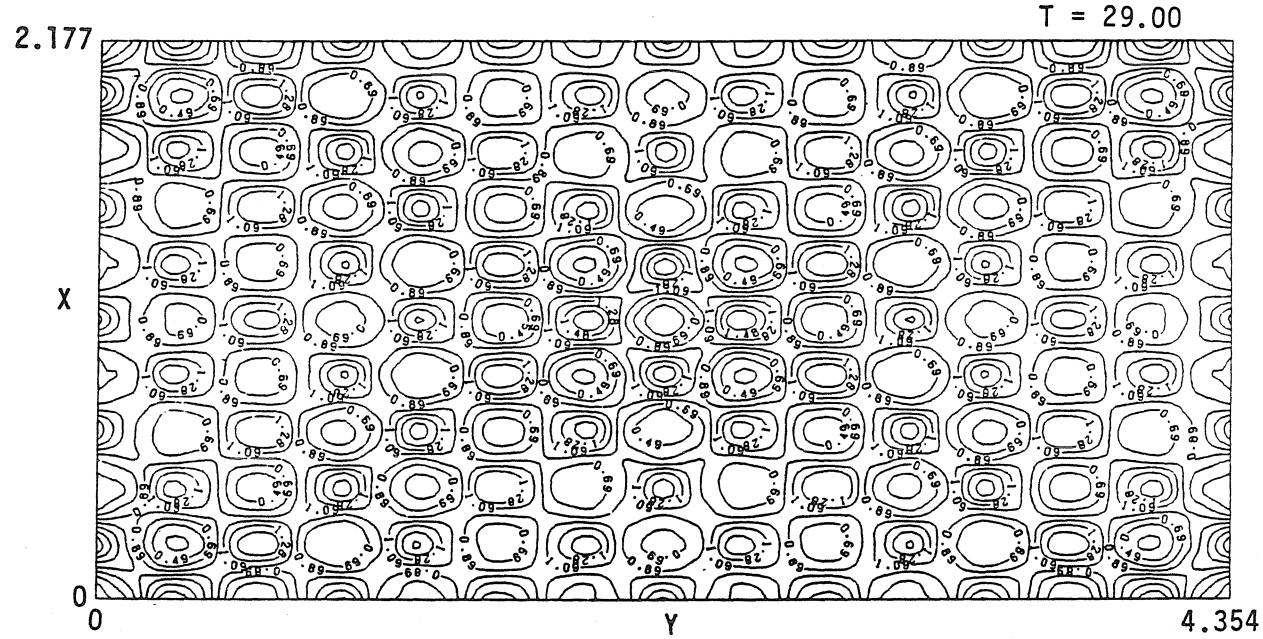

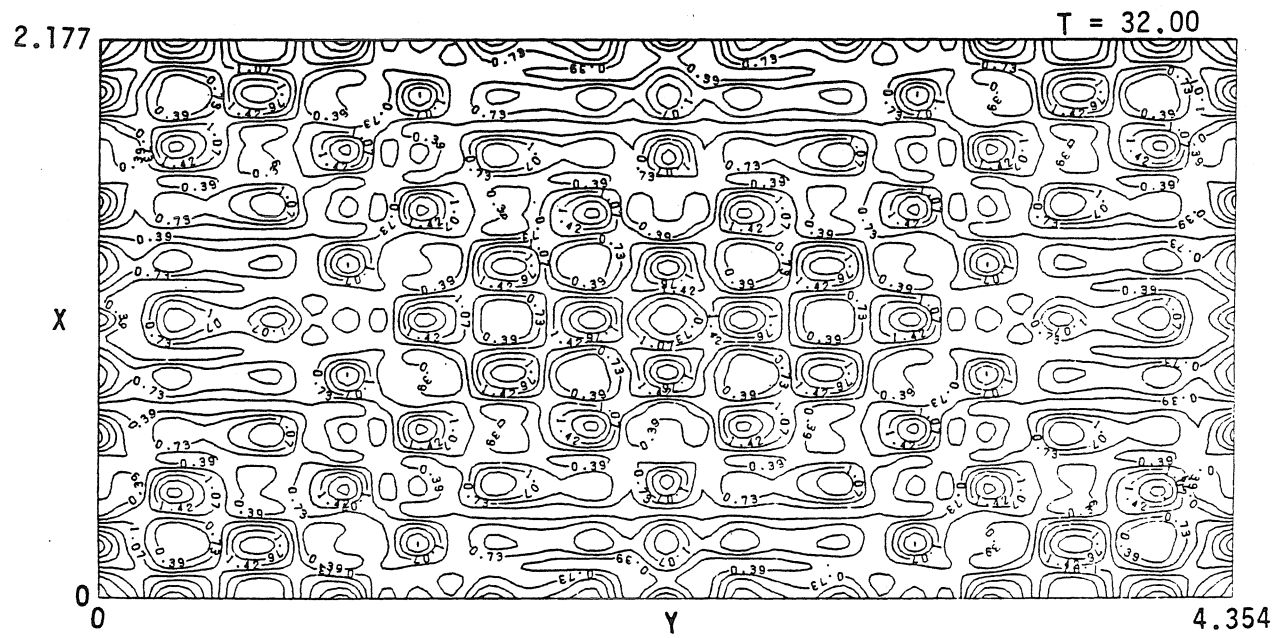

Figure 2.3. (Cont.).

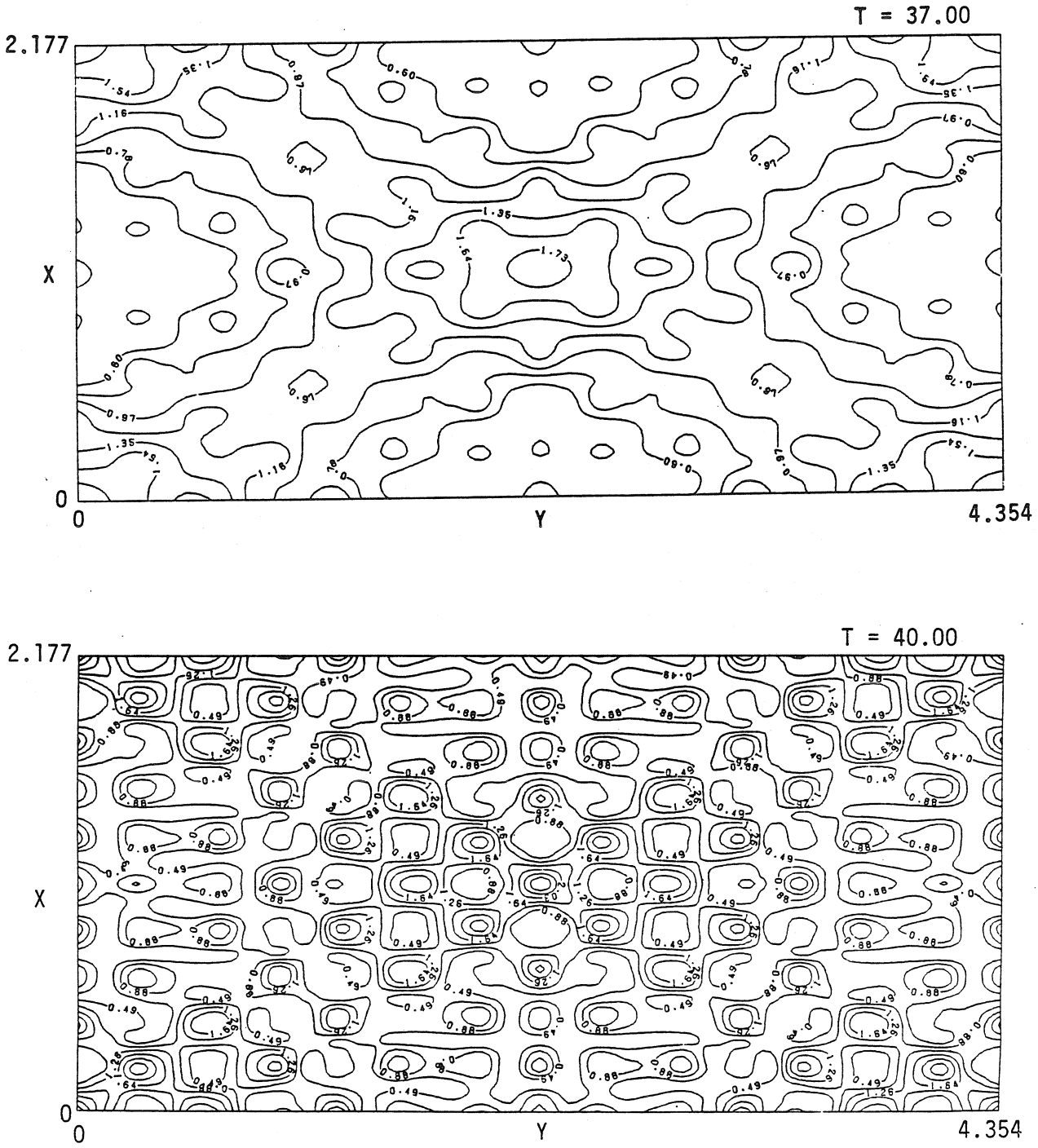

Figure 2.3. (Cont.).

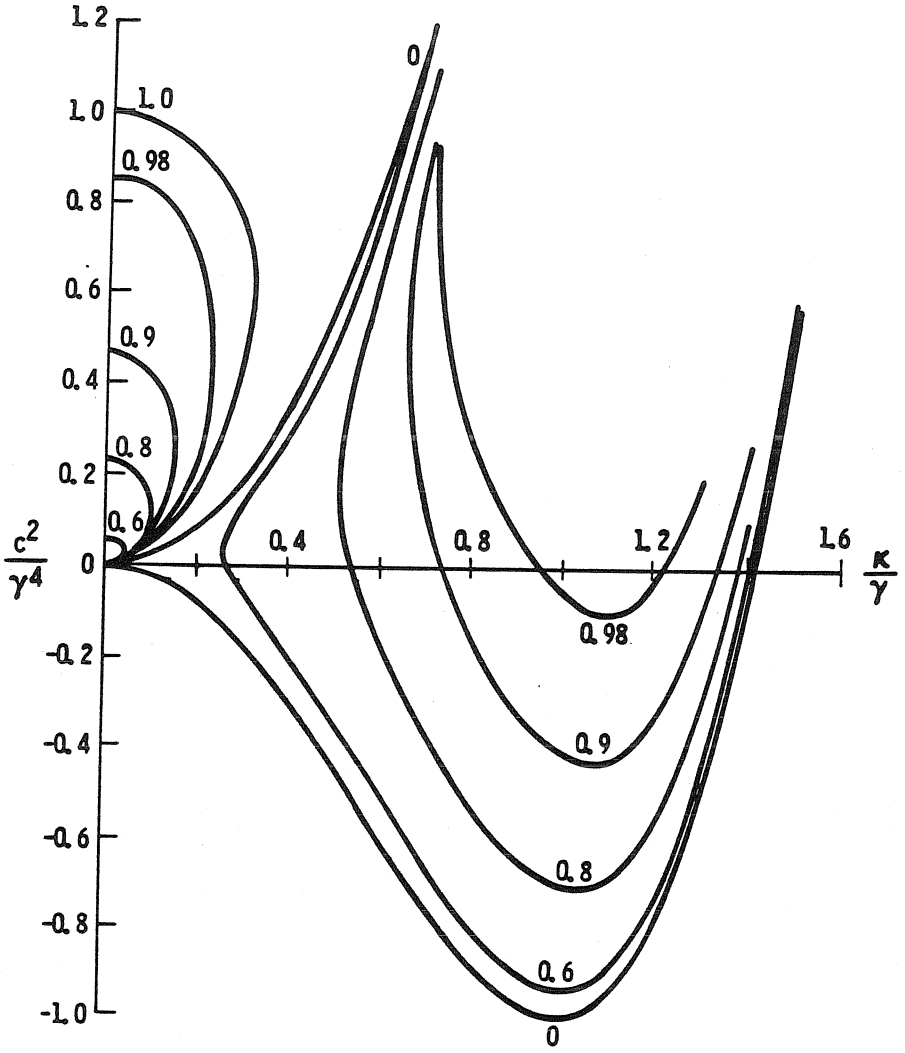

Figure 3.1. Stability results for even perturbations of periodic wave train solutions of the nonlinear Schrödinger equation in two space dimensions (where "even" signifies symmetry about the crests of the unperturbed solution). The abscissa is a dimensionless representation of the transverse wavenumber of the perturbation. The ordinate, c^2/γ^4, is a dimensionless representation of the time constant of the perturbation; that is, the perturbation will have terms proportional to $e^{i\omega_0 ct}$ and $e^{-i\omega_0 c^* t}$, or $e^{-i\omega_0 ct}$ and $e^{i\omega_0 c^* t}$, where $\omega_0 = \sqrt{gk_0}$, g is gravitational acceleration, and k_0 is the carrier wavenumber. The numeral (m) labeling each curve characterizes the unperturbed solution; m = 0 corresponds to a uniform wave, and m = 1 corresponds to a soliton. The parameter γ is given by $\gamma = \frac{1}{2} k_0 a_0 (2 - m^2)^{1/2}$, where a_0 is the carrier wave amplitude.

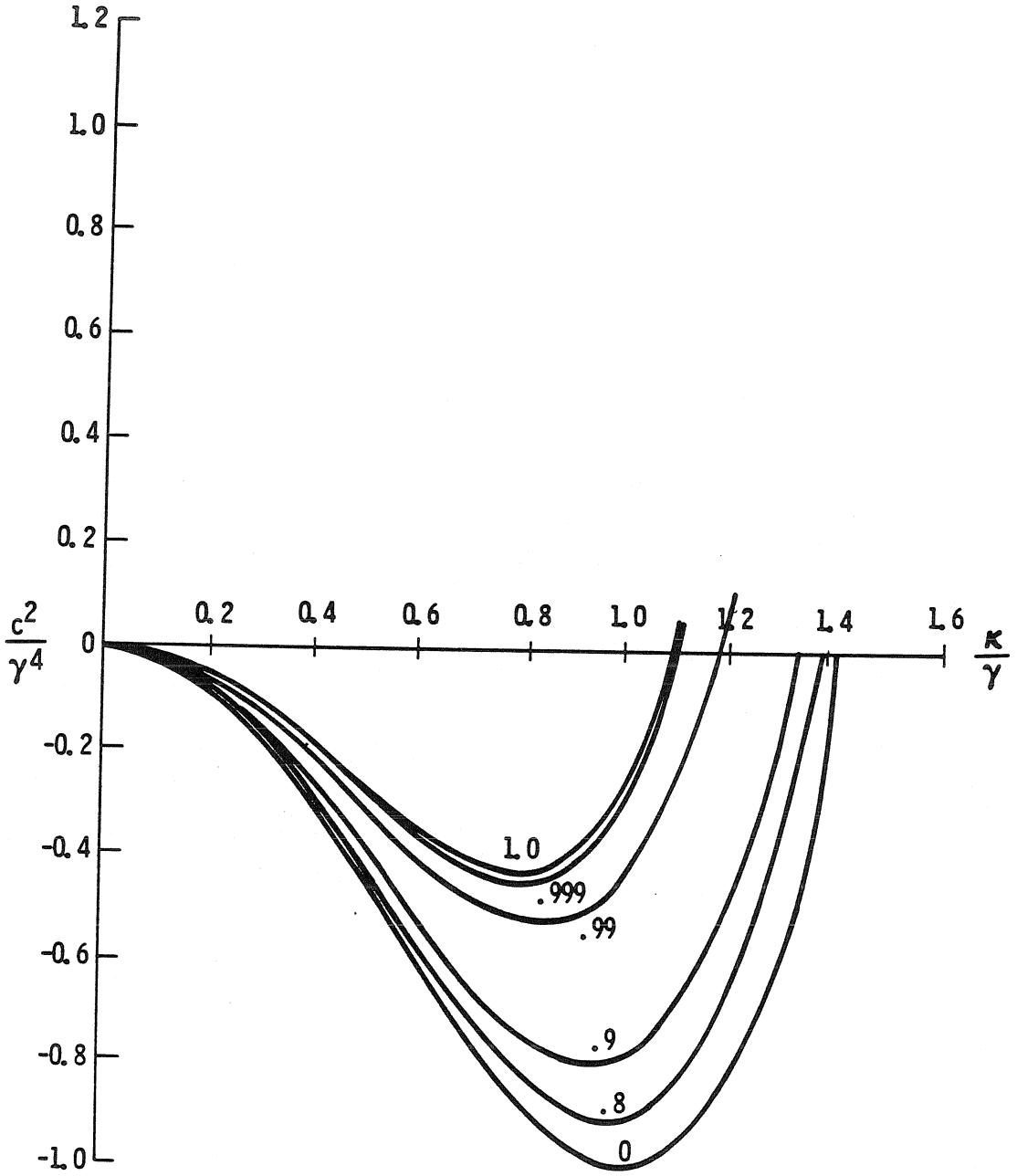

Figure 3.2. Stability results for odd perturbations of periodic wave-train solutions of the nonlinear Schrödinger equation in two space dimensions (where "odd" signifies asymmetry about the crests of the unperturbed solution). The abscissa, ordinate, curve parameter, and γ are as discussed in the description of Figure 3.1.

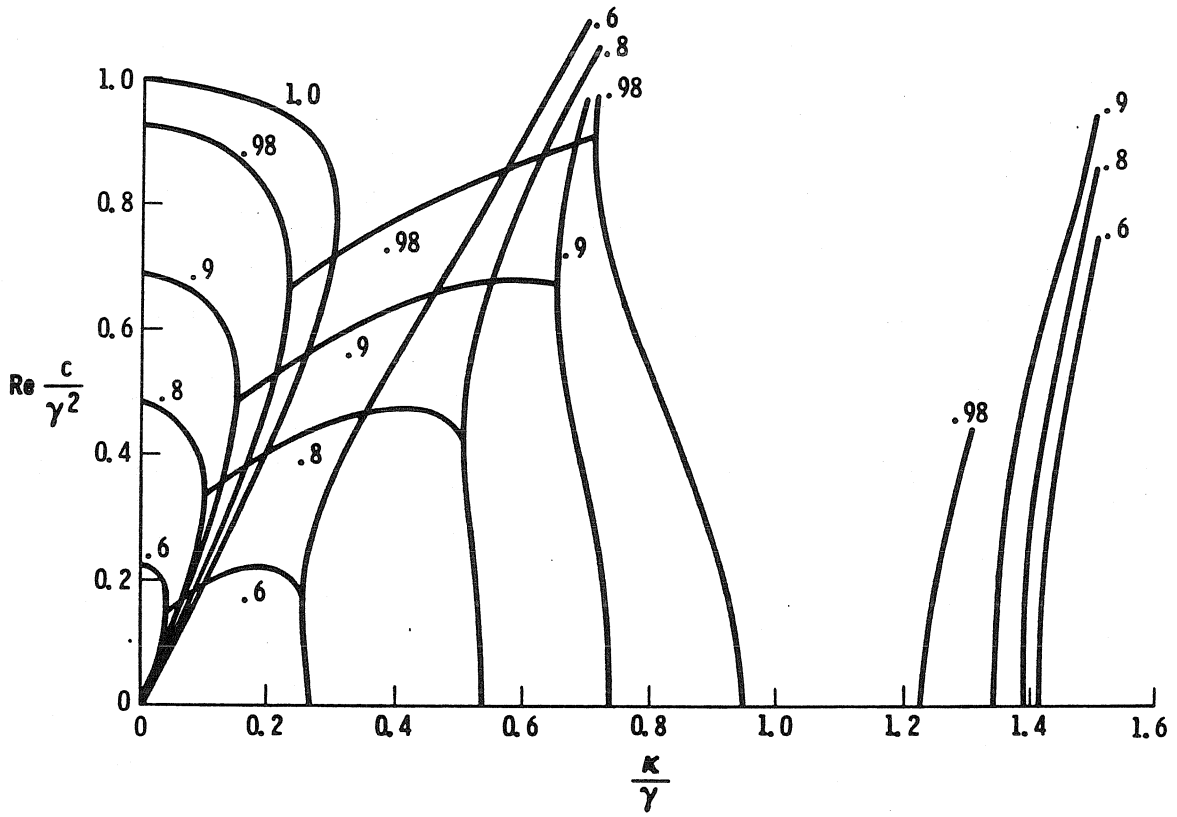

Figure 3.3. Traveling instability results for even perturbations of periodic wavetrain solutions of the nonlinear Schrödinger equation in two space dimensions (see also Figure 3.4). The ordinate is the real part of the dimensionless perturbation time constant, which is proportional to the speed of the perturbation in the transverse direction. The abscissa, curve parameter, and γ are as discussed in the description of Figure 3.1.

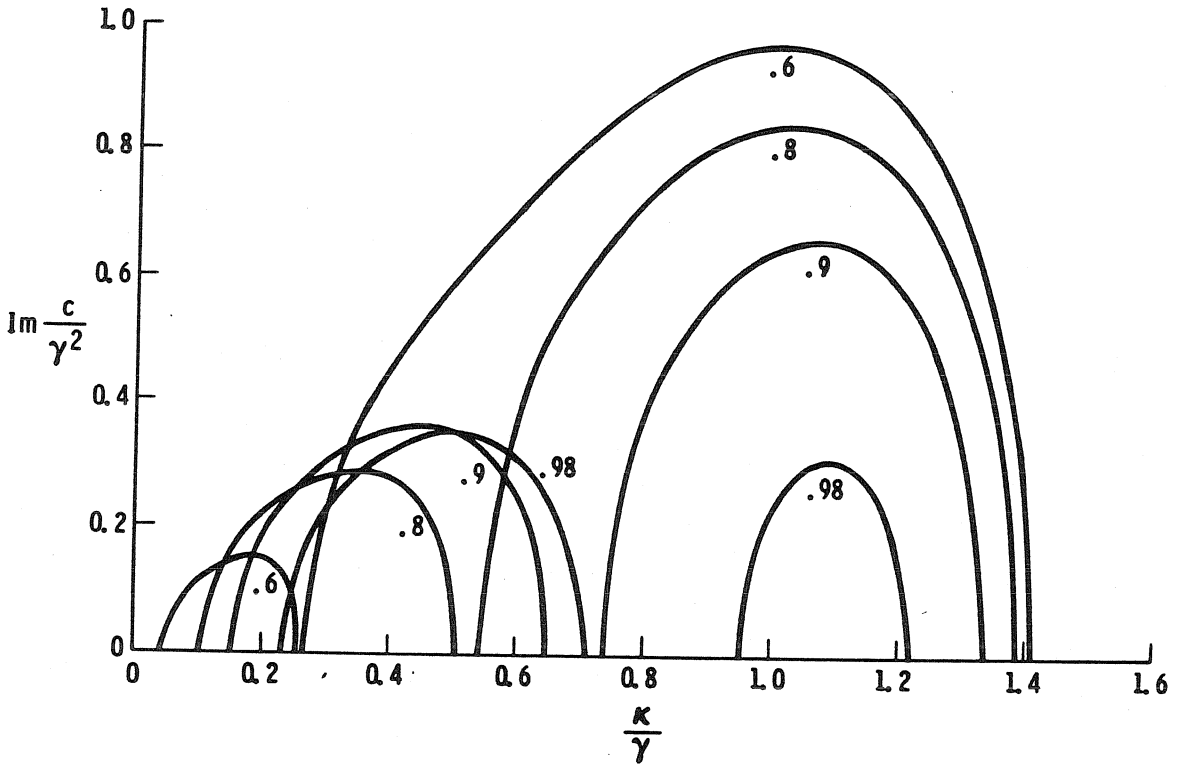

Figure 3.4. Traveling instability results for even perturbations of periodic wavetrain solutions of the nonlinear Schrödinger equation in two space dimensions (see also Figure 3.3). The ordinate is the imaginary part of the dimensionless perturbation time constant, which is proportional to the growth rate of the perturbation. The abscissa, curve parameter, and γ are as discussed in the description of Figure 3.1.

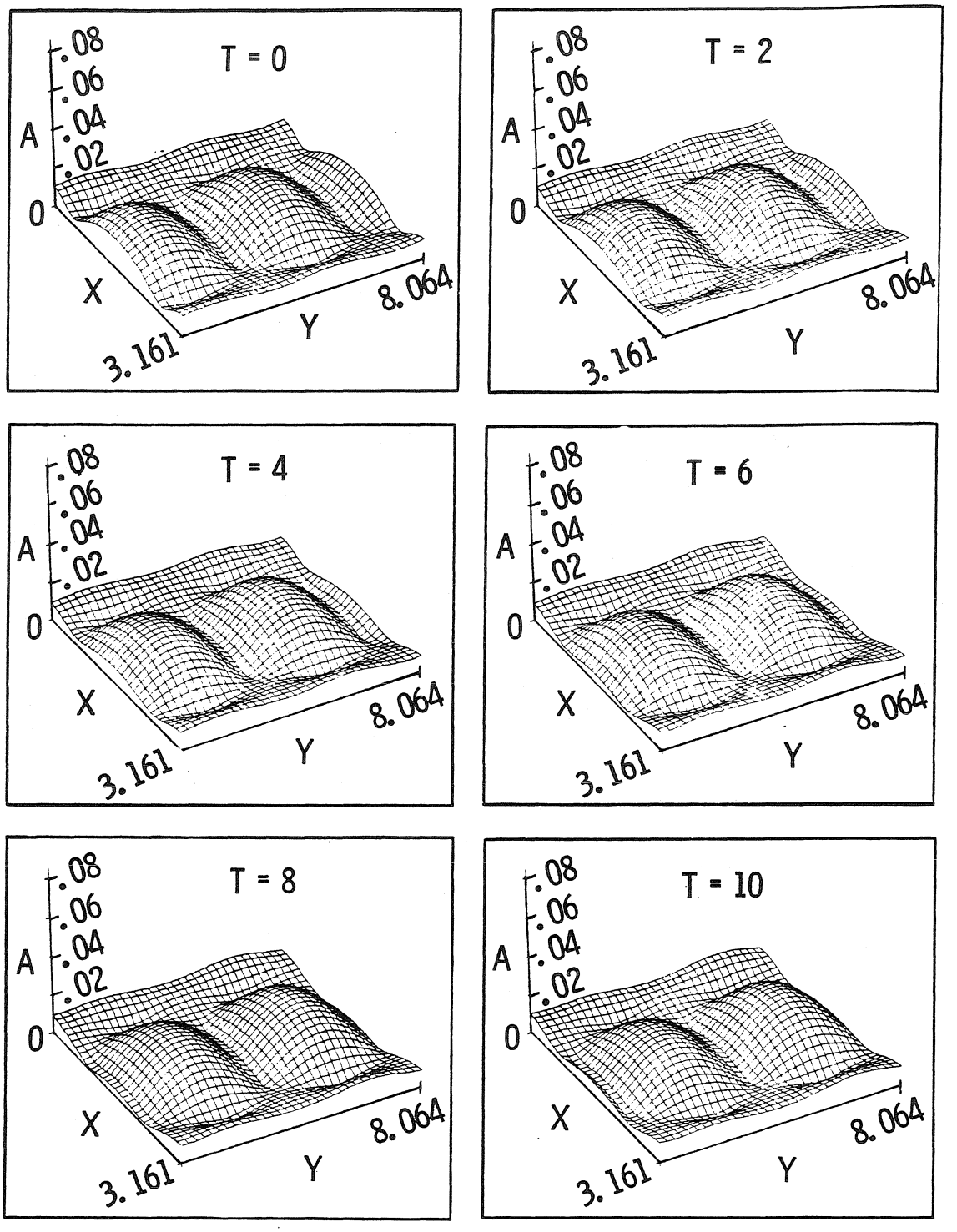

Figure 3.5. Time development of the perturbation amplitude for an even, stable perturbation. The x-axis lies in the direction of propagation of the carrier wave. Note the motion in the transverse direction. The plot is in the group velocity frame.

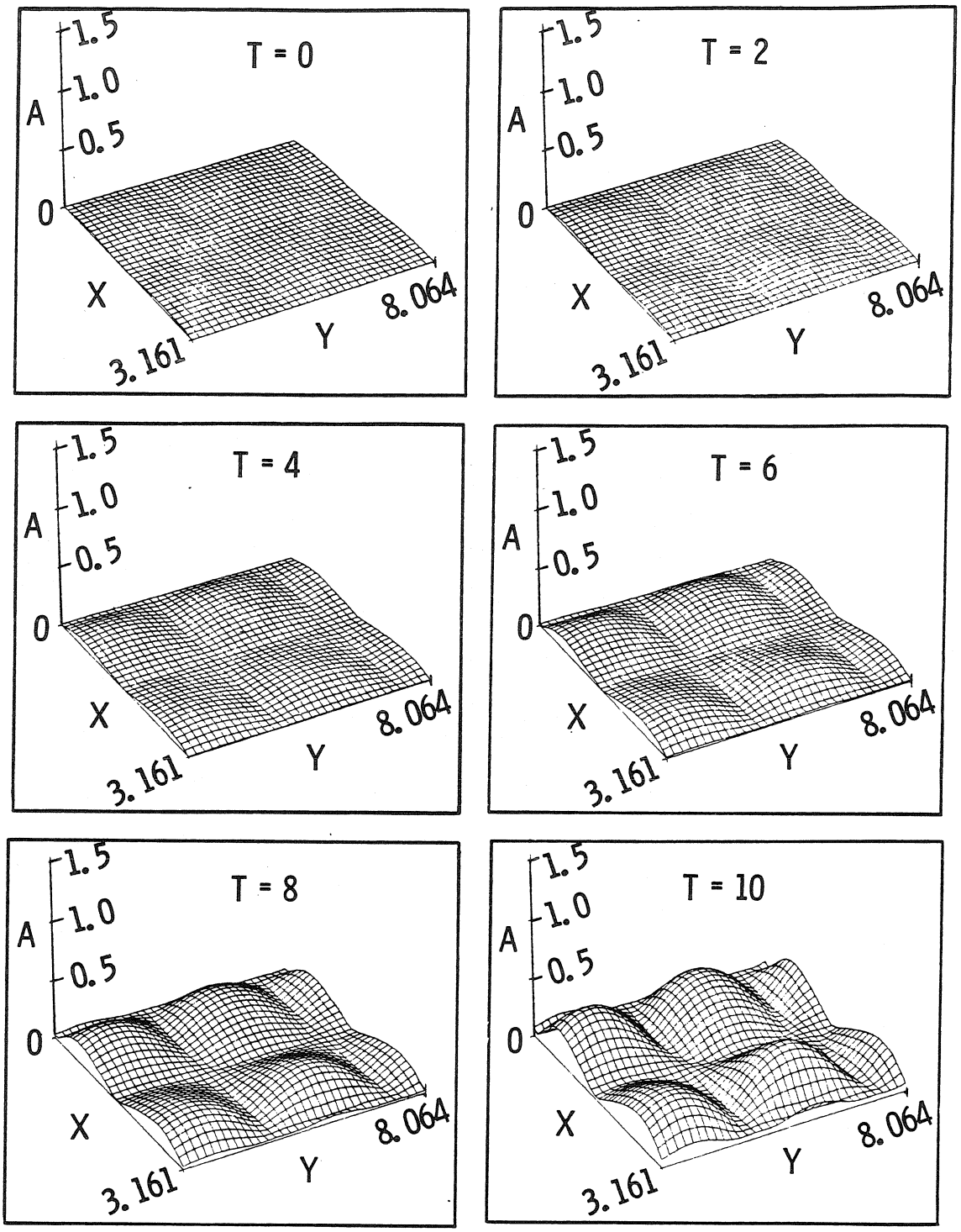

Figure 3.6. Time development of the perturbation amplitude for an odd, unstable perturbation. The x-axis lies in the direction of propagation of the carrier wave, and the plot is in the group velocity frame.

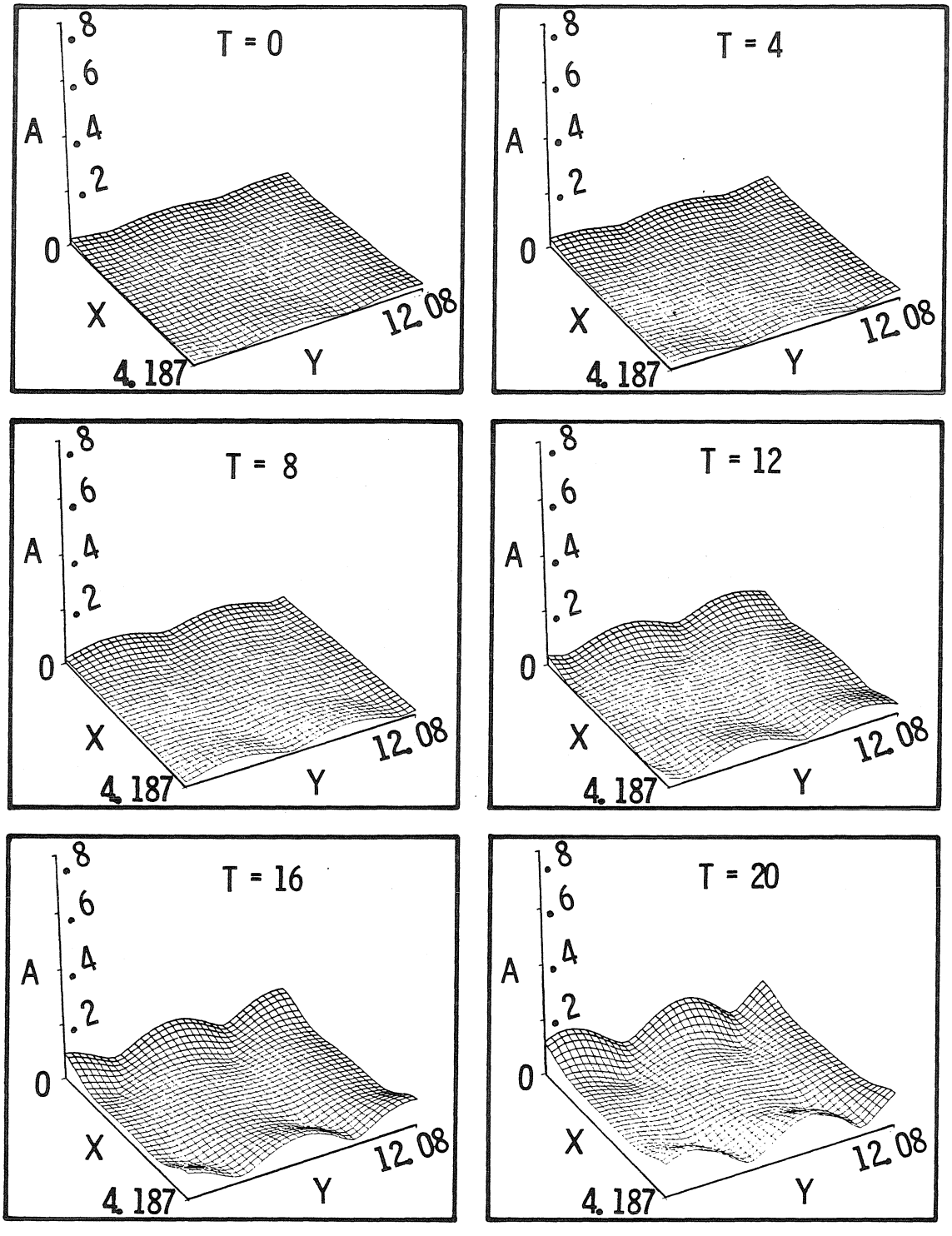

Figure 3.7. Time development of the perturbation amplitude for an even, unstable, traveling perturbation. The x-axis lies in the direction of propagation of the carrier wave, and the plot is in the group velocity frame. Note the motion in the transverse direction.

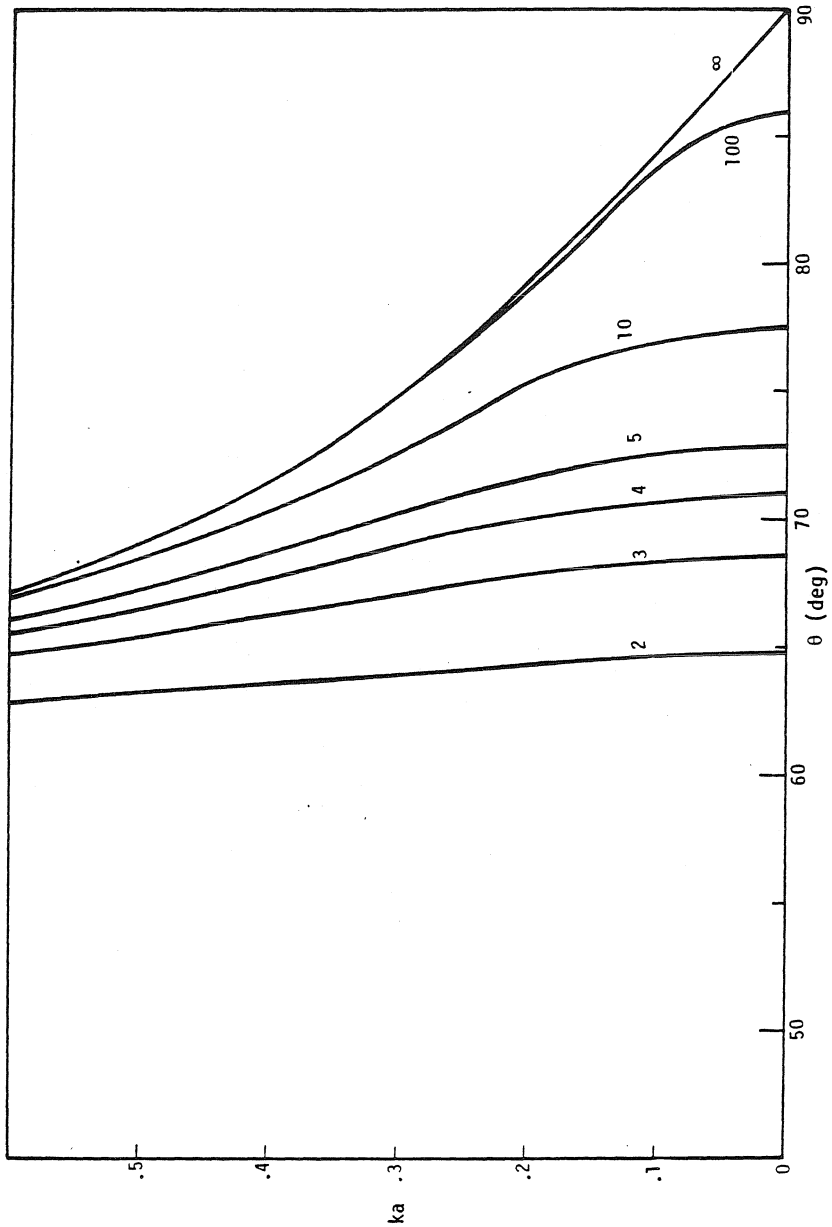

Figure 4.1. Slope at which bifurcation may occur ($k_0 a_c$) as a function of angular separation of the modulation and carrier wave (θ). The parameter appearing by each trace is the associated value of $N = k_0/k_x$.

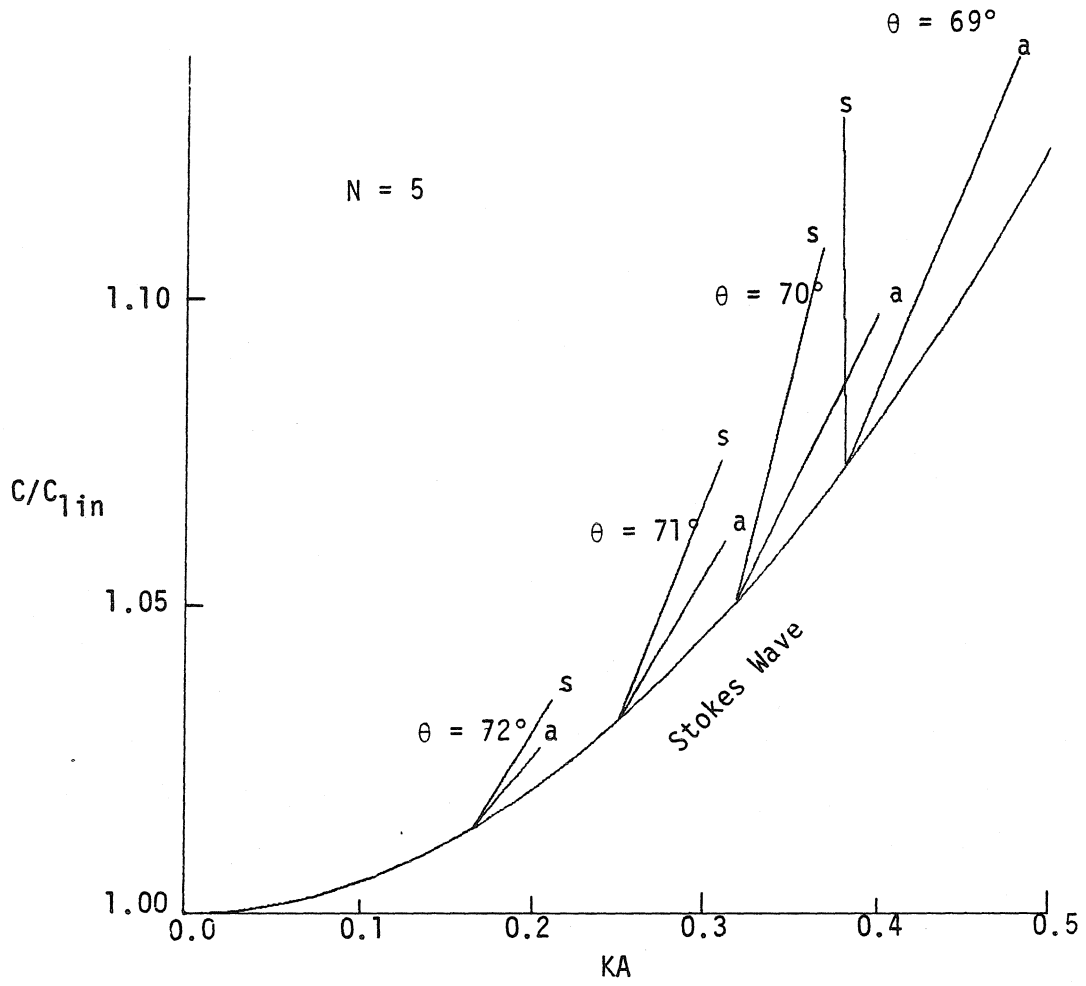

Figure 4.2. Ratio of nonlinear to linear wave speed for Stokes waves and bifurcations with $|N| = |k_o/k_x| = 5$, and the indicated values of θ. The notation "a" indicates an asymmetric bifurcation $\left[a_{01}^{(1)}/a_{10}^{(1)} = 0 = a_{0,-1}^{(1)}/a_{10}^{(1)}\right]$, and "s" indicates a symmetric bifurcation $\left[a_{01}^{(1)}/a_{10}^{(1)} = 1\right]$.

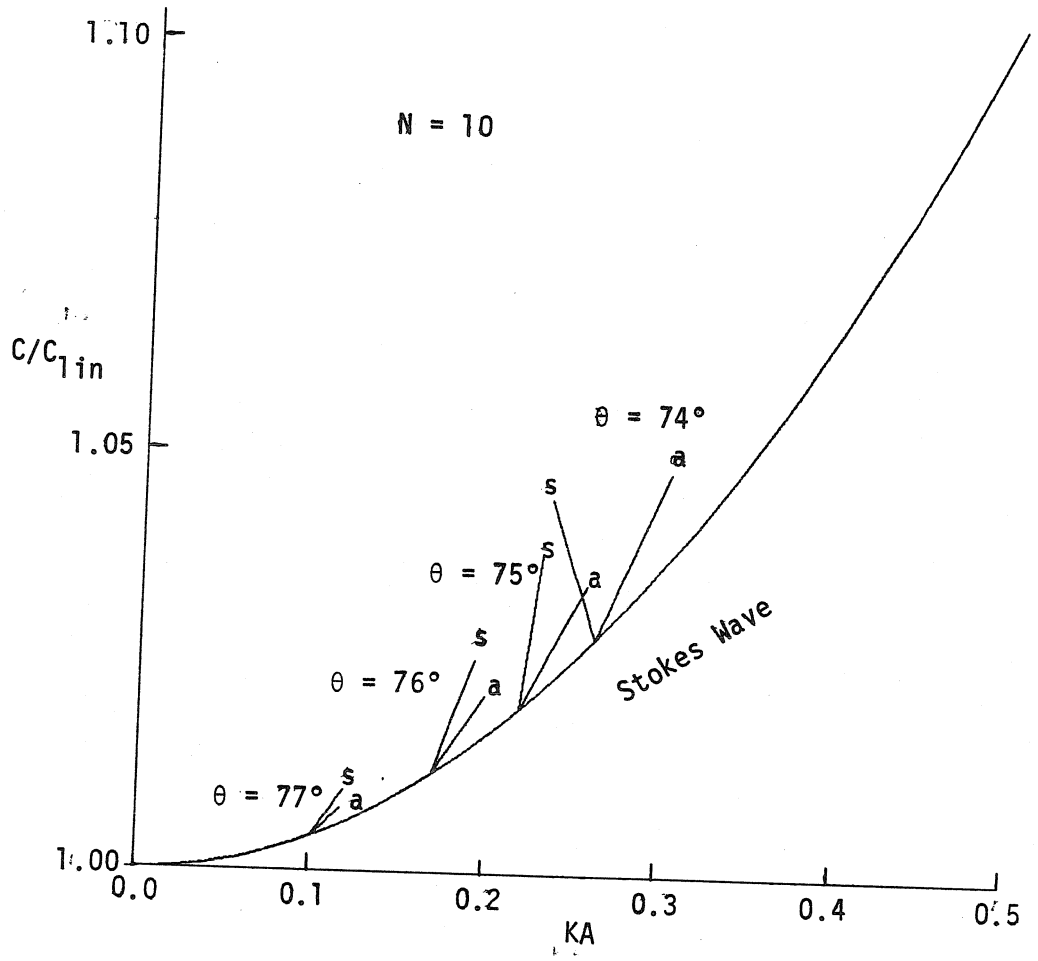

Figure 4.3. Ratio of nonlinear to linear wave speed for Stokes waves and bifurcations with $|N| = |k_o/k_x| = 10$, and the indicated values of θ. The notation "a" indicates an asymmetric bifurcation $\left[a_{01}^{(1)}/a_{10}^{(1)} = 0 = a_{0,-1}^{(1)}/a_{10}^{(1)}\right]$, and "s" indicates a symmetric bifurcation $\left[a_{01}^{(1)}/a_{10}^{(1)} = 1\right]$.

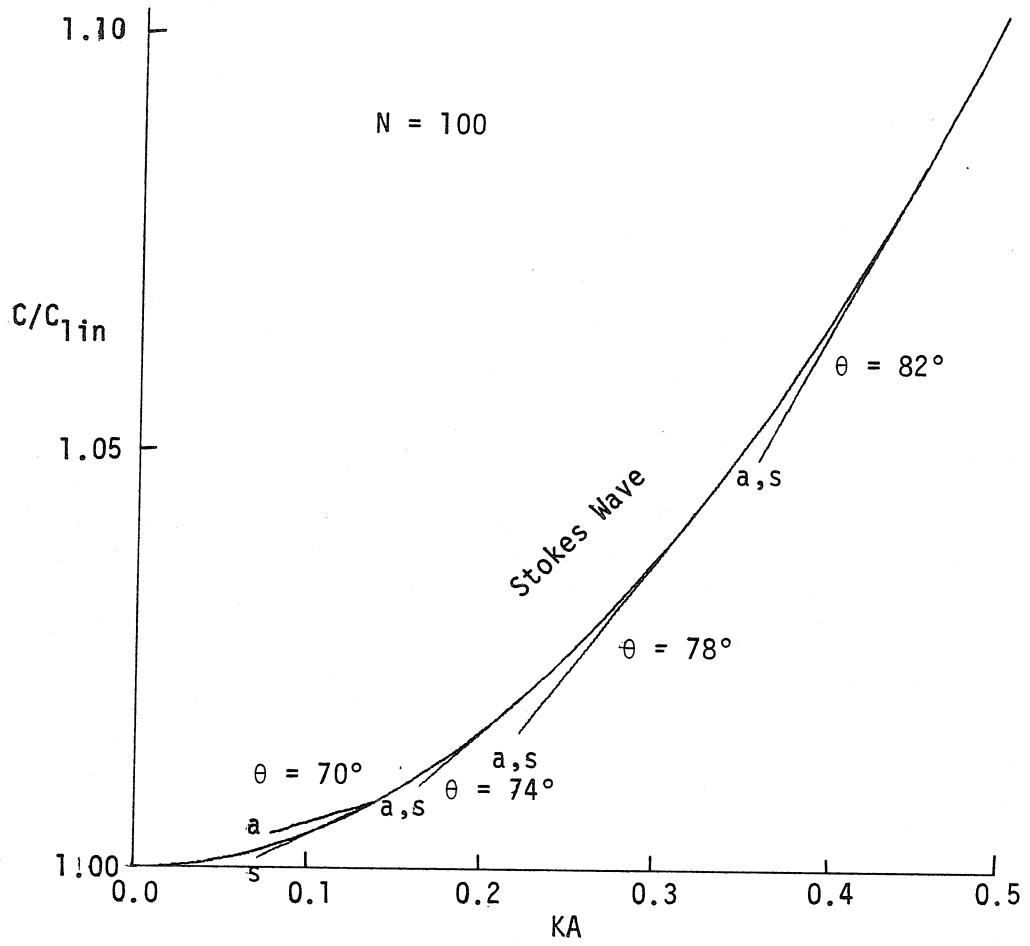

Figure 4.4. Ratio of nonlinear to linear wave speed for Stokes waves and bifurcations with $|N| = |k_o/k_x| = 100$, and the indicated values of θ. The notation "a" indicates an asymmetric bifurcation $\left[a_{01}^{(1)}/a_{10}^{(1)} = 0 = a_{0,-1}^{(1)}/a_{10}^{(1)}\right]$, and "s" indicates a symmetric bifurcation $\left[a_{01}^{(1)}/a_{10}^{(1)} = 1\right]$. Note that the symmetric and asymmetric bifurcations coincide for large θ.

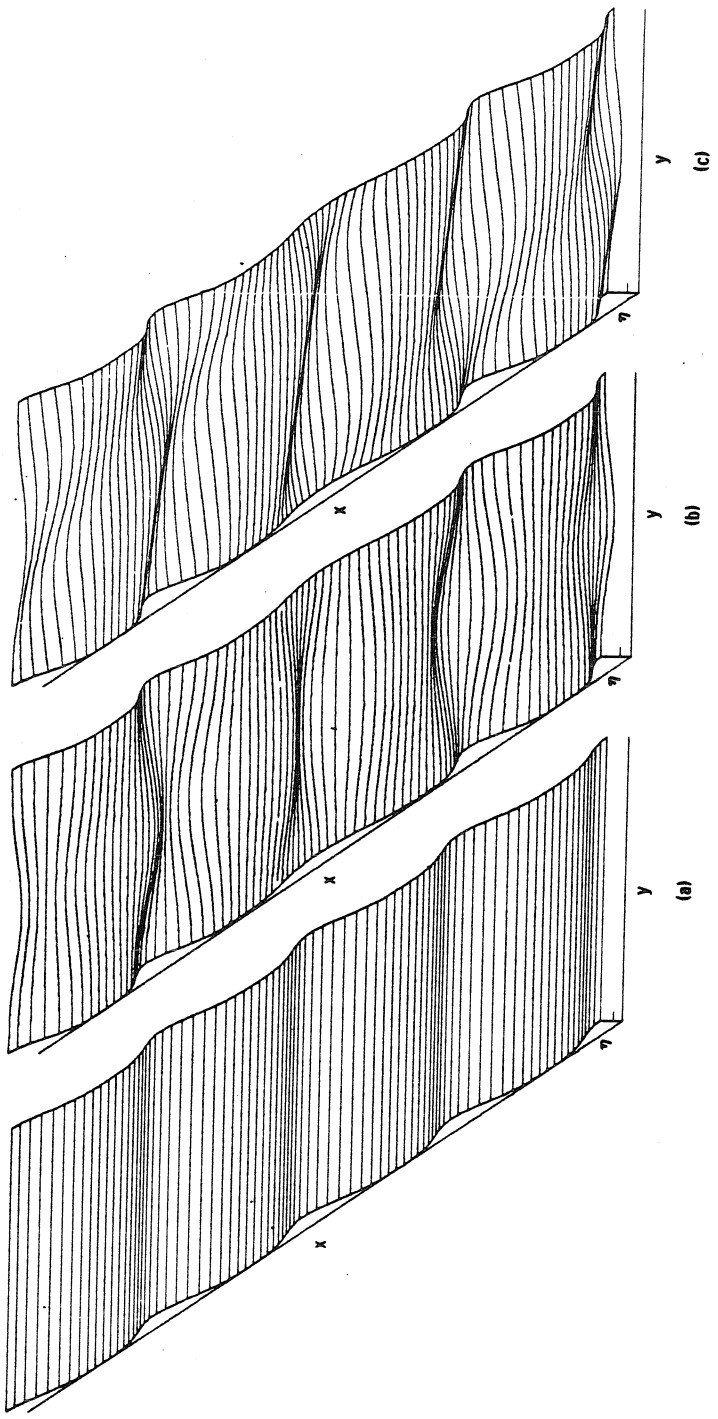

Figure 4.5. Surface displacement for:
(a) a Stokes wave with ka = .319
(b) a bifurcation from (a) with N = 5, $\theta = 70°$, and $a_{10}^{(1)} = .25 = a_{01}^{(1)}$
(c) a similar bifurcation with $a_{10}^{(1)} = .5$, $a_{01}^{(1)} = 0$.

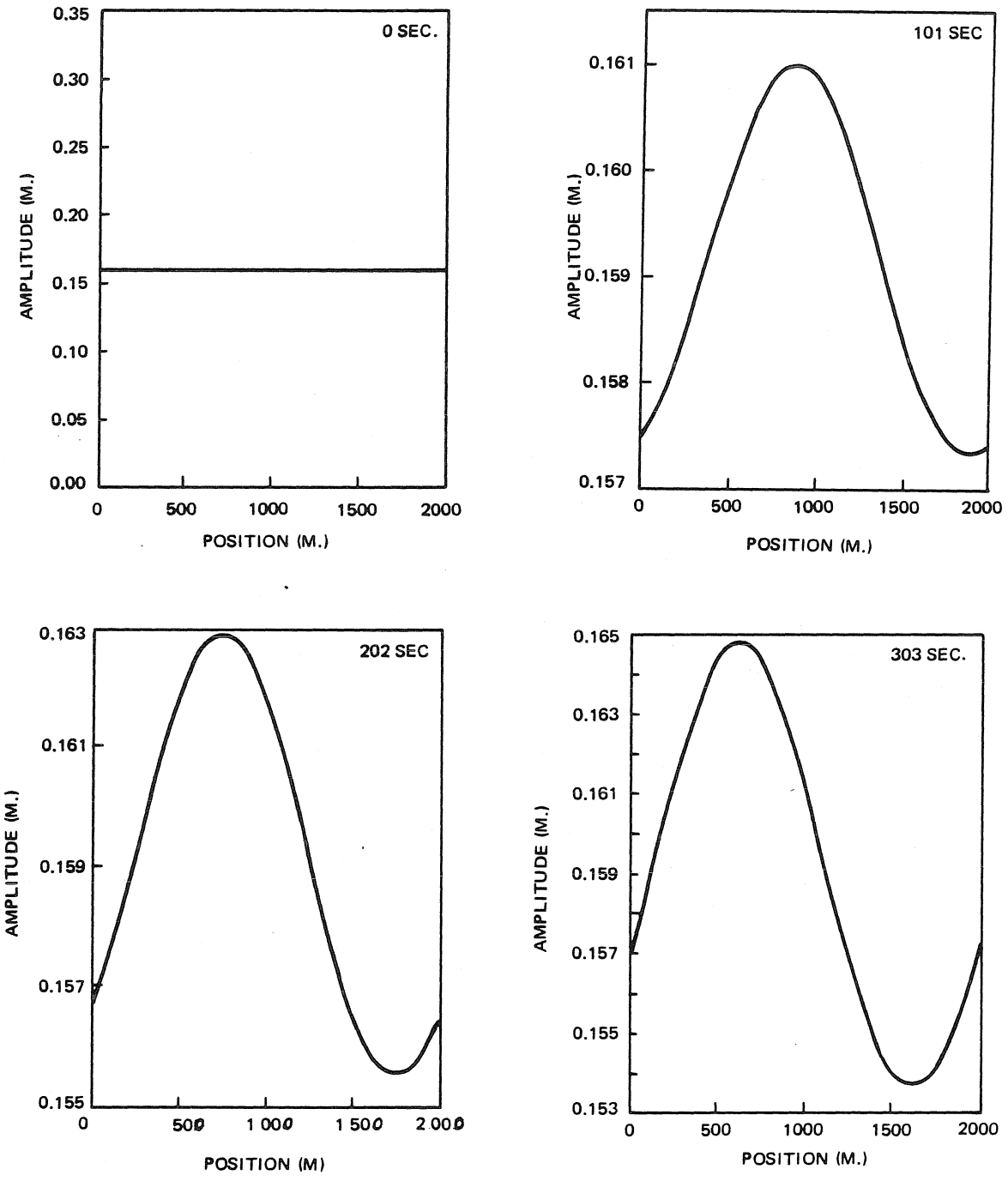

Figure 5.1. Time development (in the group velocity frame) of the amplitude of an initially uniform surface wave of slope ka = 0.1 subjected to the steady (with respect to the bottom) current pattern

$$U = 0.025 c_g \sin(k_0 x/200)$$

Scale is established by assuming a carrier wavelength of 10 m.

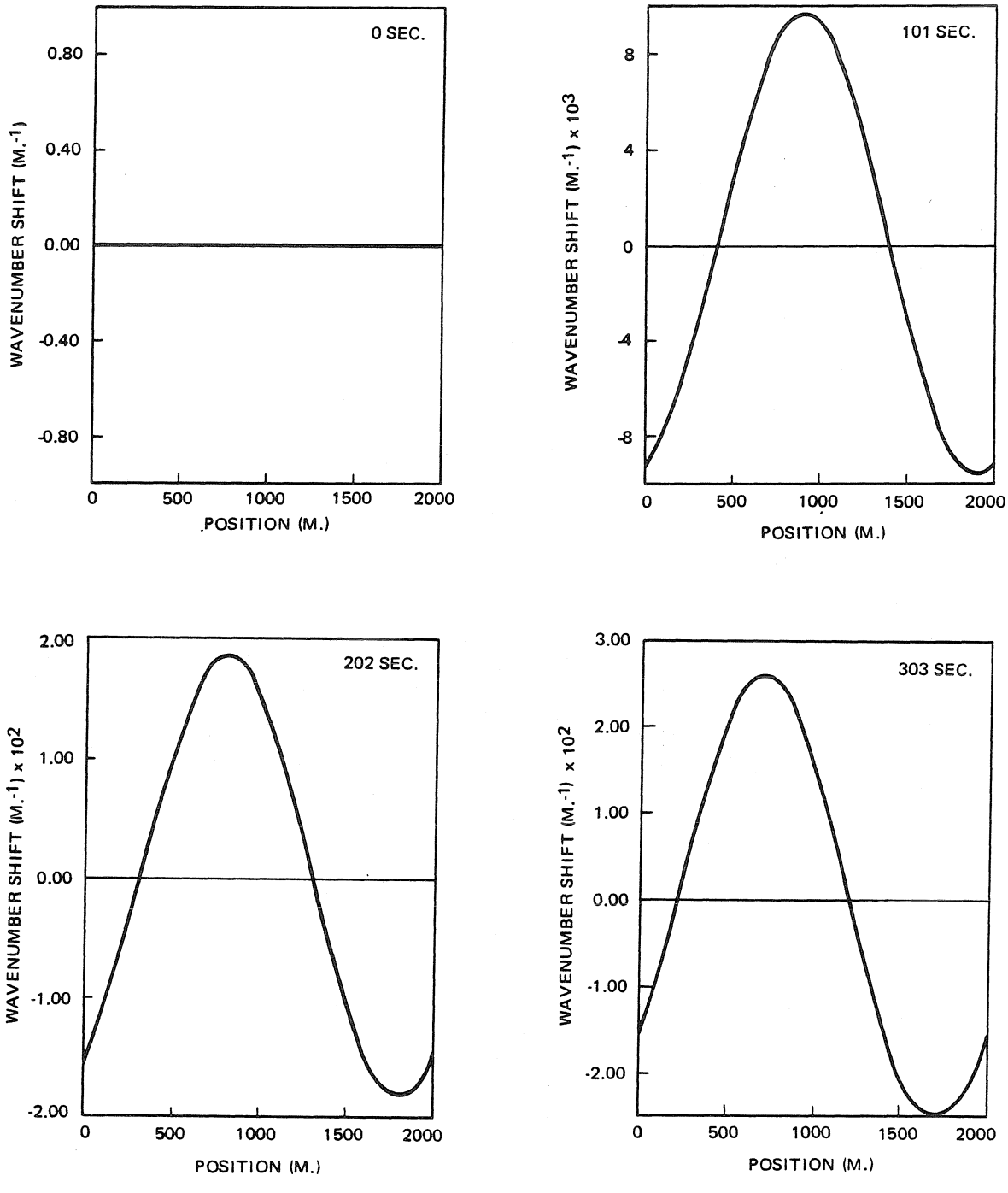

Figure 5.2. Time development (in the group velocity frame) of the wavenumber shift profile of an initially uniform surface wave of slope ka = 0.1 subjected to the steady (with respect to the bottom) current pattern $U = 0.025c_g \sin(k_0 x/200)$. Scale is established by assuming a carrier wavelength of 10 m.

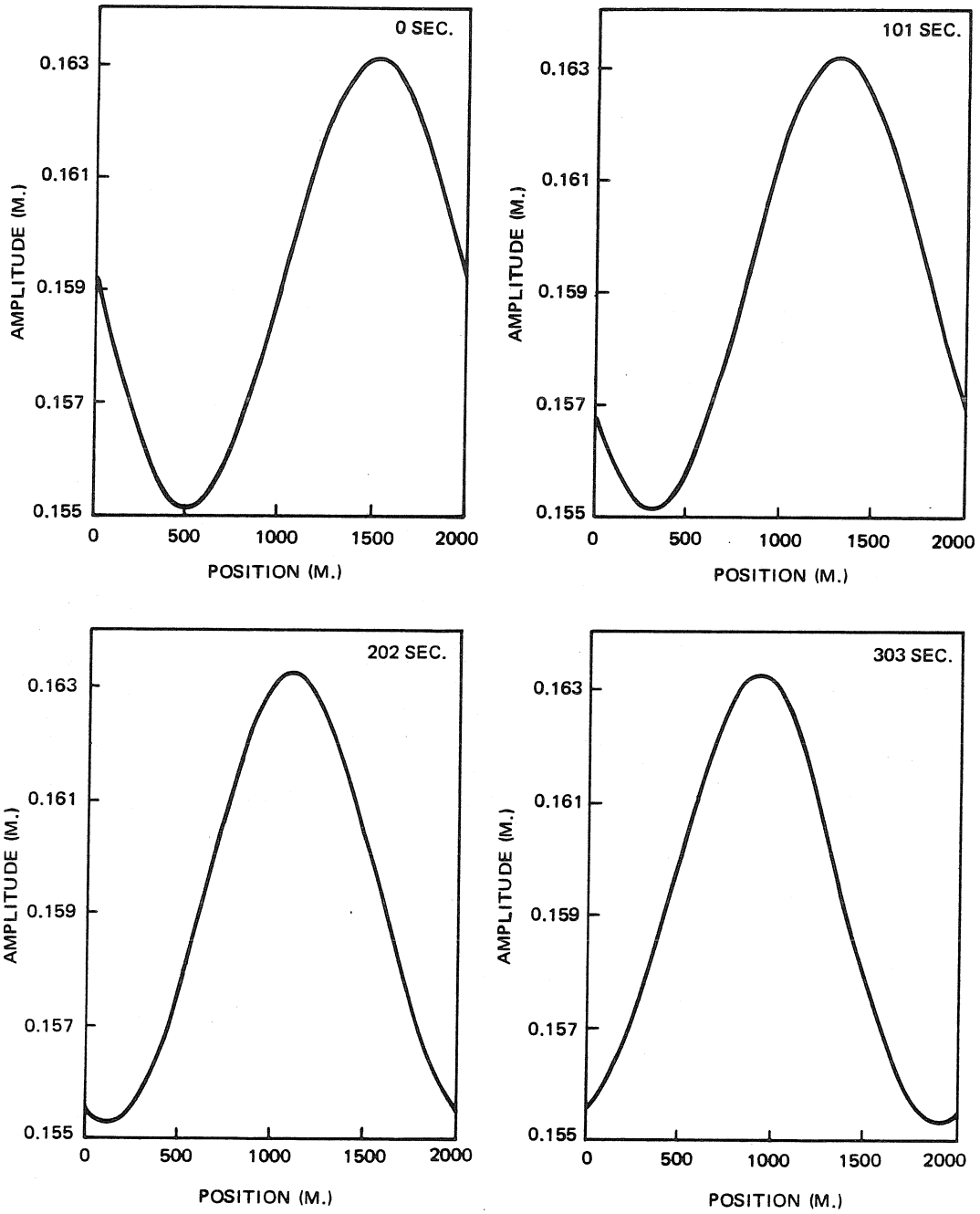

Figure 5.3. Time development (in the group velocity frame) of the amplitude of a surface wave subjected to the steady (with respect to the bottom) current pattern $U = 0.025c_g\sin(k_0x/200)$ which appears instantly at the initial time. The initial condition is the sum of a uniform wave of slope ka = 0.1 and the forced perturbation associated with the current pattern. Scale is established by assuming a carrier wavelength of 10 m.

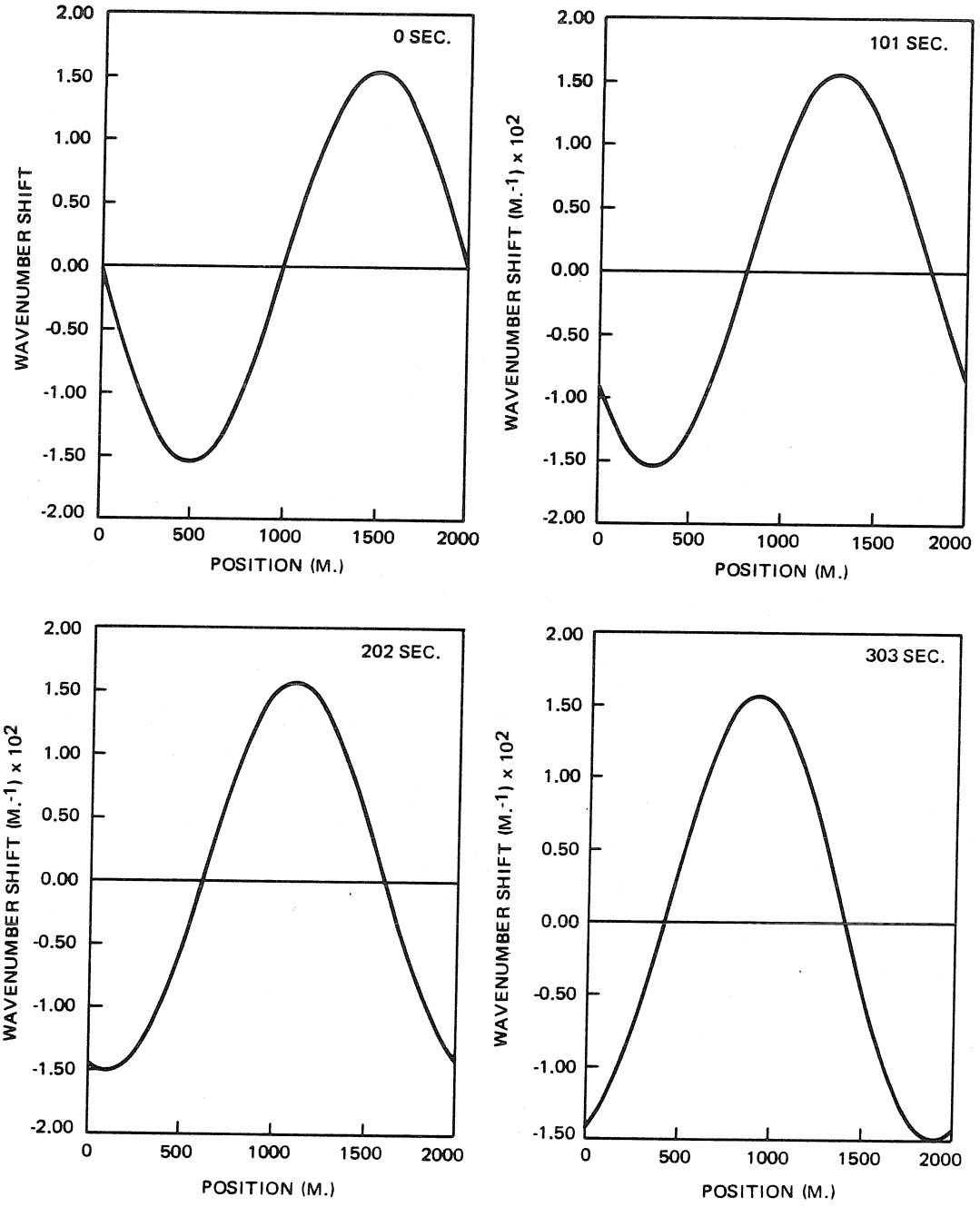

Figure 5.4. Time development (in the group velocity frame) of the wavenumber shift profile of a surface wave subjected to the steady (with respect to the bottom) current pattern $U = 0.025c_g \sin(k_0 x/200)$ which appears instantly at the initial time. The initial condition is the sum of a uniform wave of slope ka = 0.1 and the forced perturbation associated with the current pattern. Scale is established by assuming a carrier wavelength of 10 m.

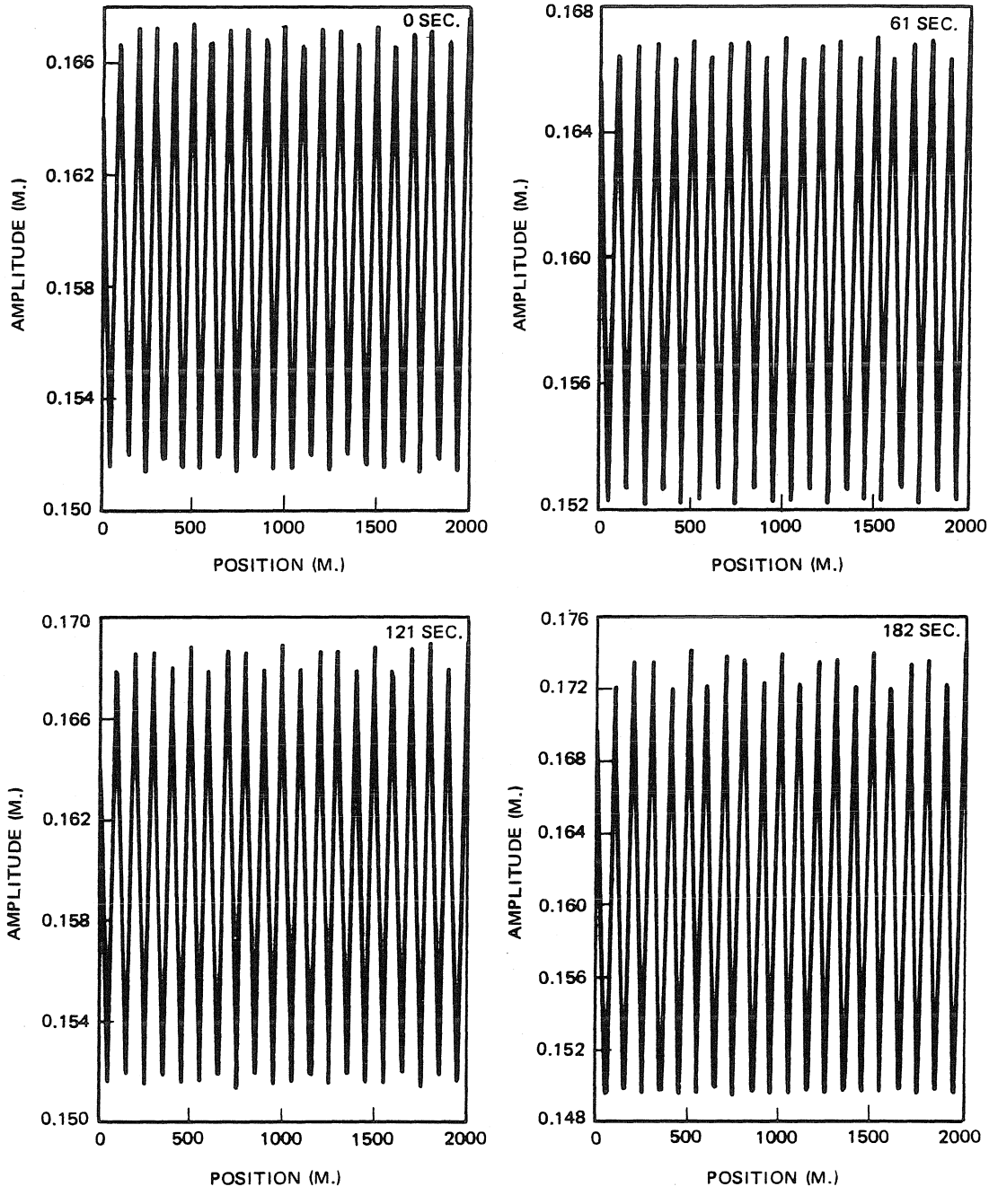

Figure 5.5. Time development (in the group velocity frame) of the amplitude of a surface wave of slope ka = 0.1 in a region free of current. Initially the envelope consists of a uniform component and a sinusoidal component of much smaller magnitude and wavelength ten times that of the carrier. This initial condition grows due to the Benjamin-Feir instability. Scale is established by assuming a carrier wavelength of 10 m.

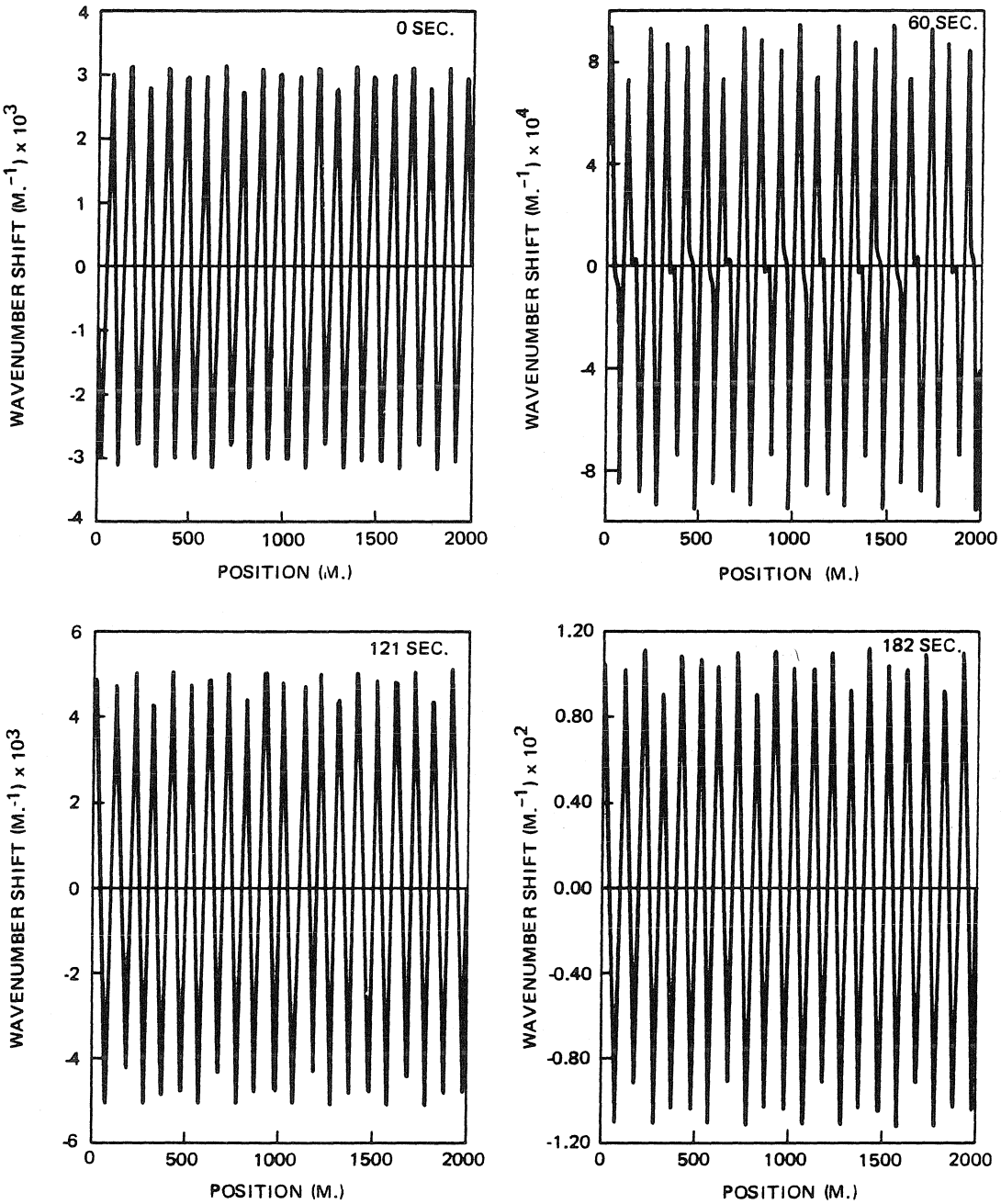

Figure 5.6. Time development (in the group velocity frame) of the wavenumber shift profile of a surface wave of slope ka = 0.1 in a region free of current. Initially the envelope consists of a uniform component and a sinusoidal component of much smaller magnitude and wavelength ten times that of the carrier. This initial condition grows due to the Benjamin-Feir instability. Scale is established by assuming a carrier wavelength of 10 m.

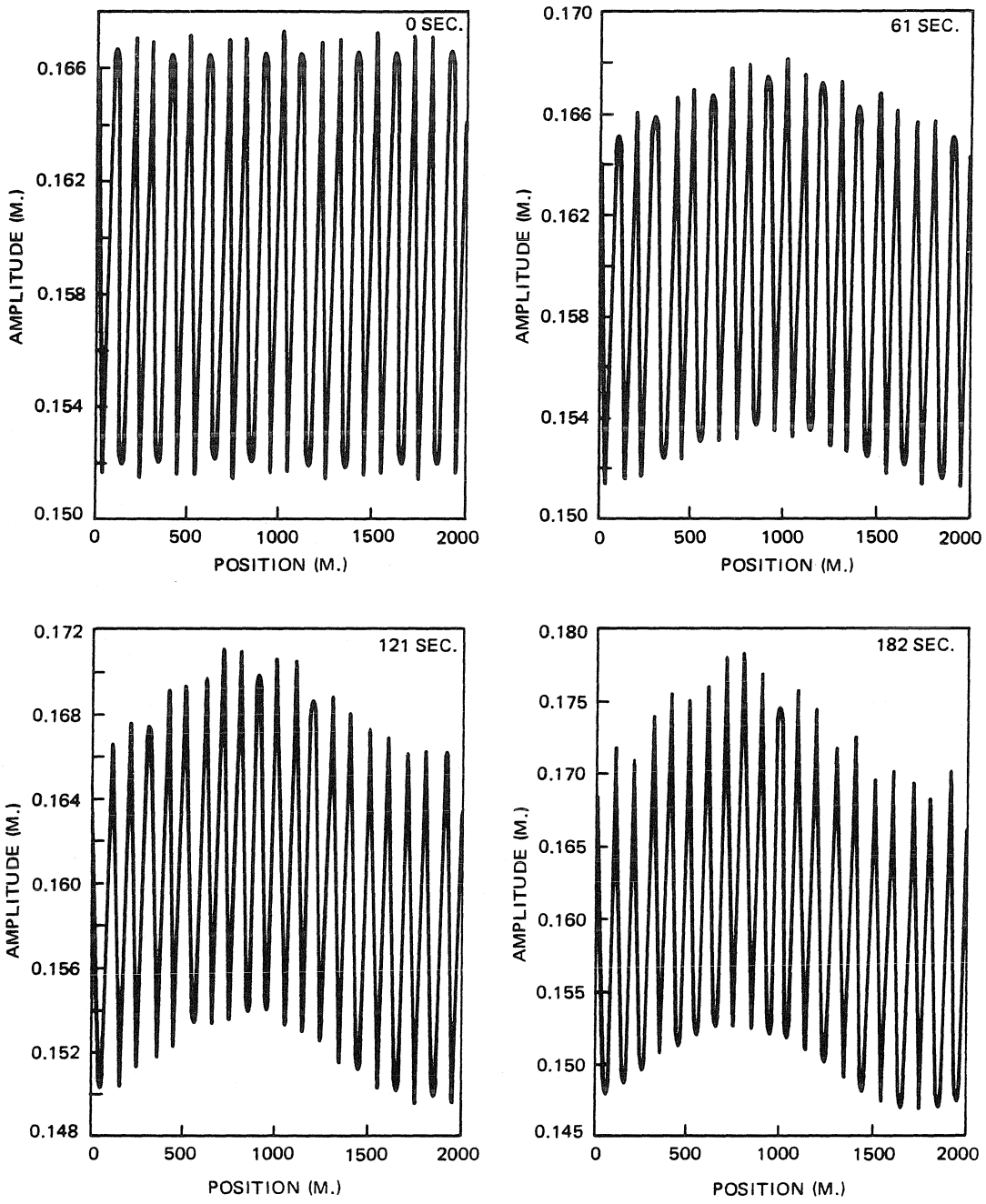

Figure 5.7. Time development (in the group velocity frame) of the amplitude of a surface wave of slope ka = 0.1 subjected to the steady (with respect to the bottom) current pattern $U = 0.025c_g \sin(k_0 x/200)$ which appears instantly at the initial time. Initially the envelope consists of a uniform component and a sinusoidal component of much smaller magnitude and wavelength ten times that of the carrier. This initial condition is Benjamin-Feir unstable. Scale is established by assuming a carrier wavelength of 10 m.

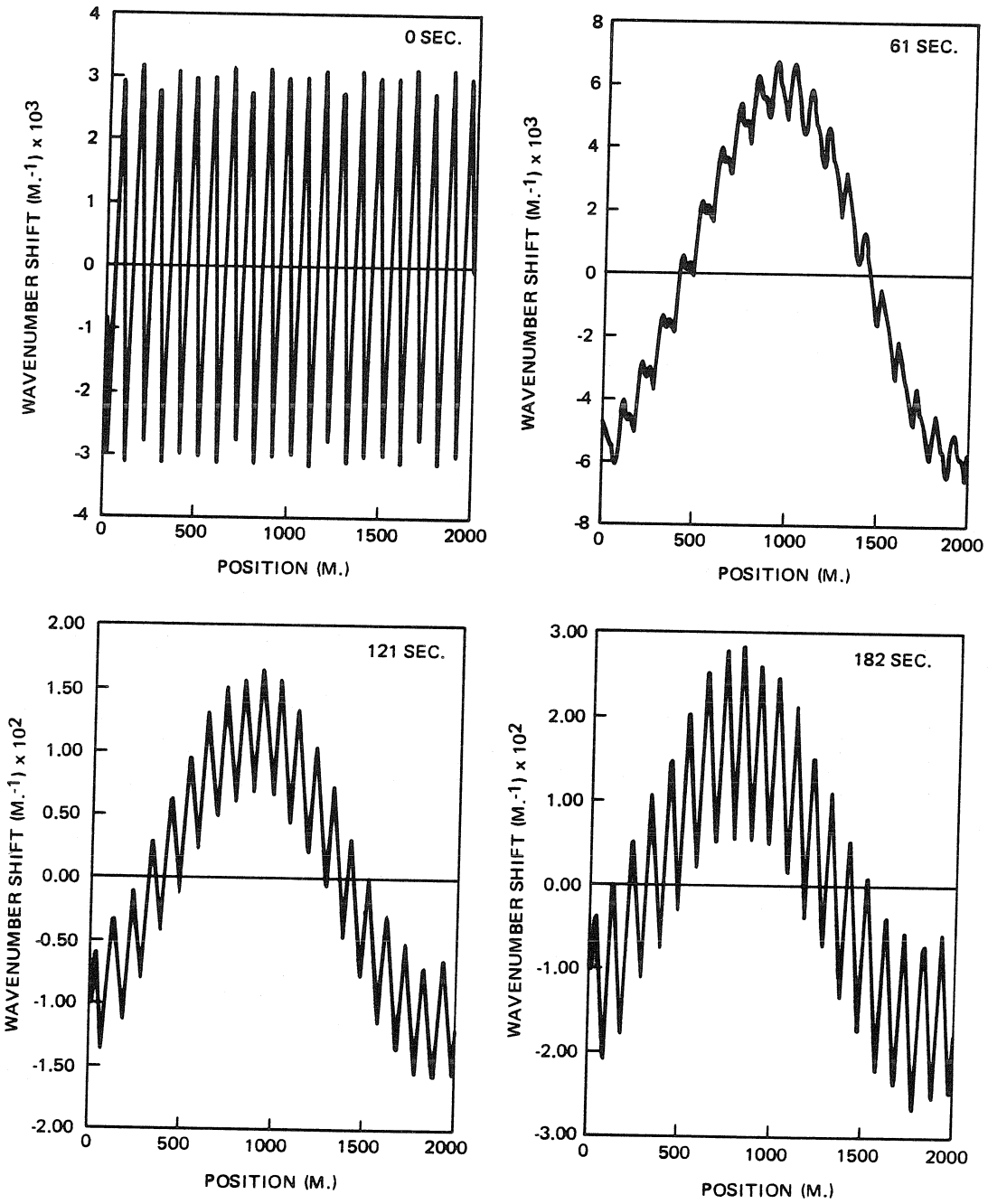

Figure 5.8. Time development (in the group velocity frame) of the wavenumber shift profile of a surface wave of slope ka = 0.1 subjected to the steady (with respect to the bottom) current pattern $U = 0.025c_g\sin(k_0x/200)$ which appears instantly at the initial time. Initially the envelope consists of a uniform component and a sinusoidal component of much smaller magnitude and wavelength ten times that of the carrier. This initial condition is Benjamin-Feir unstable. Scale is established by assuming a carrier wavelength of 10 m.

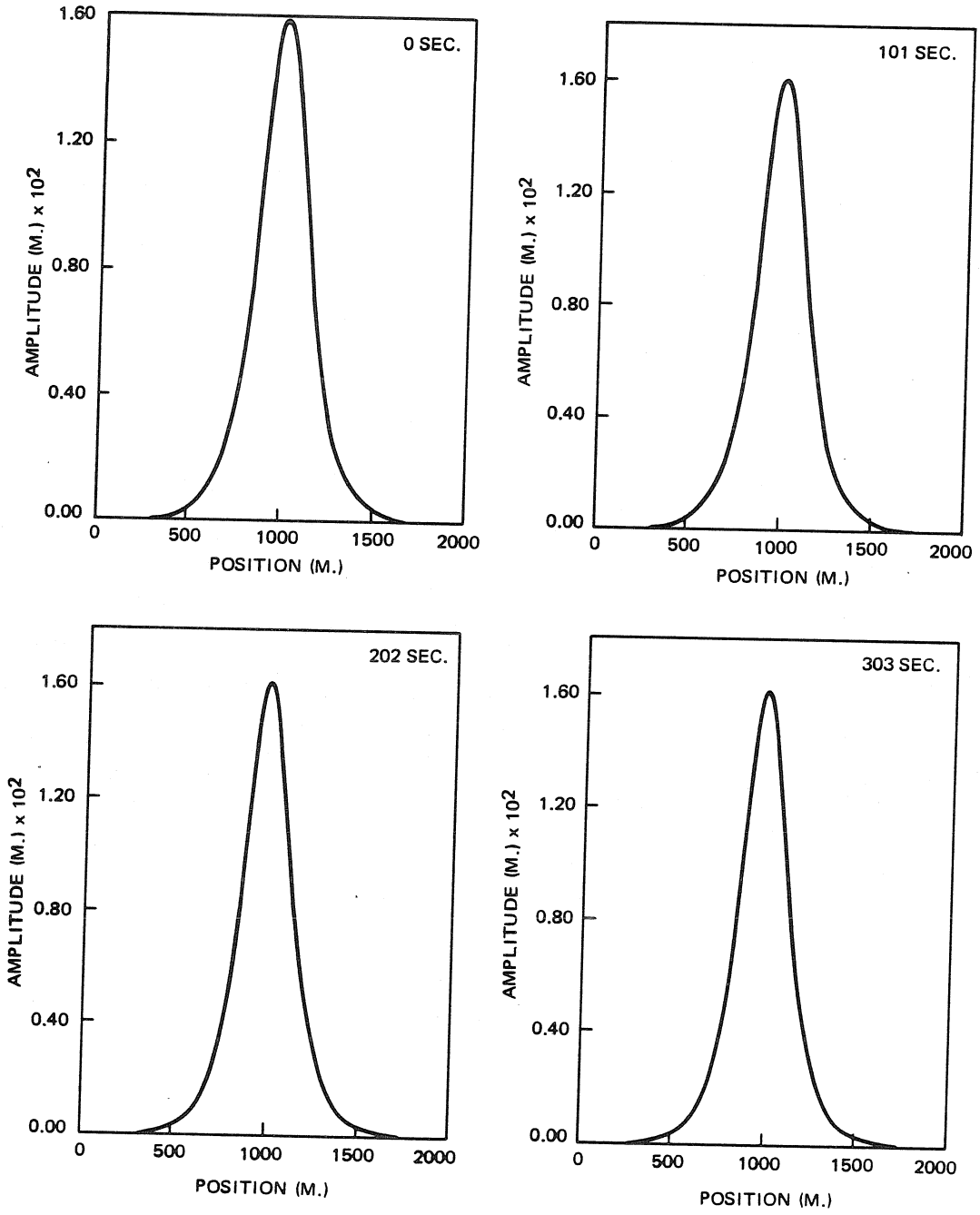

Figure 5.9. Time development (in the group velocity frame), computed via the nonlinear Schrödinger equation, of the amplitude profile of an envelope soliton subjected to the steady (with respect to the bottom) current pattern $U = 0.025c_g \sin(k_0 x/200)$ which appears instantly at the initial time. The carrier wave has slope $ka = 0.01$. Scale is established by assuming a carrier wavelength of 10 m.

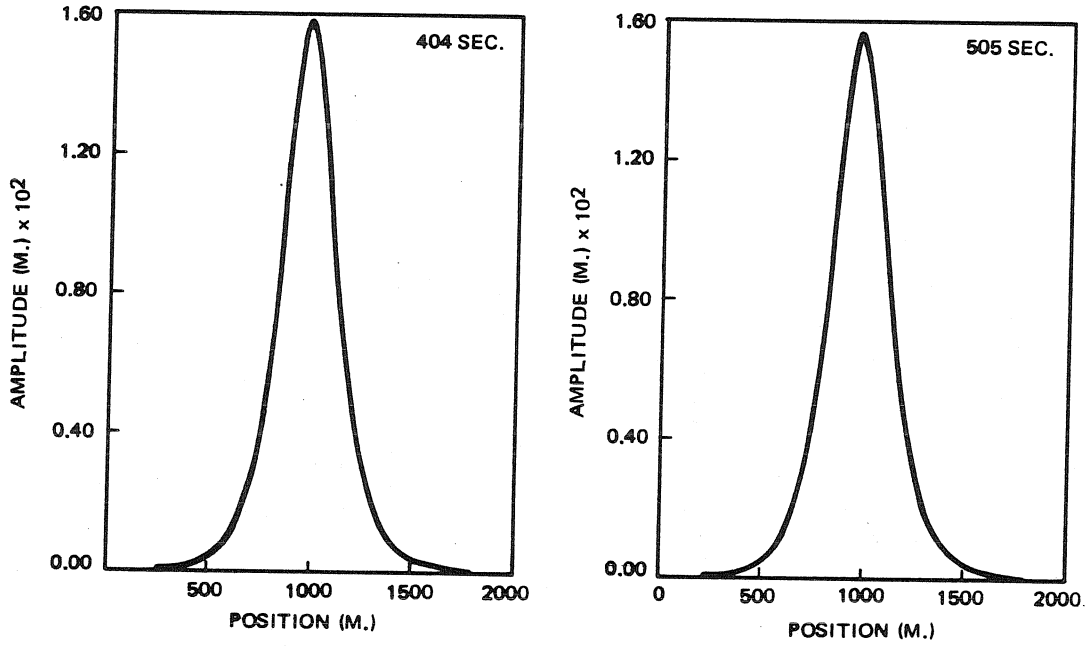

Figure 5.9. (Cont.)

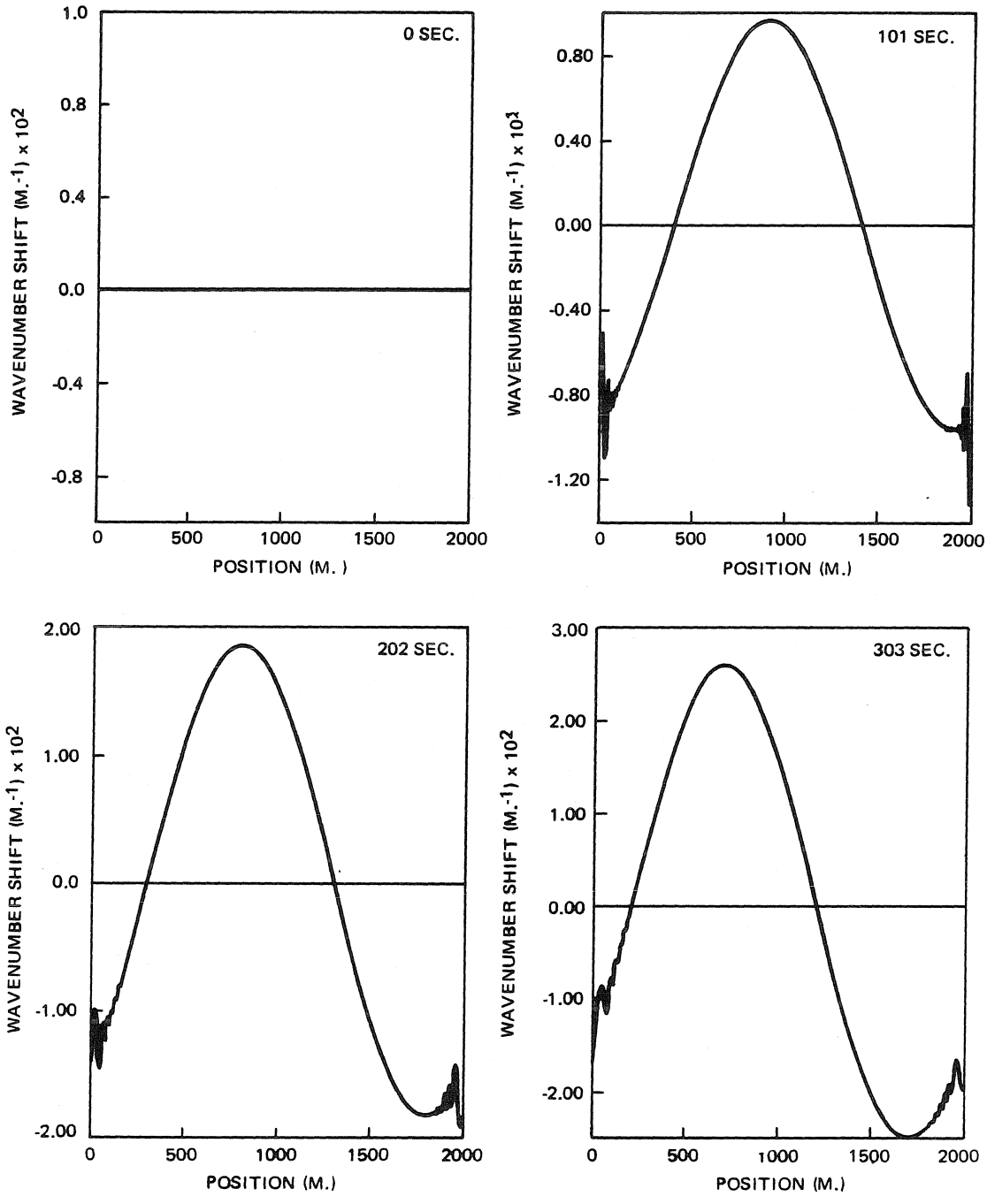

Figure 5.10. Time development (in the group velocity frame), computed via the nonlinear Schrödinger equation, of the wavenumber shift profile of an envelope soliton subjected to the steady (with respect to the bottom) current pattern $U = 0.025c_g \sin(k_0 x/200)$ which appears instantly at the initial time. The carrier wave has slope ka = 0.01. Scale is established by assuming a carrier wavelength of 10 m.

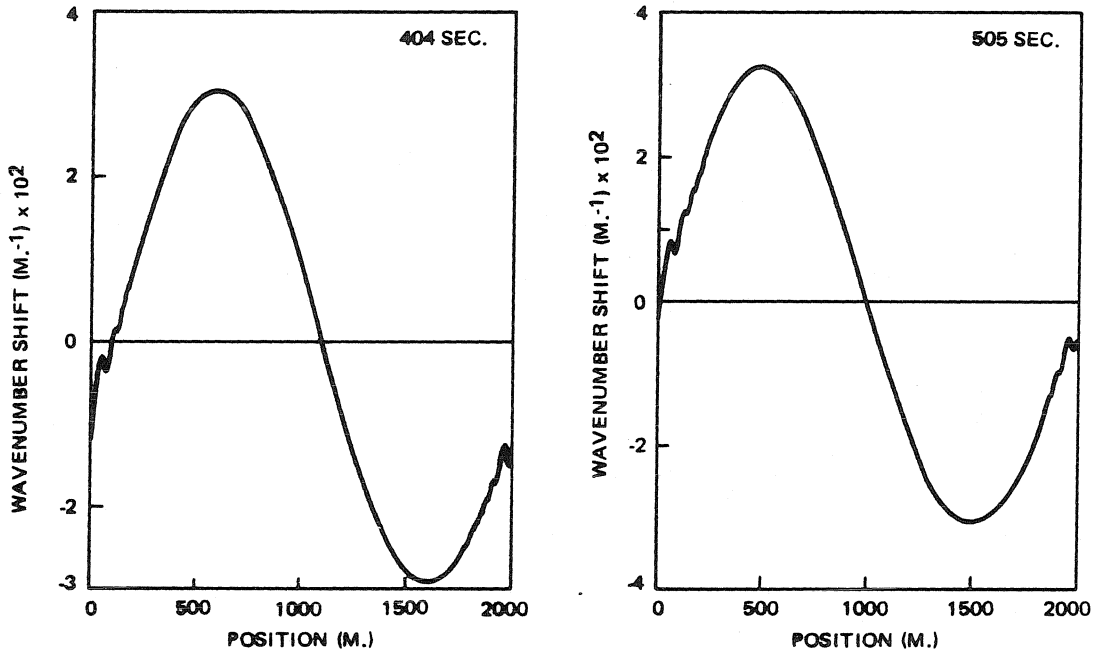

Figure 5.10. (Cont.)

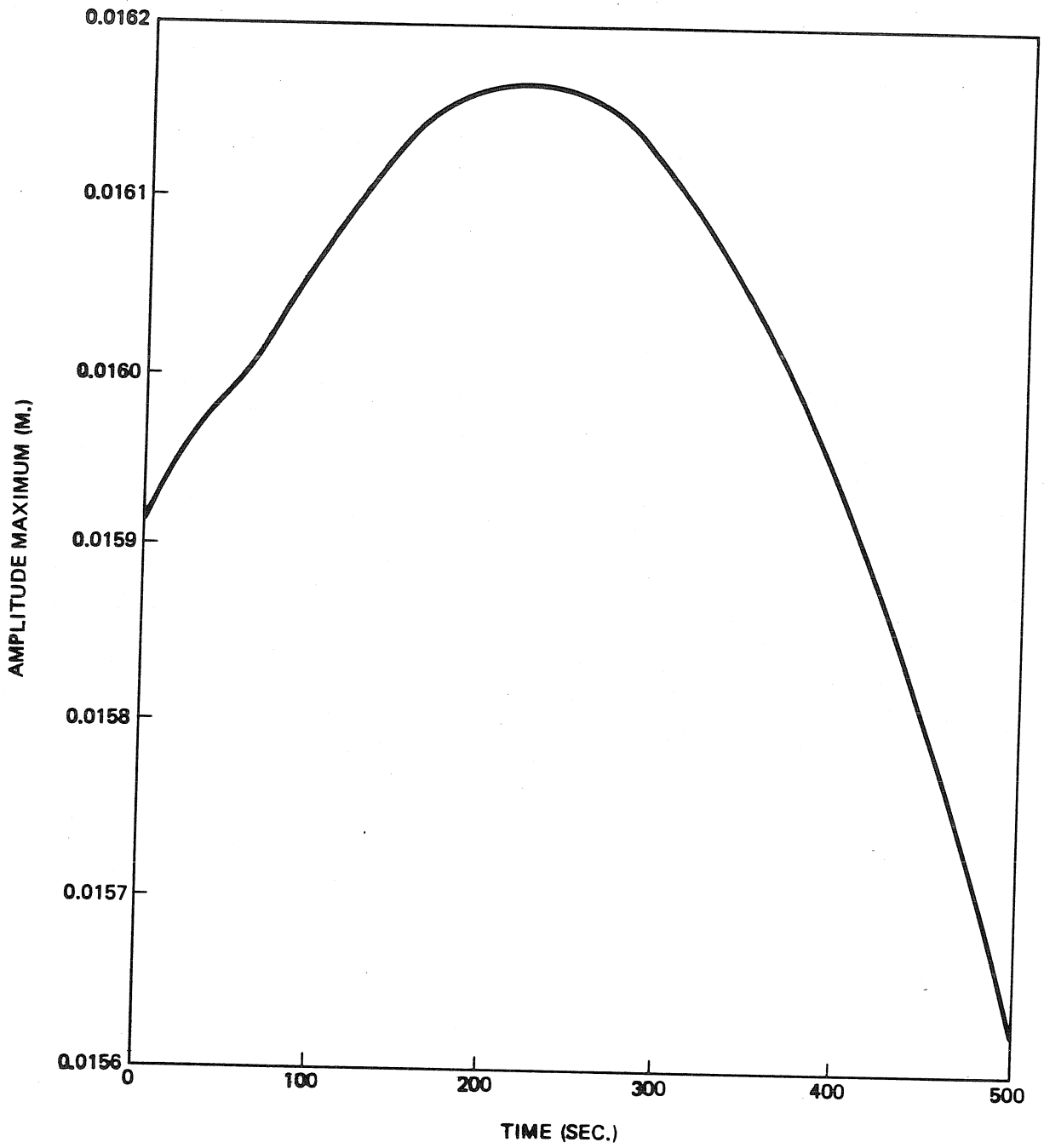

Figure 5.11. Amplitude maximum as a function of time, computed via the nonlinear Schrödinger equation, for an envelope soliton subjected to the steady (with respect to the bottom) current pattern $U = 0.025c_g \sin(k_0 x/200)$ which appears instantly at the initial time. The slope of the carrier wave is $ka = 0.01$. Scale is established by assuming a carrier wavelength of 10 m.

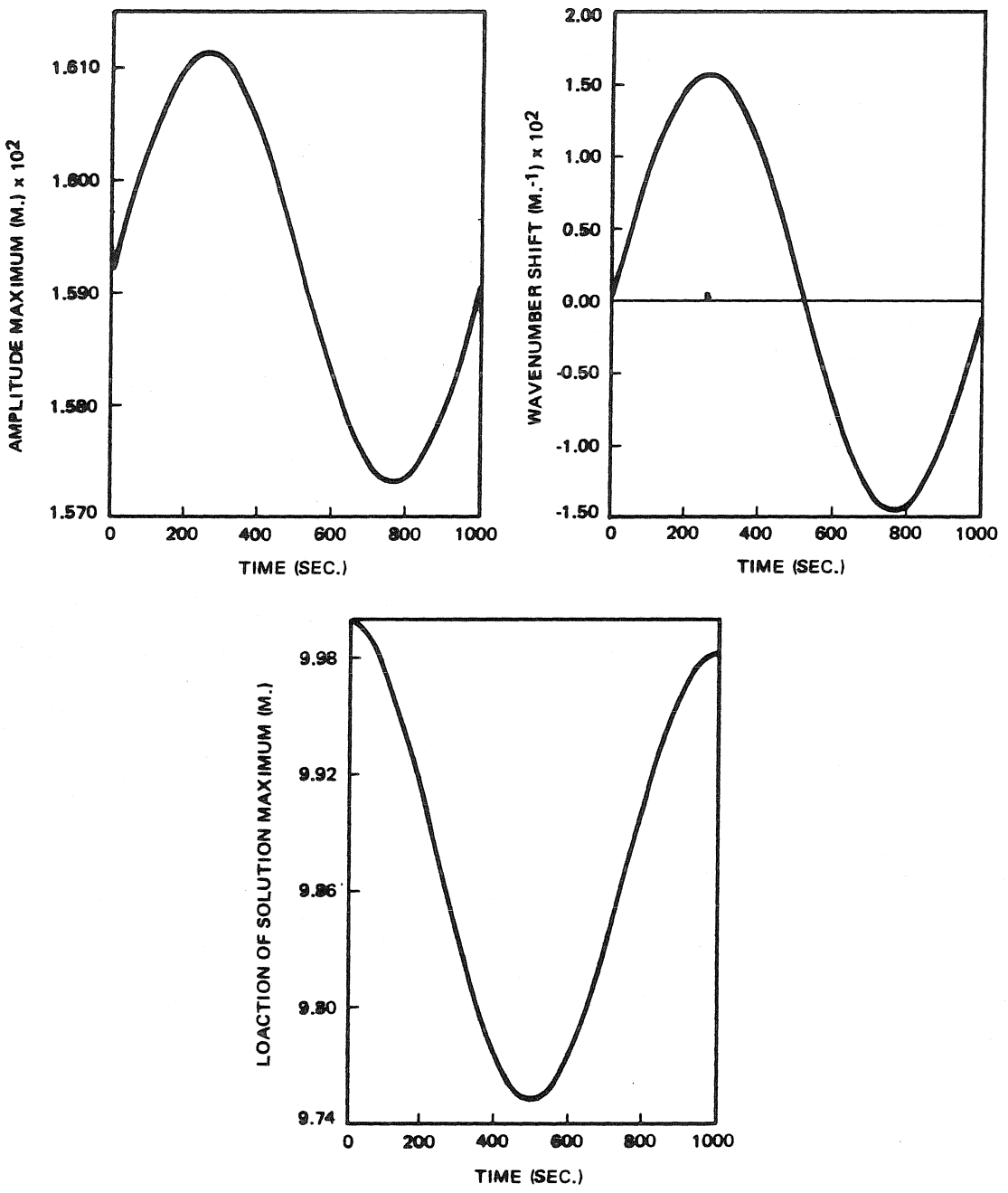

Figure 5.12. Time development of (a) the maximum of an envelope soliton, (b) the location in the group velocity frame of the soliton maximum, and (c) the associated wavenumber shift $2\beta\xi$ [see equations (5.49) and (5.64)] according to the perturbation approach. The soliton is subjected to the steady (with respect to the bottom) current pattern $U = 0.025c_g \sin(k_0 x/200)$ which appears instantly at the initial time. The carrier wave has slope $ka = 0.01$. Scale is established by assuming a carrier wavelength of 10 m.

Table 1.1. A comparison of the cutoff wavenumber for instability, N_u, with Thyagaraja's [16] bound, $\hat{N}$, on the mean component computed with energy content as a weighting function.

Case	N_u	$\hat{N}$
1	1.4	6.3
2	2.8	25.3
3	3.5	39.0
4	4.7	69.3
5	5.7	101.0
6	14.1	628.8

Table 1.2. A comparison of (1) $\max(N_{rms})$, the maximum over time of the mean component computed with energy content as a weighting function, to N_u, the cutoff number for instability, and $\hat{N}$, Thyagaraja's [16] bound on N_{rms}; and (2) N_{99}, the least component such that 99% of the energy is contained in wavenumbers of equal or lesser magnitude, to $\hat{N}_{99}$, Thyagaraja's [16] bound on N_{99}.

Case	$\max(N_{rms})$	N_u	$\hat{N}$	N_{99}	$\hat{N}_{99}$
1	1.2	1.4	6.3	3	63
2	2.4	2.8	25.3	7	253
5	5.0	5.7	101.0	15	1010
6	9.4	14.1	628.8	28	6288

REFERENCES

[1] Ablowitz, M. J. and Segur, H. (1979), "On the Evolution of Packets of Water Waves," J. Fluid Mech. 92, 691.

[2] Benjamin, T. B. and Feir, J. E. (1967), "The Disintegration of Wave Trains in Deep Water. Part 1. Theory," J. Fluid Mech. 27, 417.

[3] Chen, B. and Saffman, P. G. (1980), "Numerical Evidence for the Existence of New Types of Gravity Waves of Permanent Form on Deep Water," Studies in Applied Mathematics. 62, 1-21.

[4] Fermi, E., Pasta, J. and Ulam, S. (1955), Collected Papers of Enrico Fermi, 2, 978.

[5] Fornberg, B. and Whitham, G. B. (1978), "A Numerical and Theoretical Study of Certain Nonlinear Wave Phenomena," Philosophical Transactions of the Royal Society of London, Vol. 289, 373-404.

[6] Keener, J. P. and McLaughlin, D. W. (1977), "Solitons under Perturbations," Phys. Rev. A, Vol. 16, No. 2, 777-790.

[7] Lake, B. M., Yuen, H. C., Rungaldier, H. and Ferguson, W. E. (1977), "Nonlinear Deep-Water Waves: Theory and Experiment. Part 2. Evolution of a Continuous Wavetrain," J. Fluid Mech. 83, 49.

[8] Lighthill, M. J. (1965), "Contributions to the Theory of Waves in Nonlinear Dispersive Systems," J. Inst. Math. Appl. 1, 269-306.

[9] Longuet-Higgins, M. S. (1978), "The Instability of Gravity Waves of Finite Amplitude in Deep Water. II. Subharmonics," Proceedings of the Royal Society of London, Vol. A360, 471-505.

[10] Longuet-Higgins, M. S. and Stewart, R. W. (1960), "Changes in the Form of Short Gravity Waves on Long Waves and Tidal Currents," J. Fluid Mech. 8, 565-583.

[11] Longuet-Higgins, M. S. and Stewart, R. W. (1961), "The Changes in Amplitude of Short Gravity Waves on Steady Non-Uniform Currents," J. Fluid Mech. 10, 529-549.

[12] Peregrine, D. H. and Thomas, G. P. (1979), "Finite-Amplitude, Deep-Water Waves on Currents," Phil. Trans. Roy. Soc. A 292, 371-390.

[13] Rowlands, G. (1974), "On the Stability of Solutions of the Non-Linear Schrödinger Equation," J. Inst. Maths. Applics. 13, 367-377.

[14] Saffman, P. G. and Yuen, H. C. (1978), "Stability of a Plane Soliton to Infinitesimal Two-Dimensional Perturbations," Physics of Fluids, Vol. 21, No. 8, August, 1450-1451.

[15] Stokes, G. G. (1849),"On the Theory of Oscillatory Waves," Trans. Cambridge Philos.Soc. 8, 441-455. Math Phys. Pap. 1, 197-229.

[16] Thyagaraja, A. (1979), "On Recurrent Motions in Certain Physical Systems, Phys. Fluids 22, 2093.

[17] Whitham, G. B. (1962), "Mass, Momentum and Energy Flux in Water Waves," J. Fluid Mech. 12, 135-147.

[18] Whitham, G. B. (1974), Linear and Nonlinear Waves (Book), John Wiley & Sons, New York.

[19] Yuen, H. C. and Ferguson, W. E. Jr. (1978a), "Relationship between Benjamin-Feir Instability and Recurrence in the Nonlinear Schrödinger Equation," Phys. Fluids 21, 1275-78.

[20] Yuen, H. C. and Ferguson, W. E. Jr. (1978b), "Fermi-Pasta-Ulam Recurrence in the Two-Space Dimensional Nonlinear Schrödinger Equation," Phys. Fluids 21, 2116-18.

[21] Yuen, H. C. and Lake, B. M. (1975), "Nonlinear Deep Water Waves: Theory and Experiment," Phys. Fluids 18, 956-960.

[22] Yuen, H. C., Lake, B. M. and Ferguson, W. E. (1977), The Significance of Nonlinearity in the Natural Sciences, Plenum Press, 67.

[23] Zakharov, V. E.(1968), "Stability of Periodic Waves of Finite Amplitude on the Surface of a Deep Fluid," Journal of Applied Mechanics and Technical Physics, Vol. 2, 190-194, (Zhurnal Prikladnoi Mekhaniki Teknicheskoi Fiziki, Vol. 9, No. 2, 86-94).

[24] Zakharov, V. E. and Rubenchik, A. M. (1973), "Instability of Waveguides and Solitons in Nonlinear Media," Soviet Physics JETP, Vol. 38, No. 3, March, 494-499 (Zh. Eksp. Teor. Fiz., Vol. 65, 997-1011, September, 1973).

[25] Zakharov, V. E. and Shabat, A. B. (1971), "Exact Theory of Two-Dimensional Self-Focusing and One-Dimensional Self-Modulating Waves in Nonlinear Media," Zh. Eksp Teor. Fiz. 61, 118-134. Translated in Sov. Phys. JETP 34, 62-69 (1972).